Experiments with Entangled Photons

Bell Inequalities, Non-local Games and Bound Entanglement

Muhammad Sadiq

Thesis for the degree of Doctor of Philosophy in Physics
Department of Physics
Stockholm University
Sweden.

ISBN 978-91-7649-358-8

Printed in Sweden by Holmbergs, Malmö 2016.

Distributor: Department of Physics, Stockholm University.

Abstract

Quantum mechanics is undoubtedly a weird field of science, which violates many deep conceptual tenets of classical physics, requiring reconsideration of the concepts on which classical physics is based. For instance, it permits persistent correlations between classically separated systems, that are termed as entanglement. To circumvent these problems and explain entanglement, hidden variables theories–based on undiscovered parameters–have been devised. However, John S. Bell and others invented inequalities that can distinguish between the predictions of local hidden variable (LHV) theories and quantum mechanics. The CHSH-inequality (formulated by J. Clauser, M. Horne, A. Shimony and R. A. Holt), is one of the most famous among these inequalities. In the present work, we found that this inequality actually contains an even simpler logical structure, which can itself be described by an inequality and will be violated by quantum mechanics. We found 3 simpler inequalities and were able to violate them experimentally.

Furthermore, the CHSH inequality can be used to devise games that can outperform classical strategies. We explore CHSH-games for biased and unbiased cases and present their experimental realizations. We also found a remarkable application of CHSH-games in real life, namely in the card game of duplicate Bridge. In this thesis, we have described this application along with its experimental realization. Moreover, non-local games with quantum inputs can be used to certify entanglement in a measurement device independent manner. We implemented this method and detected entanglement in a set of two-photon Werner states. Our results are in good agreement with theory.

A peculiar form of entanglement that is not distillable through local operations and classical communication (LOCC) is known as bound entanglement (BE). In the present work, we produced and studied BE in four-partite Smolin states and present an experimental violation of a Bell inequality by such states. Moreover we produced a three-qubit BE state, which is also the first experimental realization of a tripartite BE state. We also present its activation, where we experimentally demonstrate super additivity of quantum information resources.

To my wife.

Acknowledgements

First of all I offer my profound thanks to Mohamed Bourennane, for being such a generous supervisor. He deserves a special mention of my deep gratitude. This work was accomplished as a result of his encouragement and efforts, providing me continuous support.

After this, my most humble thanks to Ingemar Bengtsson, for helping me at every stage of my life in Sweden. I am also very thankful to my co-supervisor Hoshang Heydari for occasional help that he has provided me during his stay, here in Fysikum. I am grateful to my collaborators and colleagues, I have had pleasure to work with during my PhD , thanks Adán Cabello, Marek Zukowski, Pawel Horodecki, Marcin Pawlowski Piotr Badziąg, Maciej Kurant, , Mohamed Nawareg, Elias Amselem and Armin Tavakoli.

All former and new members of KIKO including Hannes, Guillermo, Hatim, Massimiliano, Tewodros,Victoria, Marco, David, Adrian, Arash, Saeed, Waqas, Breno,Victor, Atia,Christian Kothe, Magnus, Amir, Ramiz and Benjamin, thanks for an inspiring and pleasant atmosphere. In particular, Johan, Elias, Nawareg, Hammad, Alley, Kate, Ashraf, Ole, and Ian deserve special thanks for useful and friendly discussions that we had during all these years and, for nice and pleasing memories.

Finally, special thanks also go to my family and friends, for their cooperation and extra support that provided me confidence to present this work.

Contents

List of Papers

The following papers, referred to in the text by their Roman numerals, are included in this thesis.

PAPER I: **Bell inequalities for the simplest exclusivity graph**
Muhammad Sadiq, Piotr Badziąg, Mohamed Bourennane, Adán Cabello *Phys. Rev. A*, **87**, 012128 (2013).
DOI: PhysRevA.87.012128

PAPER II: **Quantum Bidding in Bridge**
Muhammad Sadiq, Armin Tavakoli, Maciej Kurant, Marcin Pawlowski, Marek Zukowski, Mohamed Bourennane, *Phys. Rev. X*, **2**, 021047 (2014).
DOI: 10.1103/PhysRevX.4.021047

PAPER III: **Experimental Measurement-Device-Independent Entanglement Detection**
Nawareg Mohamed, Muhammad Sadiq, Elias Amselem, Mohamed Bourennane, *Scientific Reports*, **5**, 8048 (2015).
DOI: 10.1038/srep08048

PAPER IV: **Experimental bound entanglement through a Pauli channel**
Elias Amselem, Muhammad Sadiq, Mohamed Bourennane, *Scientific Reports*, **3**, 1966 (2013).
DOI: 10.1038/srep01966

PAPER V: **Experimental Three-Qubit Bound Entanglement**
Muhammad Sadiq, Mohamed Nawareg, Pawel Horodecki, Mohamed Bourennane, submitted (2015).

PAPER VI: **Superadditivity of two quantum information resources**
Mohamed Nawareg, Muhammad Sadiq, Pawel Horodecki, Mohamed Bourennane, submitted (2015).

Author's Contribution

PAPER I: I performed all the experimental work, which include designing and building the setup, measuring and analyzing the data, and helped in writing the paper.

PAPER II: I designed the experiment. Built the setup and measured the data with the help of Armin Tavakoli. I analyze the data and helped in writing the paper.

PAPER III: We, (M. Nawareg and I) designed the experiment, built the setup and measured the data together. I helped in writing paper.

PAPER IV: Elias and I performed all the experimental work together. This includes building the experiment and measuring the data.

PAPER V: I and M. Nawareg designed the experiment, built the setup and measured the data together. I helped in data analysis and writing paper.

PAPER VI: M. Nawareg and I designed the experiment, built the setup and measured the data together. I helped in data analysis and writing paper.

Sammanfattning

Kvantmekanik är tveklöst en konstig gren av naturvetenskapen och bryter mot många grundläggande antaganden inom klassisk fysik. Den kräver omprövning av de koncept som den klassiska fysiken bygger på. Exempelvis tillåts korrelationer mellan system som klassisk betraktas som åtskillda, detta kallas snärjelse. För att kringgå dessa problem och förklara snärjelse har gömda-variabel-teorier konstruerats, dessa bygger på okända parametrar. John S. Bell och andra fysiker fann olikheter som kan urskilja mellan förutsägelser från lokala gömda variabel (local hidden variable, LHV) teorier and kvantmekanik. CHSH-olikheten, funnen av J. Clauser, M. Horne, A. Shimony och R.A. Holt, är en av de mest kända. Under arbetet som presenteras i denna avhandling har vi funnit att CHSH-olikheten har en ännu enklare logisk struktur, som i sig kan beskrivas med en olikhet och som bryts av kvantmekaniken. Vi har funnit tre stycken enklare olikheter och brutit dem experimentellt.

Vidare kan CHSH-olikheten användas för att konstruera spel där utfallet blir bättreöm kvantmekaniska tillstånd tillåts. Vi har undersökt både viktade och oviktade CHSH-spel. Vi har även funnit en anmärkningsvärd verklighetsanknuten tillämpning av ett CHSH-spel, nämligen i kortspelet kontraktsbridge. Denna tillämpning, tillsammans med dess experimentella realisering, presenteras i avhandlingen. Icke-lokala spel kan även användas för att garantera snärjelse på ett apparatoberoende sätt. Vi har implementerat en sådan metod och verifierat snärjelse i en mängd två-foton Werner states. Våra resultat överensstämmer väl med teoretiska beräkningar.

En speciell form av snärjelse som inte är destillerbar genom lokala operationer och klassisk kommunikation (local operations an classical communication, LOCC) kallas bunden snärjelse (bound entanglement, BE). Vi har skapat och undersökt BE i fyr-foton Smolin-tillståndet och presenterar experimentell brytning av en Bell-olikhet. Vidare har vi för första gången skapat ett tre-foton BE-tillstånd och presenterar dess aktivering. Här demostrerar vi experimentellt super additivitet av kvantresurser.

List of Figures

List of Tables

1. Introduction

Quantum mechanics is one of the most fascinating fields in modern physics, and the heart of its fascination comes from counterintuitive and non-classical concepts. Concepts like wave-particle duality, absence of exact predictability, and inseparability of the universe at a larger scale, makes it an astounding subject [1]. Although it contains such bizarre ideas, quantum mechanics has provided the basic framework for the most precise theories in human history.

One of the most inexplicable ideas that quantum mechanics introduces is the inseparability of the universe, that is different parts of the universe are connected in a way that no matter how far they are apart, they will still influence each other. It is hard to say precisely what "influence" means here, and some of my colleagues would wince at my use of the word. But I will show in this thesis that there is something here which allows us to achieve classically impossible tasks. In fact, the founders of quantum mechanics were unaware of this implication of the theory, until the leading opponent, Albert Einstein with his colleagues– Boris Podolsky and Nathan Rosen–proposed a thought experiment to defeat quantum mechanics. In this thought experiment, using the principle of locality, they were able to argue that quantum mechanics is incomplete [2]. This thought experiment, using initials of the authors, is now known as the EPR paradox.

Since then, the EPR paradox has raised many debates and divided the scientific community into two groups, one who believed (and still believes) that quantum mechanics is indeed incomplete and therefore, we need a more down-to-earth theory, called *Hidden variables theory*. On the other hand, a second group believes, due to the enormous success of the theory, that the EPR argument must contain some flaws or incorrect assumptions which are not true for quantum mechanics. The most famous of these debates was between Einstein and Niels Bohr [3]. The other notable person was Erwin Schrödinger, who named the correlations between EPR pairs as *entanglement* [4; 5]. Nevertheless, the problem was not settled until it came to John S. Bell others who found that there are ways to distinguish between the predictions of local hidden variable (LHV) theories and quantum mechanics and formulated testable inequalities based on these differences [6–8]. These inequalities are such that, classical mechanics is bound to them but quantum mechanics violates them. These inequalities are in general called Bell inequalities. Among these, an in-

equality derived by J. Clauser, M. Horne, A. Shimony and R. A. Holt, named for their initials the CHSH inequality is the most famous.

Currently the situation is that numerous experiments have violated these inequalities in favor of quantum mechanics [9–16]. There are many interpretations of quantum mechanics that suggest different possibilities, however, we are almost certain that quantum mechanics violates local realism and allows correlation between well separated parts of a system. These kinds of quantum correlations between separated systems are referred to as entanglement. Thus, it is easy to see that in the form of entanglement quantum mechanics offers resources that are not present in classical systems and hence its uses in information sciences can break the limitations of conventional information transfer, cryptography and computation.

With this introduction it is easy to explain what we are after in this thesis. This work consist of the experiments that I carried out during my PhD, two of these have already formed part of my licentiate thesis. These experiments can be categorized into two parts. The first part is related to Bell inequalities and so called “non-local games" based on it, whereas the second part is about experimental preparation and activation of Bound entanglement.

Bell inequalities are important, since these can indicate when a system possesses non-classical properties and hence can be used to achieve classically impossible tasks. Recently, it is shown that the application of graph theory to Bell inequalities can bring new insights [17]. Using these techniques we present in **paper I** that the CHSH inequality contains another even simpler logical structure that can itself be represented by an inequality. We show that there are two more inequalities similar to this inequality and we also present the experimental violation of these inequalities.

In the **paper II** included with this thesis we will see how Bell inequalities or more specifically the CHSH inequality can be viewed as non-local games. Games in which two parties, say Alice and Bob receive some binary number x and y from a referee and to win they have to reply with numbers a and b such that $a \oplus b = x \wedge y$. Two types of this game can be defined according to the statistical distribution of received binary number x and y; if these are uniformly distributed we call the game unbiased CHSH-game, and in the other case it is called a biased CHSH-game. We will explore CHSH-game for both unbiased and biased cases and see how quantum mechanics can help us to increase probability of winning in these games [18]. For unbiased case we will see that we do not always have a quantum advantage. Also, in this work we present a remarkable application of CHSH-game, to the famous card game of contract bridge. This, according to our knowledge, is the first real life application of CHSH-game or quantum communication complexity protocol.

Paper III is another application of non-local games where using quantum

inputs instead of classical ones used in CHSH-games, one can certify entanglement in a measurement device independent way. This method was recently discovered in [19], and further elaborated in [20]. In our paper we present an experimental realization of this method, and detect entanglement in a two-qubit Werner state. Our results are in good agreement with the theory.

The other papers are about bound entanglement and its activation. In **paper IV**, we produced four-partite bound entangled states, known as Smolin states, using a noisy lossless quantum channel. Here, we started with a product of Bell states, which undergoes some changes while transmitting through this error channel which caused phase and bit flips. This error channel could transform the input free entangled states from bound entangled states to separable states. We investigated these states experimentally and were able to produce bound entangled states that violated CHSH inequality.

In **paper V** and **paper VI**, we experimentally prepared a high fidelity mixed three qubit polarization bound entangled state. This is the first experimental realization of a three-qubit bound entangled state. In **Paper VI**, we present activation scheme for this state with the help of a free entangled pair. This is the cleanest activation experiment ever done. Remarkably, our experiment also demonstrates the super additivity of quantum information sources, where by source we mean entanglement resource. Our experiment shows that considering two bound entangled states together can give you some free entanglement. It is like "something-out-of-nothing" or adding two zeros and getting something more than zero.

1.1 Outline

The aim of this thesis is to give experimental and theoretical background of the work described in the included papers. To do this, I have divided the thesis into two parts. In part one, we will cover common theoretical and experimental background, and in the second part all the experiments are briefly described with their specific background. More details can be found in the papers attached to this thesis.

Part one is consisting of chapter 2 and 3. In chapter 2, I shall discuss the theoretical concepts needed to understand the later chapters, whereas chapter 3, gives the common experimental background. Chapter 4, 5 and 6 are based on paper I, II and III, and chapter 7 describes the experiments about bound entanglement and its activation presented in paper IV, V and VI.

2. Preliminary Concepts

This chapter serves as a brief theoretical background to the later work and hence, introduces relevant terms and concepts. We first define pure and mixed states, density operator and then introduce the concept of qubit–the simplest non-trivial quantum system–and its state space. Then main topics like EPR paradox, Bell inequalities and entanglement will be presented. The chapter will be concluded with a brief introduction to the contextuality of quantum mechanics.

2.1 Pure and Mixed States

The *State* of a physical system is one of the basic notions of physics and refers to those aspects of a system with which we differentiate it from other similar systems. For instance we humans, are all made of similar kind of particles, however no two persons are exactly the same i.e. a system consisting of elementary particles can be configured to give various personalities or states. In classical dynamics, often the state of a system can conveniently be represented by a single point in the phase space. However in quantum mechanics things are a bit different. One reason for this is the fact that quantum mechanics is a probabilistic theory and these probabilities, in predicting the outcome of a process, are usually not because of our lack of knowledge– as it is the case in classical statistical mechanics–rather it is due to a fundamental feature of the theory that cannot be avoided even in principle[1]. Nevertheless, there are situations when quantum mechanics allows maximal knowledge of the state of a system. This is usually true just after a suitably chosen measurement. For example, immediately after a spin measurement along z-direction we know with certainty the state of the spin of the system along this direction. In such cases the states are known as *Pure state*.

In quantum mechanics pure states are postulated to be unit vectors in a complex vector space called *Hilbert space*[2]. That is, not every vector in Hilbert

[1] In this thesis, we only stick to the standard or Copenhagen interpretation and more or less all the description will be given according to this point of view.

[2] More precisely *Hilbert Space* is a complex vector space such that an inner product is defined for all pairs of its vectors and also the norm induced by this inner product

space represents a unique physical state, rather each direction or complex ray corresponds to a single unique physical state. This implies that a vector of Hilbert space can be multiplied by a complex number without altering the state it represents. Mathematically this fact can be expressed as,

$$|\psi\rangle \sim c|\psi\rangle = A\, e^{i\phi}|\psi\rangle \tag{2.1}$$

where $|\psi\rangle$ is a vector in Hilbert space, $c \in \mathbb{C}$ and $A, \phi \in \mathbb{R}$. Usually, the factor 'A' in the above equation is utilized to normalize the state vectors.

One should note here that this description was meant to describe the situations when there is no lack of knowledge about the state of a system. However, in almost all practical situations we usually have statistical systems or ensembles and we only know the probability with which a given system or member could be in a number of possible pure states. Such states of a system are called *mixed states*. Note that, in these cases the probabilities–if they have appropriate meaning, as we will see in the next section–come into the picture because of our ignorance or lack of knowledge and hence these states cannot be described by vectors in Hilbert space, but a description of the state based on density operator can be given.

2.2 The Density Operator

Consider an ensemble (or system consisting) of pure states, in which the probability of finding a member in a given state $|\psi_i\rangle$ is p_i, then the *Density operator* $\hat{\rho}$ of the ensemble can be written as

$$\hat{\rho} = \sum_{i=1}^{k} p_i |\psi_i\rangle\langle\psi_i|. \tag{2.2}$$

Here, three things should be noted. First, $|\psi_i\rangle$ represent pure states and are vectors in the associated Hilbert space. Secondly, as p_i represent probabilities, these are real numbers such that

$$\sum_i p_i = 1 \qquad \text{and} \qquad p_i \geq 0. \tag{2.3}$$

Thirdly, the decomposition given by the above equation is not unique, meaning that we can mix different pure states to get the same density matrix. This fact brings in some philosophical issues as one can imagine two or more observers considering the same system as a mixture of different pure states. In such case one can even ask if the probabilities, of the system to be found in a certain

makes it a complete metric space [21].

pure states for one observer, will have some meaning for the other observer who considers the system as a mixture of some other pure states. Since these probabilities will not even be defined for the second observer. We will not be considering such issues here in this thesis.

Also, note that in Eq. (2.2), the vectors $|\psi_i\rangle$ need not to be orthonormal, in such case the number of terms in Eq. (2.2), i.e. k can exceed the dimensionality of the relevant Hilbert space[22].

For a pure state $|\psi\rangle$, the density operator reduces to

$$\hat{\rho} = |\psi\rangle\langle\psi| \tag{2.4}$$

since, for a pure state we have maximal knowledge of the system and hence all p_i will be zero except the one that corresponds to the relevant state. In this case the density operator is also called the *Projection operator*, since it can project a given state on to the 1-D subspace of $|\psi\rangle$. Also, for pure states, $\hat{\rho}^2 = \hat{\rho}$ and $Tr\,(\hat{\rho}^2) = 1$, where $Tr()$ represents summation over diagonal element of a matrix. Note that for mixed states $Tr\,(\hat{\rho}^2) < 1$ and ρ cannot be written in the form given in Eq. (2.4). Therefore, the density operator also provides a way to distinguish between pure and mixed states.

In short, the density operator is represented by a positive semi-definite[1] Hermitian matrix[2] with unit trace. Note that the eigenvalues of a density operator represent the probabilities of corresponding pure states and unit-trace guarantees that these probabilities will sum to 1.

2.3 Qubit: The Simplest Quantum System

Quantum-bit or *qu-bit* is the quantum analogue of classical bit, one of the basic concepts in classical information theory. The word *Bit* is derived from binary digit and can be defined as the amount of information gained when learning the state of a two dimensional (2-D) classical system. There are only two possible states of a 2-D classical system; therefore a bit can only take two possible values. These values are usually represented by 0 and 1.

Following the same line we can define a *Qubit* as the amount of information gained when learning the state of a 2-D quantum system. Interestingly this is very different compared to the classical case. Recall that in quantum mechanics states of a system are represented by vectors in Hilbert space and since it is a vector space therefore the sum of any two such vectors could also

[1] Meaning that eigenvalues can only be positive or zero.

[2] A complex square matrix A is called Hermitian matrix when it is equal to its conjugate transpose, i.e. $A = A^{\dagger}$.

represent a legitimate yet different physical state. This is the famous *superposition principle* and suggests that a 2-D quantum system can be configured in infinitely many different physical states. Now, if we assume that the two dimensions in Hilbert space are represented by two orthonormal state vector $|0\rangle$ and $|1\rangle$ then we can write a general qubit $|Q\rangle$ as,

$$|Q\rangle = \alpha|0\rangle + \beta|1\rangle \tag{2.5}$$

where $\alpha, \beta \in \mathbb{C}$. These basis states are often referred to as *computational basis*. Furthermore, whenever a projective measurement is done along the state vector $|0\rangle$ (or $|1\rangle$) then, for the state in Eq. (2.5) the probability of getting an answer as $|0\rangle$ (or $|1\rangle$) will be $|\alpha|^2$ (or $|\beta|^2$). As the probabilities should add up to 1, so we have following restriction on α and β,

$$|\alpha|^2 + |\beta|^2 = 1 \tag{2.6}$$

It will not be out of context to mention here that the power of quantum mechanics actually comes from this superposition principle. To see this, imagine a unitary operation U carried out on a qubit as defined in Eq. (2.5), since it is a linear combination of our basis vector $|0\rangle$ and $|1\rangle$, therefore the result of this operation will be simultaneously calculated for both states. On the other hand, the classical bit requires individual operations on both possible input states. This suggests that a quantum computer will essentially have parallel processing capabilities and is the main motivation for its invention.

2.4 Bloch Sphere: The State Space of a Qubit

We have seen that any type of state, pure or mixed, can be easily represented by a density matrix and hence it is an appropriate tool to explore the state space of

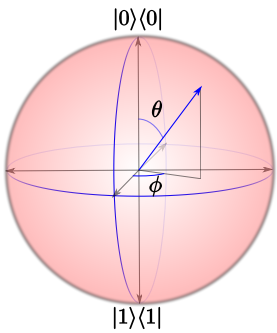

Figure 2.1: The Bloch Ball: All points on the surface of the sphere represent density matrices of pure states, whereas interior represent mixed states.

a quantum system. A qubit is a 2-D quantum system and therefore its density operator can be represented by a 2×2 Hermitian matrix with unit trace as

$$\hat{\rho} = \begin{pmatrix} \frac{1}{2}+z & x-iy \\ x+iy & \frac{1}{2}-z \end{pmatrix} \tag{2.7}$$

where x, y and z are real numbers. But a density matrix should also be semi-definite. This requirement can be fulfilled easily if we demand that the product of eigenvalues should be greater than 0. It can be checked that this condition will lead to the following inequality

$$x^2+y^2+z^2 \leq \left(\frac{1}{2}\right)^2 \tag{2.8}$$

This is interior of a sphere with unit diameter. Therefore the state space of a qubit is a ball with diameter equal to 1 unit. This ball is called *Bloch Ball*. All points on the surface of this ball represent pure states whereas the interior represents mixed states.

On the Bloch ball different states of a qubit can be easily visualized. To see this, note that due to the phase freedom we can parameterize Eq. (2.5) as,

$$|Q\rangle = cos\left(\frac{\theta}{2}\right)|0\rangle + e^{i\phi}\ sin\left(\frac{\theta}{2}\right)|1\rangle \tag{2.9}$$

where $0 \leq \theta \leq \pi$ and $0 \leq \phi < 2\pi$. Now, if one identifies a state with this θ, ϕ and $r' = \frac{1}{2}$ as spherical coordinate (r', θ, ϕ) of a point on a sphere then the corresponding point on the Bloch ball will represent the density matrix of that particular state. This point can be clarified further if one decompose the density matrix in terms of *Pauli matrices* and identity matrix. To see this, note that the set of Pauli matrices given as,

$$\hat{\sigma_x} = \begin{pmatrix} 0 & 1 \\ 1 & 0 \end{pmatrix} \qquad \hat{\sigma_y} = \begin{pmatrix} 0 & -i \\ i & 0 \end{pmatrix} \qquad \hat{\sigma_z} = \begin{pmatrix} 1 & 0 \\ 0 & -1 \end{pmatrix} \tag{2.10}$$

and $\mathbb{1}_2$ (2×2 identity matrix), form a complete set of basis in the sense that any 2×2 matrix can be written as linear combination of these four matrices. Using this fact one can write a density matrix as,

$$\hat{\rho} = \frac{1}{2}(\mathbb{1}_2 + \vec{r}.\vec{\sigma}) \tag{2.11}$$

where

$$\vec{r} = 2\begin{pmatrix} x \\ y \\ z \end{pmatrix} \equiv \begin{pmatrix} sin\,\theta\ cos\,\phi \\ sin\,\theta\ sin\,\phi \\ cos\,\theta \end{pmatrix}, \qquad \vec{\sigma} = \begin{pmatrix} \hat{\sigma}_x \\ \hat{\sigma}_y \\ \hat{\sigma}_z \end{pmatrix} \tag{2.12}$$

Here $\vec{r}$ is known as a *Bloch vector* with $|\vec{r}| \leq 1$, and equality hold for pure states only.

From the above equation one can see clearly that the θ and ϕ in Eq. (2.9) define the state on the Bloch ball through the Bloch vector. The reader should note that the orthogonal states on the Bloch sphere are directly opposite to each other e.g. when $\theta = 0^\circ(180^\circ)$ in Eq. (2.12) then the point on the Bloch sphere represents the density matrix of the state $|0\rangle$ ($|1\rangle$), which is the eigenstate of $\hat{\sigma}_z$ matrix associated to the directions along the z-axis. Similarly $\hat{\sigma}_x$ and $\hat{\sigma}_y$ matrices are associated to the directions along x and y axes respectively and corresponding points where these axes cut the Bloch Ball represent density matrices of their eigenstates. It is also interesting to note that center or the origin of this space actually represents the completely mixed state $\frac{1}{2}\mathbb{1}_2$.

2.5 Multi-Qubit Systems

In most experimental cases and also in this thesis we will encounter systems consisting of more than one qubit. States of such quantum systems are described by vectors in product Hilbert spaces. These spaces are tensor product of individual qubit spaces, e.g. the tensor product of two qubit $|Q\rangle_1$ and $|Q\rangle_2$ residing in the Hilbert spaces $\mathcal{H}^1$ and $\mathcal{H}^2$ will be $\mathcal{H} = \mathcal{H}^1 \otimes \mathcal{H}^2$. If the basis vector of individual spaces are given as

$$|0\rangle_i = \begin{pmatrix} 1 \\ 0 \end{pmatrix} \qquad |1\rangle_i = \begin{pmatrix} 0 \\ 1 \end{pmatrix} \tag{2.13}$$

where $i = 1,2$ for qubit $|Q\rangle_1$ and $|Q\rangle_2$, then the basis vector of the composite systems will be,

$$\begin{aligned} |00\rangle \equiv |0\rangle_1 \otimes |0\rangle_2 &= \begin{pmatrix} 1 \\ 0 \\ 0 \\ 0 \end{pmatrix} & |01\rangle \equiv |0\rangle_1 \otimes |1\rangle_2 &= \begin{pmatrix} 0 \\ 1 \\ 0 \\ 0 \end{pmatrix} \\ |10\rangle \equiv |1\rangle_1 \otimes |0\rangle_2 &= \begin{pmatrix} 0 \\ 0 \\ 1 \\ 0 \end{pmatrix} & |11\rangle \equiv |1\rangle_1 \otimes |1\rangle_2 &= \begin{pmatrix} 0 \\ 0 \\ 0 \\ 1 \end{pmatrix} \end{aligned} \tag{2.14}$$

Using these basis vectors one can represent a general 2-qubit pure state as,

$$|Q_{12}\rangle = c_0|00\rangle + c_1|01\rangle + c_2|10\rangle + c_3|11\rangle \tag{2.15}$$

where $c_i \in \mathbb{C}$ such that $\sum_{i=0}^{3} |c_i|^2 = 1$. Also, the equivalent operator $\hat{U}$, representing the action of local single qubit operators $\hat{A}$ and $\hat{B}$, will be a Kronecker product of the two matrices A and B as,

$$\hat{U} = A \otimes B = \begin{pmatrix} a_{00}\, B & a_{01}\, B \\ a_{10}\, B & a_{11}\, B \end{pmatrix} \tag{2.16}$$

Note that the dimensionality of the product Hilbert space, in this case, is 4. In general dimension of a composite qubit system consisting of N qubits will be 2^N i.e. the dimension of product spaces grows exponentially. Likewise, a pure states consisting of N qubits can be written as,

$$\begin{aligned} |Q_N\rangle &= c_0|00...000\rangle + c_1|00...001\rangle + ... + c_{N-1}|11...111\rangle \\ &= \sum_{i=0}^{N-1} c_i |i_{(2)}\rangle \end{aligned} \tag{2.17}$$

where $i_{(2)}$ represent i written as a base 2 number and again we have the restriction $c_i \in \mathbb{C}$ such that $\sum_{i=0}^{N-1} |c_i|^2 = 1$. Also note that the superposition principle will still be applicable in such product spaces e.g. one could have a physical state represented by the superposition of $|00\rangle$ and $|11\rangle$. Actually such states are more interesting and lead to counter intuitive correlation between the individual qubits as we will see in the next sections.

2.6 Entangled States

In quantum mechanics, we can distinguish between two kind of states, entangled states and separable states. An entangled state describes a system which comprises different parts that have quantum correlation among them. Here by quantum correlations we mean correlations that cannot be explained or simulated by classical correlations [23]. Interestingly, these correlations exist even if these parts are billions of light years apart. In general entangled states are defined as those states which are not separable, whereas separable states are those states that can be written as a convex sum of product states [24; 25]. Mathematically for separable states

$$\hat{\rho} = \sum_i p_i\, \hat{\rho}_1^i \otimes \hat{\rho}_2^i \otimes .... \otimes \hat{\rho}_n^i \tag{2.18}$$

where $\sum_i p_i = 1$ with $p_i \geq 0$ and subscript 1 to n refer to different individual parts of the system. Moreover, when $n = 2$, in the above expression i.e. for bipartite case entanglement and separability have straight forward meaning. However in multi-partite case, a state can be entangled even if only

two of its subsystems (or parts) are entangled and all other parts are separable. Conversely one can have m-partite separability in an entangled state when $1 < m < n$. Therefore, we can distinguish two special cases here, when $m = 1$ entanglement is sometimes referred to as genuine n-partite entanglement. Whereas, in the case of $m = n$ we get separable states. Note that this is the only case when a state is not entangled. This fact also demonstrates that entanglement with all of its bizarreness is a more common thing than separable states.

As mentioned earlier, correlations offered in entangled states could sometimes be counter intuitive and paradoxical. In the following sections we shall look at the famous EPR paradox where Einstein and coworkers noticed this weirdness.

2.7 EPR Paradox

It has already been mentioned that quantum mechanics is a probabilistic theory and that these probabilities are the fundamental feature of the theory. Moreover, according to standard or Copenhagen interpretation of quantum mechanics non-commutating observables[1] cannot possess simultaneous definite measurement's results. The most common example of such non-commutating observables is position and momentum. According to quantum mechanics, it is impossible to have the exact knowledge of both simultaneously. Meaning that if one tries to find, say "exact position" of a particle by some measuring device then, according to quantum mechanics the very act of this measurement makes the momentum completely unpredictable. Similarly, position becomes completely uncertain if one measures the exact momentum of the particle. This aspect of quantum theory steered Einstein, Podolsky and Rosen (EPR), in 1935, to propose that either,

1. The quantum-mechanical description of reality given by the wave function is incomplete.

   Or

2. When the operators corresponding to two physical quantities do not commute the two quantities cannot have simultaneous reality.

Then, with a puzzling thought experiment they abandoned the later possibility and proposed that quantum mechanics is not a complete theory in the sense that there are observables or elements of realities which cannot be described by quantum mechanics in certain situations [2].

[1] Here by observables we mean physically measurable quantities.

EPR's conclusion is easier to follow if one considers the version of this thought experiment proposed by David Bohm [1], rather than EPR original example. Before presenting this thought experiment, we should look at the meaning of a complete theory in this context. According to EPR the necessary condition for a theory to be complete is that "*every element of physical reality must have a counterpart in the physical theory*". Moreover, they proposed sufficient condition for recognizing the element of physical reality as "*If, without in any way disturbing a system, we can predict with certainty (i.e., with probability equal to unity) the value of a physical quantity, then there exists an element of physical reality corresponding to this physical quantity*".

Now, equipped with these definitions of completeness and reality, we can consider the EPR-Bohm thought experiment. Imagine a system of two atoms (or any 2-D quantum systems i.e. qubits) each having spin $\frac{1}{2}$, meaning that any spin measurement, along a given direction will lead to a measurement's result of $\frac{1}{2}\hbar$ denoted as "spin up" or $-\frac{1}{2}\hbar$ denoted as "spin down" in that particular direction. Suppose further that the two qubits or atoms are prepared in a state of 0 total spin. An example of such state could be the singlet state given as,

$$|\psi\rangle = \frac{1}{\sqrt{2}} \left(|01\rangle - |10\rangle \right) \tag{2.19}$$

where $|0\rangle$ and $|1\rangle$ represent spin up and spin down respectively. According to quantum mechanics, this state is such that if spin of the first qubit is measured as up in some direction then the second qubit is predicted to be in a state of spin down in the same direction with probability equal to 1. Now, imagine that after preparation in this state, atoms or qubits fly in opposite direction and their distance is increasing with time, but they do not encounter any interactions which involve their spin. When the atoms are sufficiently apart one can measure the z-component of the spin for the first atom (i.e. $S_z^{(1)} = \frac{\hbar}{2}\hat{\sigma}_z^{(1)}$). Suppose that this measurement reveals the result as "spin up" then we can immediately conclude that the second atom will be in a state of "spin down", since the total spin of the two atoms should be 0. This conclusion can be drawn even if the two atoms are space-like separated before the measurement, in which case one cannot expect any interaction between the atoms. Now, as we can predict the spin of second atom without in any way disturbing it, therefore the z-component of spin for the second atom i.e. $S_z^{(2)}$, is an element of reality according to EPR criterion. But one can also choose to measure the x-component of spin for the first atom i.e. $S_x^{(1)}$, in this case if we follow the same lines of reasoning we can conclude that the x-component of the spin for the second atom i.e. $S_x^{(2)}$, is also an element of reality according to EPR criterion. Since the state given by Eq. (2.19) is rotationally invariant therefore, the same reasoning will lead us to conclude that the spin components in all directions are element of reality for the sec-

ond atom and if one does the measurement on the second atom then the same will be true for the first atom. However, according to quantum mechanics, z and x components of spin for a particle are non-commutating observables as $[S_z, S_x] \neq 0$. Since, this thought experiment suggested that both x and z components of spin are element of physical reality so, argument (2) above cannot be true. This forced EPR to suggest that argument (1) is true i.e. quantum mechanics is not a complete physical theory and a deeper theory could exist that will eventually replace quantum mechanics.

The ERP paradox led to inconclusive discussion and debates among the founding fathers of quantum mechanics and Einstein. The most famous among these were the debates between Einstein and Bohr [3]. However, a remarkable progress in this direction was made when John Stewart Bell, proposed an inequality whose experimental violation could favor quantum mechanics. This is our next topic.

2.8 Bell Inequality

If one notices carefully, the thought experiment given in the last section is based on the assumptions known as locality and realism. Therefore, before the derivation of Bell inequality we shall look at the formal definitions of these concepts.

Locality According to the principle of locality, *"A physical process occurring at one place cannot have any influence on other processes occurring at locations outside its light cone"*. This principle is based on special relativity which does not allow any type of information transfer greater than the speed of light.

Realism The concept of realism can be stated as, *"physical objects and their properties pre-exist without the influence of an observer"*. Therefore, it means that physical quantities have pre-defined values which are independent of the measurement process. In this case, one can also identify pre-existing properties of the objects as element of reality in EPR arguments.

Now, to derive the Bell inequality we shall approximately follow, Bell's 1971 argument [26] given in [27]. Consider a source which emits a system consisting of two-component that we call particles for simplicity. Here, we are only concerned with properties of the particles that form a 2-D quantum system and therefore, the possible outcomes of some measurement are represented as ± 1. Suppose after emission each of these particle comes into the possession

of two parties that we name as Alice and Bob. Moreover, consider that their measurement devices can perform measurements with different settings. These settings could be different directions for spin measurements in case of spin system but we can keep the discussion general. We denote these settings as A_i and B_i for first and second particle respectively.

Now, suppose that quantum mechanics is not complete and there exist some other variables, which may determine the properties of the particle under consideration. These variables are usually called hidden variables, since these are unknown to us now but could be discovered in the future. We represent all such variables collectively with a parameter λ. These variables could be characteristic features of the source generating the two particles and may also belong to a probability space Λ, (i.e. $\lambda \in \Lambda$) from which it is sampled through some probability distribution $P(\lambda)$, during each emission. Therefore,

$$\int_{\Lambda} P(\lambda)\, d\lambda = 1 \tag{2.20}$$

where $P(\lambda) \geq 0$. Then, the outcomes of both Alice and Bob measurement, will be a consequence of their settings and the sampled parameter λ, which will also be responsible for any kind of correlation between the outcomes.

Suppose further that the two particles fly apart and arrive at the two different laboratories, where Alice and Bob are ready to measurement with their devices as described above. We denote Alice measurement outcome by $a(A_0, \lambda) = \pm 1$, since it can depend on the controllable parameter (measurement's setting) A_1, and hidden variables given by λ. Similarly, Bob outcome is denoted by $b(B_0, \lambda) = \pm 1$. Note that, here we have utilized the locality assumption, because, we assumed that Alice's outcome $a(A_0, \lambda)$ is dependent only on her own setting A_0 but not on Bob's setting B_0, which should be true according to the principle of locality if Alice and Bob are space-like separated while choosing their settings. The same is true for Bob also. It should also be noted here that we are assuming a deterministic hidden variable model, since parameters $a(A_0, \lambda)$ and $b(B_0, \lambda)$ are not probabilities. Now, the correlation between the measurements of Alice and Bob can be represented by a correlation function of the form

$$E(A_0, B_0) = \int_{\Lambda} a(A_0, \lambda)\, b(B_0, \lambda)\, P(\lambda)\, d\lambda \tag{2.21}$$

Suppose that Alice and Bob both perform measurement with two settings de-

noted as A_0 and A_1 for Alice and B_0 and B_1 for Bob. Then

$$\begin{aligned} E(A_0,B_0)-E(A_0,B_1) &= \int_\Lambda [a(A_0,\lambda)\ b(B_0,\lambda)-a(A_0,\lambda)\ b(B_1,\lambda)]\ P(\lambda)\ d\lambda \\ &= \int_\Lambda a(A_0,\lambda)\ b(B_0,\lambda)\,[1\pm a(A_1,\lambda)\ b(B_1,\lambda)]\ P(\lambda)\ d\lambda \\ &\quad - \int_\Lambda a(A_0,\lambda)\ b(B_1,\lambda)\,[1\pm a(A_1,\lambda)\ b(B_0,\lambda)]\ P(\lambda)\ d\lambda \end{aligned}$$

A careful reader might notice here that we have quietly used the assumption of realism by considering that the parameters λ do not depend on the setting one choose i.e. say, Alice can choose between setting A_0 or A_1 without affecting λ[1]. Also note that since, $a(A_0,\lambda)=\pm 1$ and $b(B_0,\lambda)=\pm 1$, Therefore, $|a(A_0,\lambda)|=1$ and $|b(B_0,\lambda)|=1$. But for our derivation we will use even weaker restriction given as,

$$|a(A_0,\lambda)|\leq 1 \qquad\qquad |b(B_0,\lambda)|\leq 1 \tag{2.22}$$

and, of course, the outcomes of the setting represented by A_1 and B_1 are also assumed to have similar restrictions. Now using these restriction and the triangle inequality[2] we can write

$$\begin{aligned} |E(A_0,B_0)-E(A_0,B_1)| &\leq \left|\int_\Lambda a(A_0,\lambda)\ b(B_0,\lambda)\,[1\pm a(A_1,\lambda)\ b(B_1,\lambda)]\ P(\lambda)\ d\lambda\right| \\ &\quad + \left|\int_\Lambda a(A_0,\lambda)\ b(B_1,\lambda)\,[1\pm a(A_1,\lambda)\ b(B_0,\lambda)]\ P(\lambda)\ d\lambda\right| \\ &\leq \int_\Lambda [1\pm a(A_1,\lambda)\ b(B_1,\lambda)]\ P(\lambda)\ d\lambda \\ &\quad + \int_\Lambda [1\pm a(A_1,\lambda)\ b(B_0,\lambda)]\ P(\lambda)\ d\lambda \\ &= 2\pm[E(A_1,B_1)+E(A_1,B_0)] \end{aligned}$$

Note that here we have used the fact that

$$\begin{aligned} &[1\pm a(A_1,\lambda)\ b(B_1,\lambda)]\geq 0 \\ \text{and}\quad &[1\pm a(A_1,\lambda)\ b(B_0,\lambda)]\geq 0 \end{aligned}$$

meaning that these are positive numbers for which $|x|=x, \forall\, x\in\mathbb{R}^+$ is true. Now since for any choice of the sign, the right most side of the inequality is greater or equal to the left side, so we can write it as

$$|E(A_0,B_0)-E(A_0,B_1)|+|E(A_1,B_1)+E(A_1,B_0)|\leq 2 \tag{2.23}$$

[1] We also assume that they have *free will* to choose the settings they want and there is nothing which force them to choose certain setting during a run

[2] The form of triangle inequality used is $|x+(-y)|\leq |x|+|-y| \quad \forall\, x\in\mathbb{R}$.

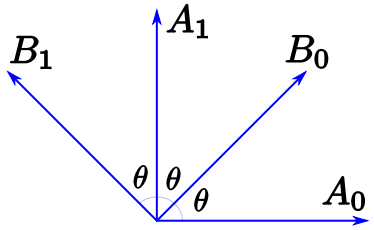

Figure 2.2: A simplest possibility for the four setting that Alice and Bob can choose to violate Bell inequality

Now, once again with the application of triangle inequality we arrive to the final result,

$$|E(A_0,B_0)-E(A_0,B_1)+E(A_1,B_1)+E(A_1,B_0)|\leq 2 \tag{2.24}$$

This can also be written in the standard form as

$$-2\leq E(A_0,B_0)-E(A_0,B_1)+E(A_1,B_1)+E(A_1,B_0)\leq 2 \tag{2.25}$$

To see if quantum mechanics violates this inequality, consider the state given in Eq. (2.19) and define Alice and Bob settings A_0 and B_0 as directions in the Bloch sphere given by $\hat{\sigma}_{A_0}=\vec{r}_{A_0}.\vec{\sigma}$ and $\hat{\sigma}_{B_0}=\vec{r}_{B_0}.\vec{\sigma}$ respectively. It can be shown that

$$E(A_0,B_0)=\langle\psi|\hat{\sigma}_{A_0}\otimes\hat{\sigma}_{B_0}|\psi\rangle=-cos\ (\theta_{A_0B_0}) \tag{2.26}$$

This will be easy to follow, if one notices that the state given in Eq. (2.19), is rotationally invariant and therefore one can rotate his reference frame such that $\vec{r}_{A_0}$ becomes the z-direction. Now, to calculate all the parameters in expression (2.24), consider the four setting A_0, A_1, B_0 and B_1 define as in Fig. 2.2. In this case expression (2.24) becomes

$$|-cos\ \theta+cos\ 3\theta-cos\ \theta-cos\ \theta|\leq 2. \tag{2.27}$$

The reader can check that for $\theta=45^\circ$ we will get $2\sqrt{2}$, much higher than what can be obtained by a local realist hidden variables theory. Note that this is the maximum violation that quantum mechanics can offer and it is known as Tsirelson bound [28]. Since the invention of Bell inequalities, numerous experiment have violated it, some can be found here [9–11; 13–15].

The proof that quantum mechanics is in conflict with local hidden variables assumption is known as Bell theorem and this particular form of the Bell inequality is called as CHSH–J. Clauser, M. Horne, A. Shimony and R. A. Holt–inequality [6].

2.8.1 Bell States

The state given in Eq. (2.19), is special in the sense that it maximally violates the Bell inequality shown in (2.25). Since we are dealing here with two qubit states and the relevant Hilbert space is 4-dimensional therefore one can easily find four states which not only violate (2.25) maximally but also form an orthonormal basis, these states are called *Bell states* and are as,

$$\begin{aligned}
|\Psi^-\rangle &= \tfrac{1}{\sqrt{2}}\left(|0\rangle_A \otimes |1\rangle_B - |1\rangle_A \otimes |0\rangle_B\right) = \tfrac{1}{\sqrt{2}}(|01\rangle - |10\rangle) \\
|\Psi^+\rangle &= \tfrac{1}{\sqrt{2}}\left(|0\rangle_A \otimes |1\rangle_B + |1\rangle_A \otimes |0\rangle_B\right) = \tfrac{1}{\sqrt{2}}(|01\rangle + |10\rangle) \\
|\Phi^+\rangle &= \tfrac{1}{\sqrt{2}}\left(|0\rangle_A \otimes |0\rangle_B + |1\rangle_A \otimes |1\rangle_B\right) = \tfrac{1}{\sqrt{2}}(|00\rangle + |11\rangle) \\
|\Phi^-\rangle &= \tfrac{1}{\sqrt{2}}\left(|0\rangle_A \otimes |0\rangle_B - |1\rangle_A \otimes |1\rangle_B\right) = \tfrac{1}{\sqrt{2}}(|00\rangle - |11\rangle)
\end{aligned} \tag{2.28}$$

where subscript A and B explicitly shows that these states are consisting of different parts. These states form an orthonormal basis for the state space of two qubits and have the property that the measurement of one qubit determines the value of the other qubit with probability equal to 1. Bell states are widely used in quantum information and communication protocols. We also used such states in all of our experiments. The next chapter will describe how one can produce and measure such states.

It should also be noticed that there are other entangled states which can violate Bell inequality though not maximally. Remarkably, some states do violate Bell inequality in a much clearer fashion, as discovered by L. Hardy [29] and presented in a very simple way in [30–32]. In the following we will describe it briefly.

2.8.2 Hardy's Proof of Non-locality

Suppose, like before, Alice can choose between two settings A_0 and A_1 to measure her dichotomic observables that can give outcomes ± 1. For simplicity we can denote these measurement settings and outcomes as 1 and 2, and 0 and 1 respectively. This scenario can be imagined as Alice has two boxes and she can choose to open one or the other, corresponding to which observable she want to measure, then getting outcome 0 or 1 could correspond to finding a box empty or full. Bob can also be considered to have similar boxes with setting $B_0 \to 3$ and $B_1 \to 4$. Then $P(0,1|i,j)$ can represents the probability of getting ith box empty and jth box full.

Now, suppose that the boxes are prepared such that,

$$\begin{aligned} P(1,1|1,4) &= 0 \\ P(1,1|2,3) &= 0 \\ P(0,0|2,4) &= 0 \end{aligned} \tag{2.29}$$

Then it is easy to see that assigning predetermined values[1] to the boxes implies that

$$P(1,1|1,3) = 0. \tag{2.30}$$

However, quantum mechanics can offer states such that Eq. (2.29) is true but not Eq. (2.30). For instance,

$$|\phi\rangle = N\left(|00\rangle - \alpha_A \alpha_B |aa\rangle\right) \tag{2.31}$$

where N is a normalization constant and,

$$\begin{aligned} |a\rangle &= \alpha_i^* |0\rangle + \beta_i |1\rangle \\ |b\rangle &= \beta_i^* |0\rangle - \alpha_i |1\rangle \end{aligned} \tag{2.32}$$

with inverse relations as,

$$\begin{aligned} |0\rangle &= \alpha_i |a\rangle + \beta_i |b\rangle \\ |1\rangle &= \beta_i^* |a\rangle - \alpha_i^* |b\rangle \end{aligned} \tag{2.33}$$

note that here * represent complex conjugation and $\langle a|b\rangle = 0$. Now one can calculate probabilities in (2.29) as,

$$\begin{aligned} P(1,1|1,4) = 0 \quad &\equiv \quad |\langle 1,b|\phi\rangle|^2 = 0 \\ P(1,1|2,3) = 0 \quad &\equiv \quad |\langle b,1|\phi\rangle|^2 = 0 \\ P(0,0|2,4) = 0 \quad &\equiv \quad |\langle a,a|\phi\rangle|^2 = 0 \end{aligned} \tag{2.34}$$

However, calculating $P(1,1|1,3) \equiv |\langle 1,1|\phi\rangle|^2$ gives $|-N\alpha_A\alpha_B\beta_A\beta_B|^2$, which should not be possible in local hidden variables model.

Another important state that we produced and used in our experiment is GHZ–Greenberger, Horne, Zeilinger–state [33]. Interestingly this state provides a direct–non-statistical contradiction–between EPR argument and quantum mechanics as we will see in the next section.

[1] Note that local Hidden variable in space-like separated case should correspond to predetermined values since once qubits are space-like separated they cannot influence each other and hence hidden variables are fixed.

2.9 GHZ State: Bell Theorem without Inequalities

Any state of the type

$$|GHZ\rangle = \frac{1}{\sqrt{2}} \left(|0\rangle^{\otimes N} + |1\rangle^{\otimes N} \right) \tag{2.35}$$

or its local rotations is known as *GHZ state*. Note that, $N \geq 3$ in the above equation. Evidently, it is a superposition of two completely distinct states, and hence sometimes also called *Schrödinger's cat state* [4]. To see how it leads to the contradiction with EPR argument we follow the lines given in [33], with an equivalent GHZ state given as,

$$|GHZ\rangle = \frac{1}{\sqrt{2}} \left(|0011\rangle + |1100\rangle \right). \tag{2.36}$$

A correlation function for this state, when measuring the individual qubits in the direction $\hat{n}_1, \hat{n}_2, \hat{n}_3$ and $\hat{n}_4$, (see appendix A), is given as,

$$\begin{aligned} E^{GHZ}(\hat{n}_1, \hat{n}_2, \hat{n}_3, \hat{n}_4) = & cos\ \theta_1\ cos\ \theta_2\ cos\ \theta_3\ cos\ \theta_4 \\ & - sin\ \theta_1\ sin\ \theta_2\ sin\ \theta_3\ sin\ \theta_4\ cos\ (\phi_1 + \phi_2 - \phi_3 - \phi_4) \end{aligned} \tag{2.37}$$

If we restrict the measurement directions $(\hat{n}_i)$, in the x-y plane i.e $\theta = \frac{\pi}{2}$ then this becomes

$$E^{GHZ}(\hat{n}_1, \hat{n}_2, \hat{n}_3, \hat{n}_4) = -cos\ (\phi_1 + \phi_2 - \phi_3 - \phi_4) \tag{2.38}$$

Now consider the cases

$$\text{When} \qquad \phi_1 + \phi_2 - \phi_3 - \phi_4 = 0 \implies E^{GHZ}(\hat{n}_1, \hat{n}_2, \hat{n}_3, \hat{n}_4) = -1 \tag{2.39}$$

$$\text{When} \qquad \phi_1 + \phi_2 - \phi_3 - \phi_4 = \pi \implies E^{GHZ}(\hat{n}_1, \hat{n}_2, \hat{n}_3, \hat{n}_4) = +1 \tag{2.40}$$

Now assuming that the outcomes of the measurements not only depends on the settings but also on the hidden variables λ, as we did in the derivation of Bell inequality and calling them as A, B, C and D respectively corresponding to the parties possessing these qubit, we get

$$\text{If} \qquad \phi_1 + \phi_2 - \phi_3 - \phi_4 = 0$$

$$\text{then} \qquad A(\lambda, \phi_1)\ B(\lambda, \phi_2)\ C(\lambda, \phi_3)\ D(\lambda, \phi_4) = -1 \tag{2.41}$$

$$\text{and If} \qquad \phi_1 + \phi_2 - \phi_3 - \phi_4 = \pi$$

$$\text{then} \qquad A(\lambda, \phi_1)\ B(\lambda, \phi_2)\ C(\lambda, \phi_3)\ D(\lambda, \phi_4) = +1 \tag{2.42}$$

There are numbers of possibility for the condition in Eq. (2.41), like

$$A(\lambda,0)\,B(\lambda,0)\,C(\lambda,0)\,D(\lambda,0) = -1 \tag{2.43}$$
$$A(\lambda,\phi)\,B(\lambda,0)\,C(\lambda,\phi)\,D(\lambda,0) = -1 \tag{2.44}$$
$$A(\lambda,\phi)\,B(\lambda,0)\,C(\lambda,0)\,D(\lambda,\phi) = -1 \tag{2.45}$$
$$A(\lambda,2\phi)\,B(\lambda,0)\,C(\lambda,\phi)\,D(\lambda,\phi) = -1 \tag{2.46}$$

Now, multiplying first three of these equation and noticing that $A(\lambda,\phi) = \pm 1 \implies |A(\lambda,\phi)|^2 = 1$ and same for B,C and D, and comparing the result with Eq. (2.46) we get

$$A(\lambda,2\phi) = A(\lambda,0) = \text{constant for all } \phi. \tag{2.47}$$

This innocent looking equation has big implications, for instance measuring this qubit in any direction, including 0 and π will give the same outcome! To further investigate the contradiction notice that the condition of Eq. (2.42) also implies that

$$A(\lambda,\phi+\pi)\,B(\lambda,0)\,C(\lambda,\phi)\,D(\lambda,0) = +1 \tag{2.48}$$

comparing it with Eq. (2.44) gives,

$$A(\lambda,\phi+\pi) = -A(\lambda,\phi) \tag{2.49}$$

which seems logical in physical respect but contradict with Eq. (2.47). This contradiction implies that local hidden variables (LHV) models cannot explain the strong correlation, shown in Eq. (2.39) and (2.40), that a GHZ state offers, assuming that all the four qubits are space-like separated and the parties can choose their measurements freely (i.e. assuming realism and free will). These states of affairs clearly demonstrate the non-locality of quantum mechanics and nature.

In the above analysis, $B(0)$ was never altered and therefore indicate that the GHZ argument can still be valid for 3 qubit GHZ state though cannot be run for a 2 qubit states[1] as, Bell himself has proposed a LHV model that can reproduced all the correlation observed when both qubit of a singlet state (like in Eq. (2.19)) are measured in $\hat{n}_1 = \hat{n}_2$ or $\hat{n}_1 = -\hat{n}_2$ basis [33].

In the end of this chapter we will look at another peculiar aspect of quantum mechanics that is known as contextuality. Interestingly, this weird aspect of quantum mechanics can be observed even without entanglement as Niels Bohr anticipated.

[1] Greenberger, Horne, Zeilinger (GHZ) were actually able to form a GHZ like argument for two qubits that were made entangled through entanglement swapping, therefore the experiment actually begins with four qubits [34].

2.10 Contextuality and Quantum Mechanics

In the last sections we saw that quantum mechanics exhibit non-local correlations between well separated subsystems. Interested reader can find an easy to take explanation of these thought experiments in [35; 36]. Here, in this section we are going to see another kind of weirdness of qunatum mechanics. If one assumes that quantum mechanics gives the correct description of the world then our world is contextual also. Meaning that, measurements in different order can lead to different outcomes. To define it more precisely, imagine three observables A, B and C such that A commutes with both B and C, but B and C do not commute. In this case a contextual theory will predict that measuring A together with B can lead to different outcome compared to measuring A together with C, or in other words, the outcome of observable A depends on the context in which it is measured. Explaining such behavior using the standard interpretation of quantum mechanics is simple, one can argue that, as the two operators (B and C) do not commute, so measuring A with B collapses the wave function in a different way compared to the collapse caused by the measurement of A with C.

In this thesis we are not concerned with the concept of contextuality, therefore I shall not go in details here. We just briefly describe how it arises in quantum mechanics, for this we follow the simple Hardy like proof given in [30] and experimentally realized in [37].

Consider five boxes that we call as box $1,2,3,4$ and 5. Either of these could be empty or full that we represents as 0 or 1 respectively. Now imagine that these boxes are prepared such that

$$P(0,1|1,2)+P(0,1|2,3)=1 \tag{2.50}$$

$$P(0,1|3,4)+P(0,1|4,5)=1 \tag{2.51}$$

where $P(0,1|i,j)$ represents the probability of getting ith box empty and jth box full. Note that according to Eq. (2.50) when box 2 is full then $P(0,1|2,3)=0$ and we must have $P(0,1|1,2)=1$ to satisfy the Eq. (2.50), i.e. box 1 must be empty, therefore both boxes cannot be full together i.e. $P(1,1|1,2)=0$. On the other hand when box 2 is empty then we must have Box 3 full or equivalently both boxes should not be empty together i.e. $P(0,0|2,3)=0$. Similarly, Eq. (2.51) implies that box 3 and 4 cannot be both full together and box 4 and 5 cannot be empty together i.e.$P(1,1|3,4)=0$ and $P(0,0|4,5)=0$.

Now assuming that the boxes states (full or empty) is predetermined or fixed before opening it, will lead to conclude that

$$P(0,1|5,1)=0 \tag{2.52}$$

However, this can be violated if one prepares a three level quantum system or a qutrit in the state given as,

$$|\psi\rangle = \frac{1}{\sqrt{3}} \left(|0\rangle + |1\rangle + |2\rangle \right) \tag{2.53}$$

and represent the projectors of the following vectors as the dichotomic observables corresponding to measuring if a box is full or empty.

$$\begin{aligned} |v_1\rangle &= \frac{1}{\sqrt{3}} \left(|0\rangle - |1\rangle + |2\rangle \right) \\ |v_2\rangle &= \frac{1}{\sqrt{2}} \left(|0\rangle + |1\rangle \right) \\ |v_3\rangle &= |2\rangle \\ |v_4\rangle &= |1\rangle \\ |v_5\rangle &= \frac{1}{\sqrt{2}} \left(|1\rangle + |2\rangle \right) \end{aligned} \tag{2.54}$$

Note that each of the vectors given in the above list is orthogonal to its adjacent vectors, and hence their projectors are compatible. To see that the state given in Eq. (2.53) obeys the preparation conditions given in Eq. (2.50), (2.51), notice that these vectors are constructed in a way that the projector or observable represented by $|v_{i+1}\rangle\langle v_{i+1}|$ has eigenvectors $|v_{i+1}\rangle$ and $|v_i\rangle$ with eigenvalues 1, and 0 respectively, since $|v_{i+1}\rangle$ and $|v_i\rangle$ are orthogonal. Therefore,

$$P(0,1|i,i+1) = |\langle v_{i+1}|\psi\rangle|^2 \tag{2.55}$$

where $i+1 = 1$, when $i = 5$. This way we actually introduce a context to each of our measurements, for instance, the state (full or empty) of the Box 2 can be measured together with the state of box 1 or box 3 corresponding to the choice of the operator $|v_2\rangle\langle v_2|$ or $|v_3\rangle\langle v_3|$ respectively.

Now, it is easy to see that our state Eq. (2.53), fulfills the preparation conditions Eq. (2.50), (2.51), however

$$P(0,1|5,1) = |\langle v_1|\psi\rangle|^2 = \frac{1}{9} \tag{2.56}$$

This is in clear contradiction to Eq. (2.52) and shows that we cannot preassign values to outcomes (realism), or measuring one observable in the context of different observables is not equivalent (contextuality). Another important point is that the violation of Bell inequalities could also be considered as the violation of non-contextuality inequalities, since in order to violate a Bell inequality Alice needs to perform her measurement in two different contexts,

namely which one of the two possible observables Bob decided to measure i.e. correlations of the types $E(A_0,B_0)$ or $E(A_0,B_1)$. Due to this contextuality is considered as a more general property of nature, whereas Bell inequality violation is just a specific example of it. Moreover, in a way Bell tests are much cleaner, at least experimentally, since locality can be arranged and seems to ensure context-independence that has been a problem in many experiments trying to verify contextuality of quantum mechanics. Nevertheless, violation of a Bell inequality implies non-locality provided that we don't want to give up realism, due to this reason in almost all interpretations of quantum mechanics one has to sacrifice one of these (realism or locality) in order to keep the other.

The proof presented here is a particular violation of famous contextuality inequality know as KCBS inequality due to its inventors Alexander A. Klyachko, M. Ali Can, Sinem Binicioğlu , and Alexander S. Shumovsky, given as,

$$\begin{aligned} &P(0,1|1,2)+P(0,1|2,3)+P(0,1|3,4)+P(0,1|4,5) \\ &+P(0,1|5,1) \overset{\text{NCHV}}{\leq} 2 \overset{\text{QM}}{\leq} \sqrt{5} \approx 2.236. \end{aligned} \tag{2.57}$$

here NCHV and QM represent upper bound for non-contextual hidden variables theories and quantum mechanics respectively.

3. Experimental Background

All the experiments presented in this thesis are realized using photonic qubits and optical setups. To facilitate understanding of these experiments, a brief introduction to the experimental background will be given in this chapter.

In the previous chapter, a 2-D quantum system or a qubit is introduced without referring to any physical system for its realization. Here, we present a polarization implementation of the qubit together with its manipulation techniques using optical components. Then the main work horse, a setup producing polarization entangled photon's pairs will be explained. In the end we will also describe how such a two-photon source can be used to build a setup producing four-photon GHZ entanglement states.

3.1 Qubits: A Polarization Implementation

Any 2-dimensional quantum system–or part of a high dimensional system when it is effectively decoupled from the rest–can be used to realize a qubit e.g. nuclear spin, trapped ion, quantum dot, electron spin etc. In our experiments we used photon's polarization to implement a qubit. One might suspect that being a spin-1 particle it could have three possible states corresponding to the eigenvalues -1, 0 and $+1$. However, due to the consequences of gauge freedom only transverse polarized photons can exist as free observable particles. Thus, one can effectively treat polarization of every single photon as a 2-level quantum system, which is a fruitful realization of a qubit.

This implementation offers a number of advantages, for instance, polarized photons can be easily generated, measured, prepared to exhibit quantum superposition and manipulated using wave-plates. Moreover photons are chargeless particles that do not interact with each other or with the environment easily. This makes them robust against decoherence and ideal for communication purposes.

Now being a qubit, all possible states or state space of a photon's polarization will be the Bloch sphere described in the previous chapter. In this case, the eigenvectors of $\hat{\sigma}_z$ operator are also known as horizontal and vertical polarizations that we represent by the state vectors $|H\rangle$ and $|V\rangle$ respectively. These two vectors define our default or computational basis. Table 3.1 gives the eigen-

Table 3.1: Pauli matrices with their eigenvectors and eigenvalues.

Observable	Eigenvalues	Eigenvectors
$\hat{\sigma}_z$	$+1$	$\|H\rangle$
	-1	$\|V\rangle$
$\hat{\sigma}_x$	$+1$	$\|+\rangle = \frac{1}{\sqrt{2}}(\|H\rangle + \|V\rangle)$
	-1	$\|-\rangle = \frac{1}{\sqrt{2}}(\|H\rangle - \|V\rangle)$
$\hat{\sigma}_y$	$+1$	$\|L\rangle = \frac{1}{\sqrt{2}}(\|H\rangle + i\,\|V\rangle)$
	-1	$\|R\rangle = \frac{1}{\sqrt{2}}(\|H\rangle - i\,\|V\rangle)$

vector and eigenvalues of all three mutually unbiased bases that correspond to the three orthogonal axes on the Bloch ball.

The reader should note here that with the definition of $|L\rangle$ we have chosen the following convention, if the electric field vector rotating counter clockwise in time while looking towards the source then the light is called *left circularly polarized*[1] and given by the equation shown in the above table. This convention also defines the sense of positive rotation for our wave-plates or all other such components.

3.2 Manipulation of Polarization Qubit

This section gives a brief description of the main optical components that we used to alter the polarization state of photons in our experiments. The simplest among these is a polarizer.

3.2.1 Polarizers

An ideal *polarizer* is an optical component that lets through only a specific polarization. Therefore, it can change mixed states to pure states. In our experiments we used absorptive linear polarizers. These are the polarizers that absorb all other polarizations while passing through only a particular linear polarization. In the lab we used the convention that when a polarizer is at 0°, it only lets through vertical polarization and hence its action can be represented

[1] i.e. polarization will be given by left or right hand rule while thumb is point towards the source. This is called “from the point of view of receiver" convention and is opposite to what is usually used in particle physics.

by

$$Pol\,(\theta = 0) = \begin{pmatrix} 0 & 0 \\ 0 & 1 \end{pmatrix}. \tag{3.1}$$

A linear polarizer can be used to prepare photons in any pure state on the z-x plane of the Bloch sphere by properly selecting its orientation that we denote by an angle θ. In this case its matrix representation can be obtained by rotating our lab frame to a frame in which the polarizer is at 0° where its action is given by Eq. (3.1), and then rotate back to the lab frame. Mathematically this will give

$$Pol(\theta) = R(-\theta)\; Pol(\theta)\; R(\theta). \tag{3.2}$$

Where $R(\theta)$ represents passive rotation in counter clockwise direction i.e.

$$R(\theta) = \begin{pmatrix} \cos\theta & \sin\theta \\ -\sin\theta & \cos\theta \end{pmatrix}. \tag{3.3}$$

Now, using Eqs. (3.1) and (3.3) in Eq. (3.2), one can calculate easily that the action of a polarizer at an angle θ from vertical, in the lab frame will be

$$Pol(\theta) = \begin{pmatrix} \sin^2\theta & -\sin\theta\,\cos\theta \\ -\sin\theta\,\cos\theta & \cos^2\theta \end{pmatrix}. \tag{3.4}$$

Polarizers can be made of thin films of some crystal like Tourmaline, Herapathite etc., or with elongated metallic nano-particles embedded on glass substrates. In the latter case, they can have high extinction ratio and wide working wavelength range. The polarizers used in experiments are of this type.

3.2.2 Wave-Plates

Wave-plates or *phase retarders* are the most important components for manipulating photon's polarization. These are the optical devices with which– by choosing their appropriate orientations perpendicular to the transmitting beam–one can transform a polarization state to another one. In the simplest case, when a wave-plate oriented at an angle $\theta = 0^{\circ}$, it produces a phase shift (ϕ) between horizontal and vertical polarizations and therefore its action on the input state can be represented by the matrix

$$W(\theta = 0, \phi) = \begin{pmatrix} 1 & 0 \\ 0 & e^{i\phi} \end{pmatrix}. \tag{3.5}$$

There are two main types depending on whether $\phi = \frac{\pi}{2}$ or $\phi = \pi$, which are known as *Quarter wave-plates* (QWP) and *Half wave-plate* (HWP) respectively. Note that with a suitable combination of these wave-plates one can realize any single qubit quantum gate [38].

The wave-plates used in the experiments are made of a birefringent material known as *Quartz*. Remember that the refractive index of a birefringent material depends on the polarization and propagation direction of the light in the material. Besides its immense availability and optical properties, quartz has two good characteristics which make it the first choice for constructing wave-plates. Firstly, it is a uniaxial crystal, meaning that there is a special direction in the crystal such that light propagating in this direction with any polarization experiences only one refractive index. This particular direction is called optical axis. There is only one such direction therefore the material is called uniaxial. On the other hand, if light propagates in a direction perpendicular to the optical axis it encounters two different refractive indices according to the polarization (horizontal or vertical), and the second good thing about quartz is that there is not a big difference between these refractive indices, which means a longer length of the material will be required to create a desire phase shift, this makes the quartz crystals a more practical choice.

Therefore, to construct a wave-plate, one can cut a quarts slice in a way that light propagate perpendicular to the optical axis when transmitting through it, as shown in the Fig. 3.1. In this case phase shift ϕ introduced between horizontal and vertical polarization will be

$$\phi = 2\pi \frac{\Delta n}{\lambda} t. \tag{3.6}$$

where t is the thickness of the crystal that light traverse and Δn represents birefringence or difference between the two refractive indices i.e. $\Delta n = n_e - n_o$. For quartz, $n_e > n_o \implies \Delta n > 0$, therefore quartz is a positive uniaxial crystal and in this case optical axis is actually slow axis. This also means that $\phi > 0$

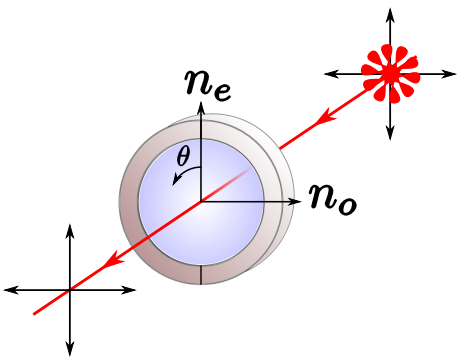

Figure 3.1: Fast and slow axis of a quartz wave-plate marked as n_o and n_e respectively. The small arrow explains the sense of positive rotation in the lab frame.

and hence we can call our wave-plates as phase retarders, since the time-term has negative sign in the wave equation.

In the lab we use the convention that $\theta = 0^\circ$ or no rotation corresponds to slow axis vertical and a wave-plates action in this case is given by Eq. (3.5). Matrix representation for arbitrary orientation angle θ, can be obtained by rotating lab frame to the frame where wave-plate is at 0°, get the phase shift as in Eq. (3.5) and then rotate back to the lab frame again, as we did in case of polarizer. One can check that this will lead to

$$W(\theta,\phi) = \begin{pmatrix} \cos^2\theta + e^{i\phi}\sin^2\theta & \sin\theta\ \cos\theta(1-e^{i\phi}) \\ \sin\theta\ \cos\theta(1-e^{i\phi}) & \sin^2\theta + e^{i\phi}\cos^2\theta \end{pmatrix} \tag{3.7}$$

Therefore, matrix representations of HWP and QWP will be

$$W(\theta,\pi) = \mathrm{HWP}(\theta) = \begin{pmatrix} \cos(2\theta) & \sin(2\theta) \\ \sin(2\theta) & -\cos(2\theta) \end{pmatrix} \tag{3.8}$$

$$W(\theta,\frac{\pi}{2}) = \mathrm{QWP}(\theta) = \frac{(1+i)}{2}\begin{pmatrix} 1-i\ \cos(2\theta) & -i\ \sin(2\theta) \\ -i\ \sin(2\theta) & 1+i\ \cos(2\theta) \end{pmatrix} \tag{3.9}$$

Note that $\mathrm{HWP}(\theta)$ is not only unitary but Hermitian also, this makes it self-inverse.

Some useful configurations of these wave-plates with which we can rotate a given input state along x, y and z-axis on the Bloch sphere are as follows.

- Rotation along x-axis,

$$\mathrm{QWP}(\frac{\pi}{2})\ \mathrm{HWP}(\theta)\ \mathrm{QWP}(\frac{\pi}{2}) = \begin{pmatrix} \cos(2\theta) & -i\sin(2\theta) \\ -i\sin(2\theta) & \cos(2\theta) \end{pmatrix} \tag{3.10}$$

- Rotation along y-axis,

$$\mathrm{HWP}(0)\ \mathrm{HWP}(\theta) = \begin{pmatrix} \cos(2\theta) & \sin(2\theta) \\ -\sin(2\theta) & \cos(2\theta) \end{pmatrix} \tag{3.11}$$

- Rotation along z-axis,

$$\mathrm{QWP}(\frac{\pi}{4})\ \mathrm{HWP}(\theta)\ \mathrm{QWP}(\frac{\pi}{4}) = \begin{pmatrix} 1 & 0 \\ 0 & e^{i(4\theta+\pi)} \end{pmatrix} \tag{3.12}$$

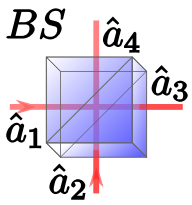

Figure 3.2: Beam splitter (BS).

Where unimportant overall phases have been neglected. Also, note that these configurations are practically simpler but not unique. Moreover, HWP($\frac{\pi}{8}$), HWP($\frac{\pi}{4}$) and HWP(0) can be used to realized Hadamard, Pauli-X(bit flip) and Pauli-Z gates respectively, whereas one way to realize Pauli-Y gate is QWP($\frac{\pi}{2}$) HWP($-\frac{\pi}{4}$) QWP(0).

3.2.3 Beam Splitters

Beam splitter (BS) is an optical device that can split an input light field into two or more output fields. Conversely, it can also be used to blend two or more fields to get a single or multiple outputs and therefore, it is an essential component for interferometry.

BSs are available in different types and shapes depending on their working principle and application's demands. The most common types are beam splitter plates and cubes. In our experiments we used cubic BSs, which are made of two right angled prisms glued together. One of these prism's hypotenuse surface has dielectric coating which determines the splitting ratio. Also, in some cases this prism should preferentially be used as input and therefore has a small dot to distinguish it from the other.

To write the transformation matrix of a lossless BS, consider two inputs and two outputs fields on the ports of a BS as shown in the Fig. 3.2. Here, we represent amplitude of individual field modes by boson annihilation operators $\hat{a}_1$, $\hat{a}_2$, and $\hat{a}_3$, $\hat{a}_4$ for inputs and outputs respectively [39; 40]. In general a lossless BS transforms these inputs to the outputs as

$$\begin{pmatrix} \hat{a}_1 \\ \hat{a}_2 \end{pmatrix} \rightarrow \begin{pmatrix} A_{00} & A_{01} \\ A_{10} & A_{11} \end{pmatrix} \begin{pmatrix} \hat{a}_3 \\ \hat{a}_4 \end{pmatrix}. \tag{3.13}$$

Where A_{ij} are elements of the matrix $\hat{A}$ bearing this transformation. Note that, operators corresponding to individual field modes should satisfy commutation relation $[\hat{a}_i, \hat{a}_j^\dagger] = \delta_{ij}$. A standard way to fulfill this requirement is to assume that the transformation is unitary since commutators are preserved by unitary transformations. Therefore, with this condition matrix $\hat{A}$ is unitary and can be

parameterized as

$$A = e^{i\phi_0} \begin{pmatrix} e^{i\phi_1}\cos\theta & e^{i\phi_2}\sin\theta \\ -e^{-i\phi_2}\sin\theta & e^{-i\phi_1}\cos\theta \end{pmatrix}. \tag{3.14}$$

Here, $e^{i\phi_0}$ is global phase and can be neglected without loss of generality. Hence, a lossless BS transforms two input modes polarized in the same direction to the output modes according to

$$\begin{pmatrix} \hat{a}_1 \\ \hat{a}_2 \end{pmatrix} \rightarrow \begin{pmatrix} e^{i\phi_1}\cos\theta & e^{i\phi_2}\sin\theta \\ -e^{-i\phi_2}\sin\theta & e^{-i\phi_1}\cos\theta \end{pmatrix} \begin{pmatrix} \hat{a}_3 \\ \hat{a}_4 \end{pmatrix}. \tag{3.15}$$

Moreover, $\tau = \cos^2\theta$, and $r = 1 - \tau = \sin^2\theta$ can respectively be recognized as transmissivity and reflectivity of the BS. Therefore, for a 50–50 BS we will have

$$\begin{pmatrix} \hat{a}_1 \\ \hat{a}_2 \end{pmatrix} \rightarrow \frac{1}{\sqrt{2}} \begin{pmatrix} e^{i\phi_1} & e^{i\phi_2} \\ -e^{-i\phi_2} & e^{-i\phi_1} \end{pmatrix} \begin{pmatrix} \hat{a}_3 \\ \hat{a}_4 \end{pmatrix}. \tag{3.16}$$

In our experiment we used 50–50 BSs which transform inputs with a given polarization–say, horizontal–to the outputs according to the above expression. Modes of the field amplitudes with orthogonal polarization will also transform in a similar manner, however with different phases in general. That is, with two orthogonal polarizations incident on a BS, there will be four kinds of phases involved. One of these can be taken as a reference and then other three can be compensated by phase-plates, which are usually QWP or HWP at 0° and tilted–not rotated–along vertical direction.

In case of a symmetric lossless 50–50 BS (i.e. $\phi_1 = 0$ and $\phi_2 = \frac{\pi}{2}$) we can write this transformation as

$$\begin{pmatrix} \hat{a}_1 \\ \hat{a}_2 \end{pmatrix} \rightarrow \frac{1}{\sqrt{2}} \begin{pmatrix} 1 & i \\ i & 1 \end{pmatrix} \begin{pmatrix} \hat{a}_3 \\ \hat{a}_4 \end{pmatrix}. \tag{3.17}$$

3.2.4 Polarizing Beam Splitters

Polarizing beam splitter (PBS) is a similar sort of optical component like a BS described in the last section, however, a PBS splits or blends input fields in a way which depends on their polarizations.

PBSs used in our experiments are cubic PBSs with two inputs and two outputs ports and completely polarizing. That is, in ideal case, they perfectly transmit horizontally polarized light while reflecting vertical polarization. Therefore, if desired, they can also be used like a polarizer. Moreover, this way they can map polarization to path, since horizontal and vertical polarization takes different paths after passing through a PBS. In this respect, a PBS

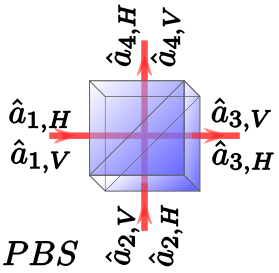

Figure 3.3: Polarization Beam-splitter cube.

can be used to perform $\hat{\sigma}_z$ measurement also, since its output ports correspond to eigenvectors $|H\rangle$ and $|V\rangle$.

One can use transformation given in Exp. (3.15) to write PBS's transformation explicitly, where for horizontal polarization we have $\theta = 0$ and for vertical polarization $\theta = \frac{\pi}{2}$.

$$\begin{pmatrix} \hat{a}_{1,H} \\ \hat{a}_{2,H} \end{pmatrix} \rightarrow \begin{pmatrix} e^{i\phi_1} & 0 \\ 0 & e^{-i\phi_1} \end{pmatrix} \begin{pmatrix} \hat{a}_{3,H} \\ \hat{a}_{4,H} \end{pmatrix} \tag{3.18}$$

$$\begin{pmatrix} \hat{a}_{1,V} \\ \hat{a}_{2,V} \end{pmatrix} \rightarrow \begin{pmatrix} 0 & e^{i\phi_2} \\ -e^{-i\phi_2} & 0 \end{pmatrix} \begin{pmatrix} \hat{a}_{3,V} \\ \hat{a}_{4,V} \end{pmatrix} \tag{3.19}$$

Note that like a BS we have an extra phase in this case also–while using both of the input ports with arbitrary polarization–which can easily be compensated by a phase plate at one of the outputs. However, in most of the cases this is not required.

3.2.5 Optical Fibers

In all of our experiments whenever possible, we transmit photons from one place to the other via propagating them through the air, since it is not birefringent and losses are negligible. However, this is not always possible; in such cases optical fibers are used.

Optical fibers are thin tubes that are not necessarily hollow from inside and usually made of silica. There are two distinguishable regions in a fiber, known as core and cladding. The core is the central region of a fiber and has slightly higher refractive index than the cladding that surrounds the core. Due to this refractive index difference total internal reflection is possible and therefore once light inserted into the fiber core it can remain there and may reach to the other end easily.

In these experiments we used two types of fibers; *single mode fibers* and *multi-mode fibers*. As the name implies, single mode fibers have small core

size which only allow the propagation of the first mode and therefore are perfect for mode selection. Also, because of their small core size, coupling light into these fibers is much harder. We used these fibers for mode selection and to transport photons before polarization measurement. Since silica can becomes slightly birefringent under stress and bends, therefore one has to be careful with these fibers, they should not move or stressed during operation. Nevertheless, when photons propagate through these fibers, their polarization is altered and has to be compensated. This is usually accomplished through manual polarization controllers.

In our experiments we used three pads homemade polarization controllers. Each of these pads has one-turn, two-turns and one-turn loop of the fiber such that they can act like QWP, HWP and QWP respectively and therefore, should be able to undo any polarization rotation. However, it is quite hard by only using polarization controller. Nonetheless, it becomes easy if one uses a phase plate together with it.

On the other hand, we used multi-mode fibers when we need to transport photons but we don't care about its polarization e.g. when bringing them to the detectors. Multi-modes fiber have comparably bigger cores and offer several modes. Multi-mode fiber used in these experiments had core size of about 50 micrometers.

3.2.6 Single Photon Detectors

For the detection of single photons we used silicon-based *avalanche photodiodes* (APD). These detectors were operated in Geiger mode, a mode where they can continuously detect photons, meaning that no trigger pulses are needed. In this mode, APDs are reverse biased well above the breakdown voltage and to avoid high current flow a special quenching circuit is used. Whenever a photon is absorbed in the sensitive region it produces an electron-hole pair which due to high electric field creates many more electro-hole pairs on their way. This leads to abruptly high avalanche current that can be easily detected. This detection reduces the biased voltage that in turn removes the electron-holes pairs or quenches the circuit. Then the bias can be increased again to make the APD ready for the next detection.

Sometimes thermal excitations can lead to the generation of a single electron-hole pair which through avalanche mechanism abruptly triggers the device on and hence results in a false detection, this type of detections often refers as dark counts.

The detectors that we used for the experiments had detection efficiencies of about 55%. Dead time of around 50 nsec and TTL output signal with 20 nsec width.

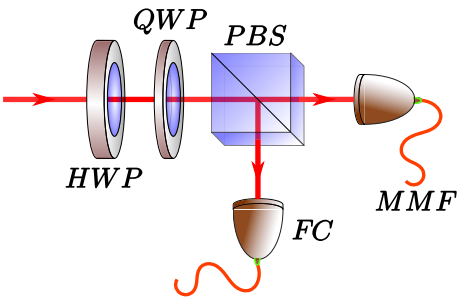

Figure 3.4: A Polarization Analyzer, used to measure photons polarization in different bases.

3.2.7 Polarization Analysis

As mentioned earlier one of the advantages of implementing qubit with the photon's polarization is that it can be simply measured by *polarization analyzer*, an optical device consists of wave-plates and/or polarizers. In our experiments we used a PBS together with wave-plates to analyze photon's polarization. By only using a PBS one can perform $\hat{\sigma}_z$ measurement. To measure the states in other bases we used the fact that a combination of HWP and a QWP can rotate $|H\rangle$ to any other pure qubit state [38], or conversely any pure qubit state can be rotated to $|H\rangle$ using these plates. Therefore, the configuration of the HWP, QWP and PBS–as shown in Fig. 3.4–can be used to analyze polarization state of a photon in any bases. Different settings of HWP and QWP leading to the projection of a given state onto the eigenvectors of Pauli matrices are given in table 3.2.

Table 3.2: Settings of HWP and QWP, with a configuration shown in Fig. 3.4, that can map output ports of a PBS to the projectors formed by the eigenvectors of Pauli matrices.

Projections	**HWP @**	**QWP @**	**PBS Output Port**
$\|H\rangle\langle H\|$	0°	0°	H
$\|V\rangle\langle V\|$	0°	0°	V
$\|+\rangle\langle +\|$	22.5°	0°	H
$\|-\rangle\langle -\|$	22.5°	0°	V
$\|L\rangle\langle L\|$	0°	-45°	H
$\|R\rangle\langle R\|$	0°	-45°	V

When a photon traverses through the analyzer–a combination of HWP, QWP and PBS–then its state is projected onto a state given by the specific setting of these wave-plates and therefore after the PBS the polarization state of a photon is not important. The purpose of the fiber coupler mark as FC in the figure is just to bring these photons to the single photon detectors (SPDs), and thus it can be done via multi-mode fibers.

3.3 Polarization Entangled Photons Source

In each of the experiments described here, we used one or more sources that produce polarization entangled photons pairs. These pairs are first generated through a non-linear process called *spontaneous parametric down conversion* (SPDC), and then entangled with an optical setup that will be described in this section. The main advantage of using SPDC process is that it always produces photons in pair, which are correlated and can easily be entangled. The first stage of building such a polarization entangled photons source is preparation of the pump laser.

3.3.1 Preparation of the Pump Laser

Sources used in all the experiments create polarization entangled photon pairs centered at 780*nm*. To generate such pairs we started with a tunable mode-locked Ti:Sapphire laser, producing around 140 femto-second long pulses with a repetition rate of 80MHz. The laser was set at 780*nm* and yield ∼8*nm* spectral width. The output was horizontally polarized with an available average power of ∼4W. The laser's beam quality was very good giving M^2 factor very close to be 1.

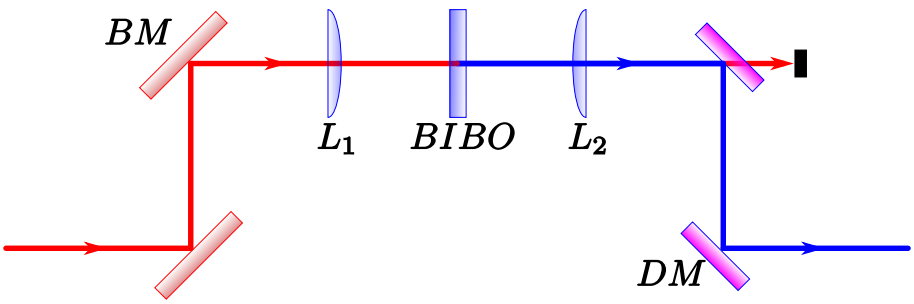

Figure 3.5: Preparation of pump laser for SPDC at 390nm, through SHG via BIBO crystal. L_1 and L_2 are lenses, whereas BM and DM are broadband and dichroic mirrors respectively.

This laser beam is then focused with a 100mm focal length lens onto a 1mm thick non-linear crystal "Bismuth triborate" (BiB_3O_6)–that usually called BIBO–for second harmonic generation(SHG) or frequency doubling. This process yields vertically polarized ultraviolet (UV) pulses with around 1.5W average power, leading to the conversion efficiency of 37.5%. The spectral width was about $1.1nm$ centered at $390nm$. Moreover, due to the walk-off in BIBO crystal beam quality was reduced and gave $M^2 = 1.70$ and $M^2 = 1.25$ along horizontal and vertical directions respectively i.e. this process rendered the beam shape elliptical. This beam was then collimated again using 100mm focal length lens as depicted in Fig. 3.5.

These collimated UV pulses contained some residual $780nm$ pump which is really crucial to eliminate since it can mixed up with the down-converted light and reduce the entanglement visibility. To remove this noise a series of *dichroic mirrors* is used. These mirrors are made to reflect a band of frequencies around $390nm$ with high efficiency, while keeping the transmission very high for $780nm$. Also, they are non-absorbing with good surface quality; this assures long lasting operation without burning even with high intensity UV light. As a result one can attenuate undesired frequencies $>100dB$ easily with few mirrors. Nevertheless, a non-collinear SPDC configuration is used, as described in the next section, which further decreases the chance of getting a pump photon in the down-conversion path.

3.3.2 Spontaneous Parametric Down-conversion (SPDC)

A very efficient and common technique presently used to generate entangled photons is spontaneous parametric down conversion (SPDC), where one exploits non-linear response of the dielectric polarization of the optical material under influence of strong light field. Since, with sufficiently high light intensity dielectric polarization is not any more proportional to electric field of the incident light, instead it is given by the relation

$$P_i = \varepsilon_0 \sum_{j=1}^{3} \chi^{(1)}_{jk} E_j + \varepsilon_0 \sum_{j,k=1}^{3} \chi^{(2)}_{jkl} E_j E_k + \varepsilon_0 \sum_{j,k,l=1}^{3} \chi^{(3)}_{jklm} E_j E_k E_l .... \qquad (3.20)$$

Here P is dielectric polarization density (i.e. average dipole moment per unit volume), ε_0 is vacuum permittivity, and χ is optical susceptibility tensor. When the interacting material have a large second order non-linearity ($\chi^{(2)}$), there is a probability–proportional to $\chi^{(2)}$–that a pump photon may split into two photons with lower energy, usually called *signal* and *idler*. Note that the conversion is spontaneous, and material role is passive–i.e. no energy is exchanged–hence the name "spontaneous parametric down-conversion". Thus, momentum

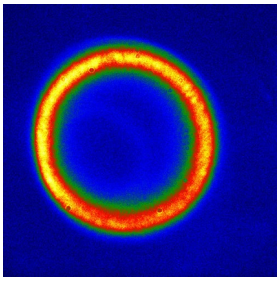

Figure 3.6: Type I spontaneous parametric down conversion in BBO.

and energy of the photons should be conserved by their own, implying that

$$\vec{k_p} = \vec{k_s} + \vec{k_i} \qquad , \qquad \omega_p = \omega_s + \omega_i. \tag{3.21}$$

Where the subscripts p, s and i refer to pump, signal and idler respectively. These are often called phase matching conditions. Note that, due to these conditions down-converted photon have strong correlations and hence can be entangled in a number ways e.g. polarization, time, path, angular momentum etc.

In this thesis we are only concerned with photons entangled in polarization and with degenerate energies i.e. $\omega_s = \omega_i$. There are a number of possible configurations, types and material for obtaining this through SPDC. We used a non-linear crystal called Beta-Barium Borate ($\beta - BaB_2O_4$), also known as BBO. It is a uniaxial crystal and can fulfill phase matching conditions (Eq. (3.21)) with required degeneracy in two ways that are known as type I and type II. In type I an extraordinary polarized pump photon splits into two ordinary polarized signal and idler, that appear in a conical pattern. A real photograph taken by a single photon sensitive camera is shown in Fig. 3.6. We are not much concerned with this type here and hence do not go in details.

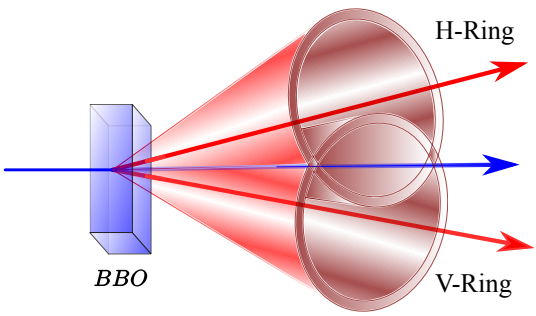

Figure 3.7: Type II spontaneous parametric down conversion in non-colinear configuration.

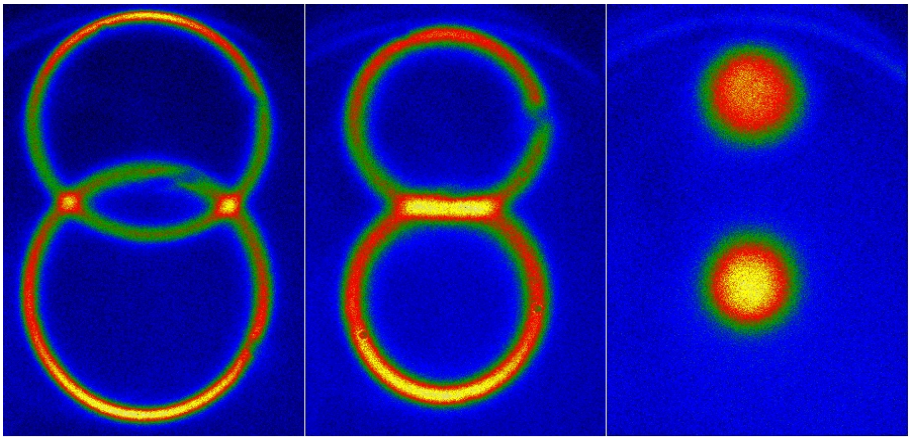

Figure 3.8: Different configuration in type II SPDC (a) Non-collinear. (b) Collinear. (c) Beam-like.

In type II version, an extraordinary polarized pump photon splits into an ordinary and an extraordinary polarized signal and idler, that in this case, emerge as individual cones as shown in Fig. 3.6. There are actually three different configurations with which one can obtain degenerate correlated photons in type II version, these are known as *non-collinear*, *collinear*, and *beam like*. A real photograph of all three configurations is shown in Fig. 3.8. Sources used in the experiments are built in the non-collinear configuration shown in Fig. 3.7 or Fig. 3.8(a), which was first implemented in [41].

In type II non-collinear case it is easy to see how the entanglement arises. Note that, upper and lower rings in Fig. 3.8 (a) have opposite polarizations that can be made to coincide with horizontal and vertical polarizations in the lab frame. Now, if one couples only a single mode centered in each of the crossing, then these photons should reveal opposite polarizations i.e. if the photon from first crossing is horizontally polarized then the photon coming from the other crossing, should have vertical polarization. Moreover, this will be true in any basis. If we also assume here that except polarization, these photons are indistinguishable in all other degrees of freedom, then as such these photons are entangled. Mathematically, if we denote amplitude of each of the field modes by the operators $\hat{a}$ and $\hat{b}$ then the simplified interaction Hamiltonian can be written as

$$\hat{H}_{int} = \kappa e^{i\phi}(\hat{a}_H^\dagger \hat{b}_V^\dagger - \hat{a}_V^\dagger \hat{b}_H^\dagger) + \kappa e^{-i\phi}(\hat{a}_H \hat{b}_V - \hat{a}_V \hat{b}_H) \tag{3.22}$$

Note that here the pump field is assumed to be intense and hence described classically by a real valued coupling constant κ proportional to the pump intensity and $\chi^{(2)}$, and ϕ is a general phase between the two processes [42; 43].

Acting with the time evolution operator $\hat{U} = e^{i\hat{H}t/\hbar}$ on the vacuum state leads to

$$|\psi\rangle \propto \sum_{n=0}^{\infty} (\tanh\tau)^n \sum_{m=0}^{n} (-1)^m |(n-m)_H, m_V\rangle |m_H, (n-m)_V\rangle. \tag{3.23}$$

Here $\tau = \kappa t/\hbar$, and the numbers $(n-m)$ and m in the first ket with subscripts H and V represent numbers of photons in mode $\hat{a}$ with corresponding polarization, whereas second ket represent photons in mode $\hat{b}$. Here we are only interested in the case when $n = 1$, putting this value in the above expression gives

$$|\psi\rangle \propto (\tanh\tau)(|1_H, 0_V\rangle|0_H, 1_V\rangle - |0_H, 1_V\rangle|1_H, 0_V\rangle) \tag{3.24}$$

Now, a normalized state with zero-photon modes suppressed can be made to give singlet state that can be written in a standard way as,

$$|\Psi^-\rangle = \frac{1}{\sqrt{2}} (|H\rangle|V\rangle - |V\rangle|H\rangle). \tag{3.25}$$

However, after emission due to the birefringence of the crystal both photons take slightly different path and speed, according to their polarization to traverse through the crystal and hence becomes distinguishable. To circumvent this problem one has to compensate for this spatial and temporal walk-offs as discuss in the next section.

3.3.3 Walk off compensation

As mentioned earlier, in the used type II configuration pump beam is extraordinary polarized and hence when traversing through the BBO crystal even with normal incident it deviates from the straight path as show in the Fig.3.9 with blue line. This deviation is termed as spatial walk-off. At 390*nm* in the phase matching direction this walk-off angle is about 77.14*mrad*. A pump photon may down-convert at any place along this path. Moreover, signal and idler beams thus produced will have a different wave-length (780*nm*) and therefore will take different paths and speeds according to their polarizations. Ordinary polarized down-converted beam will obey Snell's law and hence will not deviate from the straight path in this case–as shown in the Fig.3.9 with red arrows–though it will lead the pump beam due to lower group index. On the other hand, down-converted beam with extraordinary polarization will suffer from spatial walk-off, which is around 72.59*mrad* in this case, and hence will follow the pump beam with slight deviation and will be the fastest compare to both pump or ordinary polarized down-converted beam. This speed difference will lead to the temporal mismatch in the down-converted beams and is often referred as temporal walk-off.

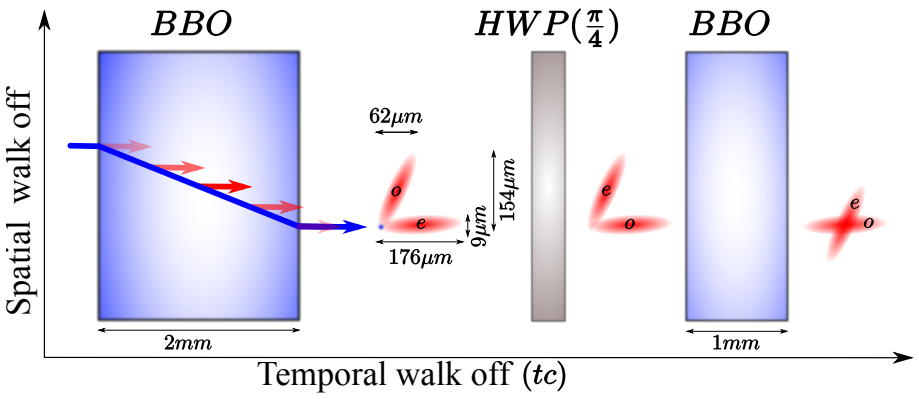

Figure 3.9: Effect of temporal and spatial walk-offs on the down-converted beams. This picture is approximate and not drawn to scale.

Fig. 3.9 depicts approximate spatial and temporal walk-offs with respect to the pump, which is shown as blue dot. In this case, the extraordinary beam is the fastest and therefore represented by a red ellipse elongated $176\mu m$ in the forward direction according to at which point in the crystal conversion occurred. For instance, photons created at the beginning of the crystal will be on the leading edge of the ellipse. Vertical spread of $9\mu m$ is due to the slight difference in the spatial walk-off angles of the pump and the extraordinary polarized down-converted beam. Similarly a red ellipse marked as 'o' represents ordinary polarized beam, which will be elongated $62\mu m$ forward due to lower group index compare to the pump beam. Vertical spread of $154\mu m$ in this beam, is due to the walk-off in the pump beam corresponding to where down-conversion occurred.

Note that, to arrive to the state given in Eq. (3.25), we assumed single modes and hence these down-converted beams should be coupled to single modes fibers. However, as such these beams do not have good overlap and therefore cannot be coupled optimally using single mode fibers. Fig. 3.9 also shows how these beams can be overlapped optimally using a HWP($\frac{\pi}{4}$) and an extra BBO crystal with half of the main crystal thickness i.e. we need 1mm thick BBO in this case. HWP($\frac{\pi}{4}$) can switch the polarization 'o' to 'e' and vice versa, and when these beams with switched polarizations pass through a 1mm BBO, then only 'e' beam suffer spatial and temporal walk-offs compare to the 'o' beam (we need not to bother about pump beam at this stage anymore). This means 'e' beam will be pushed forward about $57\mu m$ and down about $72.5\mu m$ leading to optimal overlap as shown in the Fig. 3.9.

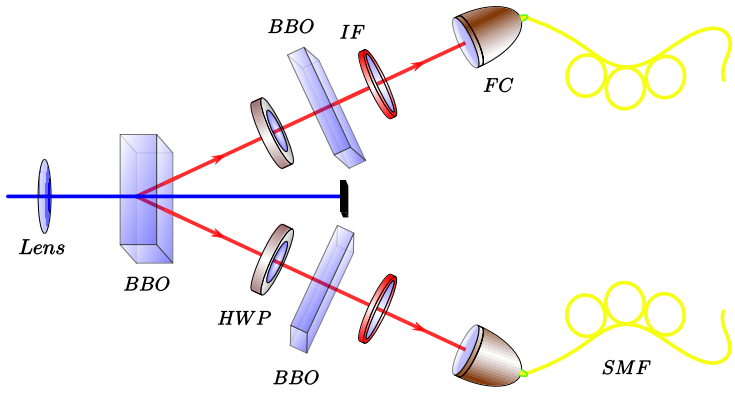

Figure 3.10: Polarization entangled photons source.

3.3.4 Two Photon Polarization Entanglement

Once the compensation is done, one needs to filter the spatial modes using single mode fibers. Usually it takes a big fraction of the whole time spent in building such a source, since purity of the state and the factor $\frac{1}{\sqrt{2}}$ in Eq. (3.25) depend on coupling alignment. To increase the purity usually frequency filtering is also needed, for this narrow band interference filter (IF) are used. However, this reduces the count rates significantly.

Fig. 3.10 depicts a polarization entangled photon source with all important optical components. With such a setup, photons emerging from each of the crossing can be made to exist in the singlet state given in Eq. (3.25) or in any of the other Bell states given in Eq. (2.28) easily.

3.4 Two-Photon Interference

Often in multi-photon experiments e.g. teleportation [44; 45], entanglement swapping [46; 47] etc, one has to remove distinguishability between two given photons due to their arrival times or alternatively one could require to measure how indistinguishable the photons are due to their other characteristics. This is usually done by observing Hong-Ou-Mandel (H-O-M) effect, also known as Hong-Ou-Mandel interference [48; 49]. This technique can also be used to measure path lengths differences and the bandwidth or the size of the wave-packets of the photons used. We utilized this technique to remove distinguishability between two photons due to their arrival times in our experiments.

To get some physical intuitions for this, consider the situation when two photons arrive at a symmetric BS simultaneously, as depicted in Fig. 3.11. We have seen earlier, for a symmetric BS there is equal probability for a photon

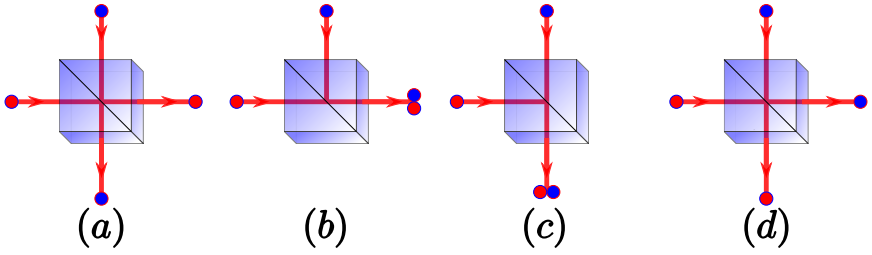

Figure 3.11: Two photons at the inputs of a symmetric BS. Each sub-figure represents the possibility corresponding to the case when (a) Both photons transmitted, (b) first transmitted, second reflected,(c) first reflected and second transmitted,(d) both reflected.

to transmit or reflect. Hence, there will be in total four possibilities corresponding to the cases; both photons transmitted, first transmitted while second reflected, first reflected and second transmitted, and both reflected. Here, one should note two things about the cases depicted in (a) and (d) of Fig. 3.11. Firstly, if we have represented photons with the circles of the same color–i.e. if the photons were indistinguishable–then one cannot distinguish between the processes (a) and (d). Secondly, there will be a relative phase difference of π between the two cases as can be seen from the BS transformation given in (3.17). Hence, the two probability amplitudes representing each of these cases will interfere destructively and therefore the photons will not end up into any of these configurations in an ideal situation.

Mathematically, two photons at the inputs of a BS, Fig. 3.12, can be represented as

$$|1,1\rangle_{a_1,a_2} = \hat{a}_1^\dagger \hat{a}_2^\dagger |0,0\rangle_{a_1,a_2}. \tag{3.26}$$

We have seen that a symmetric 50–50 BS transform operators corresponding

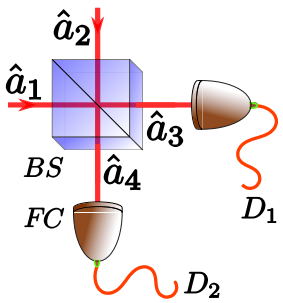

Figure 3.12: Setup to observe Hong-Ou-Mandel interference with a 50–50 symmetric BS.

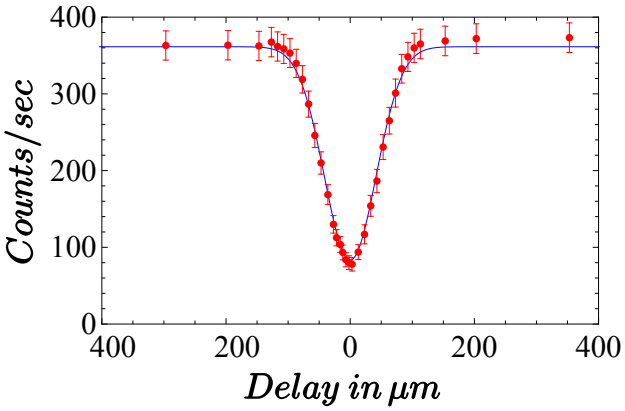

Figure 3.13: Hong-Ou-Mandel interference of two independent photons–originating from two SPDC processes–with $V_{H-O-M} = 76.9 \pm 0.9\%$. The other two photons are used as triggers.

to individual field amplitude according to (3.17), therefore

$$\begin{aligned}\hat{a}_1^\dagger \hat{a}_2^\dagger |0,0\rangle_{a_1,a_2} &\xrightarrow{BS} \frac{1}{2}\left(\hat{a}_3^\dagger - i\hat{a}_4^\dagger\right)\left(-i\hat{a}_3^\dagger + \hat{a}_4^\dagger\right)|0,0\rangle_{a_3,a_4} \\ &= (-i)\frac{1}{2}\left(\hat{a}_3^{\dagger 2} - \hat{a}_4^{\dagger 2}\right)|0,0\rangle_{a_3,a_4} \\ &= \frac{-i}{\sqrt{2}}\left(|2,0\rangle_{a_3,a_4} + |0,2\rangle_{a_3,a_4}\right).\end{aligned} \tag{3.27}$$

This calculation reveals that there will be no coincidences between the detectors D_1 and D_2, due to the cancellation of the terms $\hat{a}_3^\dagger \hat{a}_4^\dagger - \hat{a}_4^\dagger \hat{a}_3^\dagger$. However, if the photons are distinguishable then they must be described with operators corresponding to different field modes, i.e. $(\hat{a}_3^\dagger \hat{a}_4^\dagger - \hat{a}_4^\dagger \hat{a}_3^\dagger) \rightarrow (\hat{a}_{3,1}^\dagger \hat{a}_{4,2}^\dagger - \hat{a}_{4,1}^\dagger \hat{a}_{3,2}^\dagger)$, where the new subscripts 1 and 2 refer to the first and the second photon respectively. Hence these terms will not cancel and will lead to the coincidences between the detectors D_1 and D_2.

In our experiments we delay one of the photons to make them distinguishable due to their arrival times at the BS. Ideally, when the delay is zero one should not get any coincidences provided that the photons are indistinguishable, whereas maximal coincidences are achieved when delay is larger than the coherence length of interfering photons. However, we got small amount of coincidence even for zero delay, as shown in Fig. 3.13, due to experimental imperfection or slight distinguishability. The degree of distinguishability is measured with a parameter often referred as visibility of H-O-M dip and define as $V_{H-O-M} = \frac{C_\infty - C_0}{C_\infty}$ [50–52], where C_0 and C_∞ refer to the coincidences at zero and large delays respectively. For the dip shown in Fig. 3.13 we got

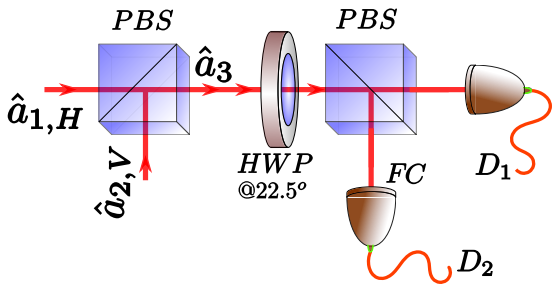

Figure 3.14: Setup to observe Hong-Ou-Mandel interference with a PBS.

$V_{H-O-M} = 76.9 \pm 0.9\%$. Note that these interfering photons are independent i.e. they are originated from two different down conversions and hence much more difficult to interfere [53].

Another way to observe H-O-M interference with a PBS is shown in Fig. 3.14. Here, we assume two photons with orthogonal polarizations at the two input ports of a PBS simultaneously i.e.

$$|1_H, 1_V\rangle_{a_1,a_2} = \hat{a}^\dagger_{1,H}\hat{a}^\dagger_{2,V}|0,0\rangle_{a_1,a_2}. \tag{3.28}$$

Now, using Eq. (3.8) and PBS transformation given in (3.18), while neglecting overall phases we get,

$$\begin{aligned}\hat{a}^\dagger_{1,H}\hat{a}^\dagger_{2,V}|0,0\rangle_{a_1,a_2} &\xrightarrow{PBS} \hat{a}^\dagger_{3,H}\hat{a}^\dagger_{3,V}|0\rangle_{a_3} \\ &\xrightarrow[@22.5^\circ]{HWP} \frac{1}{2}\left(\hat{a}^\dagger_{3,H}+\hat{a}^\dagger_{3,V}\right)\left(\hat{a}^\dagger_{3,H}-\hat{a}^\dagger_{3,V}\right)|0\rangle_{a_3} \\ &= \frac{1}{\sqrt{2}}\left(|2_H\rangle_{a_3} - |2_V\rangle_{a_3}\right).\end{aligned} \tag{3.29}$$

Which shows that there will be no coincidences between D_1 and D_2 due to the cancellation of the terms $(-\hat{a}^\dagger_{3,H}\hat{a}^\dagger_{3,V} + \hat{a}^\dagger_{3,V}\hat{a}^\dagger_{3,H})$ like before and will lead to a similar dip in coincidences–as shown in Fig. 3.13–when one of the photon is delayed related to the other.

An important characteristic feature of H-O-M interferometers is that it is much more stable than any interferometer based on second order interference e.g. Mach-Zehnder interferometer which has sub-wavelength sensitivity, whereas H-O-M interference is sensitive to path length changes on the order of the coherence length of the photons involved.

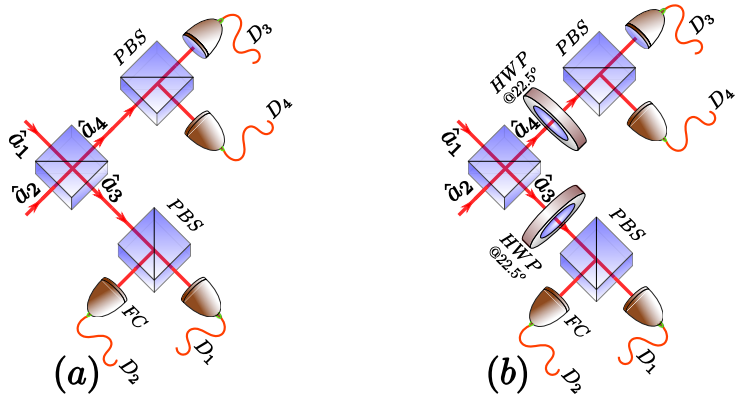

Figure 3.15: Bell state analyzer (a) based on a BS, (b) based on a PBS.

3.5 Bell State Measurement

Bell states, introduced in sec. 2.8.1 of chapter 2, not only maximally violates Bell inequality but also form an orthonormal basis for the state space of two qubits and are very important in quantum information sciences as these are the key ingredient in many of its striking applications including teleportation [44; 45], superdense coding [54], entanglement swapping [46; 47] and numerous other cryptographic protocols. Therefore, ability to measure and prepare these states is crucial. In section 3.3 we described how one can create such states using down conversion sources, whereas this section describe how we can measure if the two input photons are in one of the four possible Bell states. Note that with linear optics it has been proven that a never failing Bell measurement is impossible [55]. However, there are linear optical setups which can discriminate between all four Bell states probabilistically [56; 57]. For our purposes it is enough to look at the optical setups discriminating between only two of the four states as given in [58; 59].

Consider a BS with two detectors on each of its output modes as shown in Fig. 3.14 (a). For simplicity we will just analyze what type of coincidence one will get when the two input photons at the BS are in each of the possible Bell states. Consider the case when input photons at the BS are in Ψ^- state. Then we can write it as

$$|\Psi^-\rangle_{a_1,a_2} = \frac{1}{\sqrt{2}}\left(\hat{a}^\dagger_{1,H}\hat{a}^\dagger_{2,V} - \hat{a}^\dagger_{1,V}\hat{a}^\dagger_{2,H}\right)|0,0\rangle_{a_1,a_2}. \tag{3.30}$$

By using BS transformation (3.17) we get

$$
\begin{aligned}
&\frac{1}{\sqrt{2}}\left(\hat{a}^{\dagger}_{1,H}\hat{a}^{\dagger}_{2,V}-\hat{a}^{\dagger}_{1,V}\hat{a}^{\dagger}_{2,H}\right)|0,0\rangle_{a_1,a_2} \\
&\qquad\xrightarrow{BS}\frac{1}{2\sqrt{2}}\Bigg[\left(\hat{a}^{\dagger}_{3,H}-i\hat{a}^{\dagger}_{4,H}\right)\left(-i\hat{a}^{\dagger}_{3,V}+\hat{a}^{\dagger}_{4,V}\right) \\
&\qquad-\left(\hat{a}^{\dagger}_{3,V}-i\hat{a}^{\dagger}_{4,V}\right)\left(-i\hat{a}^{\dagger}_{3,H}+\hat{a}^{\dagger}_{4,H}\right)\Bigg]|0,0\rangle_{a_3,a_4} \\
&\qquad=\frac{1}{\sqrt{2}}\left(\hat{a}^{\dagger}_{3,H}\hat{a}^{\dagger}_{4,V}-\hat{a}^{\dagger}_{3,V}\hat{a}^{\dagger}_{4,H}\right)|0,0\rangle_{a_3,a_4} \\
&\qquad=\frac{1}{\sqrt{2}}\left(|1_H,1_V\rangle_{a_3,a_4}-|1_V,1_H\rangle_{a_3,a_4}\right).
\end{aligned}
\tag{3.31}
$$

That is, Ψ^- state at the input will lead to the coincidences between the detectors D_1, D_4 or D_2, D_3. Similarly, assuming Ψ^+ at the input will give

$$
\begin{aligned}
|\Psi^+\rangle_{a_1,a_2}&=\frac{1}{\sqrt{2}}\left(\hat{a}^{\dagger}_{1,H}\hat{a}^{\dagger}_{2,V}+\hat{a}^{\dagger}_{1,V}\hat{a}^{\dagger}_{2,H}\right)|0,0\rangle_{a_1,a_2} \\
&\xrightarrow{BS}\frac{1}{\sqrt{2}}\left(\hat{a}^{\dagger}_{3,H}\hat{a}^{\dagger}_{3,V}-\hat{a}^{\dagger}_{4,H}\hat{a}^{\dagger}_{4,V}\right)|0,0\rangle_{a_3,a_4}
\end{aligned}
\tag{3.32}
$$

Therefore, in this case we will get coincidences between D_1, D_2 or D_3, D_4. Whereas it is straight forward calculation to see that $\Phi^{\pm}$ will not lead to any kind of coincidences.

Moreover, if we consider the setup shown in Fig. 3.14 (b)– a modified version of Fig. 3.14(a) proposed in [60]–then one can check easily that input state Φ^+ will give the coincidence between the detectors D_1, D_4 or D_2, D_3, whereas Φ^- at the input will lead to the coincidence between D_1, D_3 or D_2, D_4 i.e. with this setup one can discriminate between $\Phi^{\pm}$. Therefore with successful projection, any of these setups can be used to distinguish between only two of the four Bell states.

Note that for both of these setups we assumed that the two photons arrive at the input of the BS (or the PBS) simultaneously which is necessary condition for these setups to work. To assure this one usually observe H-O-M interference.

3.6 GHZ-State Preparation

We prepare three or four photons GHZ state–introduced in section 2.9– with the method given in [61]. To do this one need two down conversion sources similar to those described in section 3.3. The whole setup is shown in Fig. 3.15. Here, circles marked as A and B are the two sources producing entangled

states given as,

$$|\phi_i\rangle = \frac{1}{\sqrt{2}}\left(|HH\rangle + e^{i\phi_i}|VV\rangle\right). \tag{3.33}$$

Where $i = 1,2$ corresponding to source A or B. When both of the sources produce a pair of the photons simultaneously we get,

$$\begin{aligned}
|\phi\rangle_{1,2'}|\phi\rangle_{3',4} =& \frac{1}{2}\left(|H_1H_{2'}\rangle + e^{i\phi_1}|V_1V_{2'}\rangle\right)\left(|H_{3'}H_4\rangle + e^{i\phi_2}|V_{3'}V_4\rangle\right)\\
\xrightarrow{PBS}& \frac{1}{2}\left(|H_1H_3\rangle + i\, e^{i\phi_1}|V_1V_2\rangle\right)\left(|H_2H_4\rangle + i\, e^{i\phi_2}|V_3V_4\rangle\right)\\
=& \frac{1}{2}\big(|H_1H_2H_3H_4\rangle + i\, e^{i\phi_2}|H_1H_3V_3V_4\rangle\\
&+ i\, e^{i\phi_1}|V_1V_2H_2H_4\rangle - e^{i(\phi_1+\phi_2)}|V_1V_2V_3V_4\rangle\big).
\end{aligned} \tag{3.34}$$

Note that the terms with $|H_1H_3V_3V_4\rangle$ or $|V_1V_2H_2H_4\rangle$ will not lead to the coincidence between all of the four modes marked as $1,2,3$ and 4 i.e. no 4-photon click among them. Therefore, if one requires having one photon in each of the four modes–that can be accomplished by post selecting only the events when we get a click in each of the four paths–will lead to the state that one can write with proper normalization as

$$\frac{1}{\sqrt{2}}\left(|H_1H_2H_3H_4\rangle - e^{i(\phi_1+\phi_2)}|V_1V_2V_3V_4\rangle\right). \tag{3.35}$$

This can give GHZ state easily, since the phases ϕ_1 and ϕ_2 can be adjusted to give ± 1. Note that this method of only observing coincidences, sometimes called *conditional detection* or *observation in coincidence basis* [53].

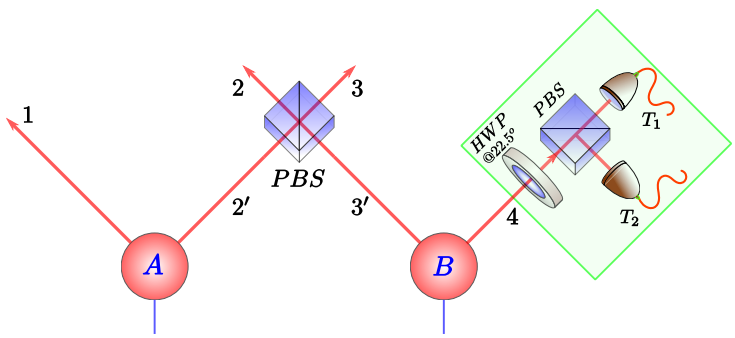

Figure 3.16: Setup to obtain a four-photon GHZ state, post selected by coincidence between each of the four modes marked as 1, 2, 3 and 4. Also, a three-photon GHZ state can be obtained in modes 1,2 and 3 when the fourth photon at T_1 or T_2 is used as trigger.

Moreover, placing a HWP @ 22.5° in one of the modes, e.g. in mode 4, will lead to

$$\begin{aligned}\frac{1}{\sqrt{2}}\left(|H_1H_2H_3H_4\rangle - e^{i(\phi_1+\phi_2)}|V_1V_2V_3V_4\rangle\right)\\ \xrightarrow[@22.5]{HWP} \frac{1}{2}|H_4\rangle\left(|H_1H_2H_3\rangle - e^{i(\phi_1+\phi_2)}|V_1V_2V_3\rangle\right)\\ =|V_4\rangle\left(|H_1H_2H_3\rangle + e^{i(\phi_1+\phi_2)}|V_1V_2V_3\rangle\right)\end{aligned} \tag{3.36}$$

Therefore, using H_4 or V_4 as a trigger one can get a three photon GHZ state in modes $2,3$ and 4. Note that photons in modes $2'$ and $3'$ need to be indistinguishable in order to arrive to these results, which one assured by observing H-O-M interference.

3.7 Quantum Teleportation

One of the most fascinating applications that quantum information provides is the possibility of teleportation. This was first discovered by Bennett et al. [44] and experimentally realized in [45; 62]. Before expounding the idea of quantum teleportation, one should note that photons– or any other elementary particles–are in principle indistinguishable and the differences in their response only arise due to the various states they can acquire in different situations. Therefore, to teleport a photon from one place to another it is enough to copy its state onto a photon located at the destination. The procedure to solely achieve this is referred as *quantum teleportation*. Moreover, it has also been discovered that copying a quantum state is not possible. This is often referred as no-cloning theorem [63; 64], and implies that a successful teleportation can only be accomplished when teleporting machine does not retain any information whatsoever about the state being teleported and therefore the original state at the input will be destroyed in this process.

To teleport a state from one party that we call Alice to the other party Bob, they need to have an entangled pair shared between them. Suppose Alice and Bob each have a photon from an entangled pair prepared in Ψ^- and the state Alice wants to teleport to Bob is given as

$$|\psi\rangle_1 = \alpha|H_1\rangle + \beta|V_1\rangle. \tag{3.37}$$

The singlet state or Ψ^- given in Eq. (2.28), can be written as

$$|\Psi^-\rangle_{2,3} = \frac{1}{\sqrt{2}}\left(|H_2V_3\rangle - |V_2H_3\rangle\right). \tag{3.38}$$

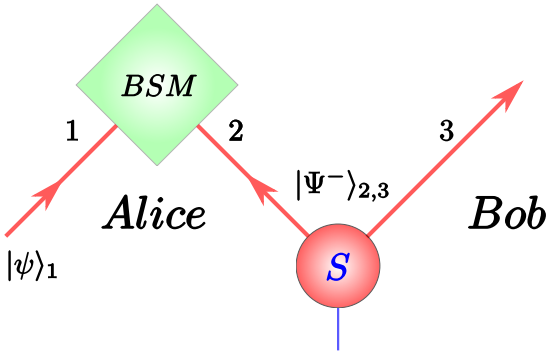

Figure 3.17: Principle of quantum teleportation. Alice teleport $|\psi\rangle_1$ to Bob with the help of an entangled pair $|\Psi^-\rangle_{2,3}$ shared between them.

Considering them together gives

$$|\psi\rangle_1 \otimes |\Psi^-\rangle_{2,3} = \frac{1}{\sqrt{2}}(\alpha|H_1\rangle + \beta|V_1\rangle) \otimes (|H_2V_3\rangle - |V_2V_3\rangle) \tag{3.39}$$

Now, using the Bell basis given in Eq. (2.28) one can write

$$\begin{aligned}
|H_1H_2\rangle &= \frac{1}{\sqrt{2}}(|\Phi^+\rangle_{1,2} + |\Phi^-\rangle_{1,2}),\\
|H_1V_2\rangle &= \frac{1}{\sqrt{2}}(|\Psi^+\rangle_{1,2} + |\Psi^-\rangle_{1,2}),\\
|V_1H_2\rangle &= \frac{1}{\sqrt{2}}(|\Psi^+\rangle_{1,2} - |\Psi^-\rangle_{1,2})\\
|V_1V_2\rangle &= \frac{1}{\sqrt{2}}(|\Phi^+\rangle_{1,2} - |\Phi^-\rangle_{1,2})
\end{aligned} \tag{3.40}$$

Using these we can write Eq. (3.39) as,

$$\begin{aligned}
|\psi\rangle_1 \otimes |\Psi^-\rangle_{2,3} = \\
&\frac{1}{2}\Big(|\Phi^+\rangle_{1,2} \otimes (-\beta|H_3\rangle + \alpha|V_3\rangle)\\
&+ |\Phi^-\rangle_{1,2} \otimes (\beta|H_3\rangle + \alpha|V_3\rangle)\\
&+ |\Psi^+\rangle_{1,2} \otimes (-\alpha|H_3\rangle + \beta|V_3\rangle)\\
&- |\Psi^-\rangle_{1,2} \otimes (\alpha|H_3\rangle + \beta|V_3\rangle)\Big)
\end{aligned} \tag{3.41}$$

It is clear from this equation that if Alice performs a Bell state measurement (BSM) and communicates the result of her measurement to Bob then the pho-

ton that Bob had–after performing an appropriate local unitary transformation-will be in the same state as of the photon that Alice wanted to teleport. For instance, when Alice's measurement project the two photons in the modes 1 and 2 to Ψ^-, then she needs to tell this result to Bob and only then Bob will know that his photon is in the desired state without performing any local transformation. In all other cases he needs to perform some local unitary transformations to get the desired state as apparent from Eq. (3.41).

Note that this teleportation cannot be achieved without classical information transfer as Alice needs to tell her results to Bob. Therefore, this procedure does not allow information transfer faster than the speed of light and therefore, will not violate relativity.

4. Bell Inequalities for the Simplest Exclusivity Graph

The aim of this chapter is to introduce the background needed for the **Paper I**, where we discovered three new Bell inequalities based on exclusivity graphs and presented their experimental violations.

In chapter 2, we have seen that quantum mechanical systems possess non-local[1] and contextual correlations that not only lead to the violation of Bell and non-contextual inequalities, but also allow us to achieve classically impossible tasks. However, identifying when such tasks are possible is difficult and still under research. Recently, it is shown that linking non-contextual inequalities to graphs could be fruitful [17], as it is discovered in the same paper that the classical bounds for local hidden variable (LHV) theories and non-contextual hidden variable (NCHV) theories can be extracted from the associated graphs of their respective inequalities, by just calculating the so called independence numbers of these graphs. Whereas the quantum mechanics is upper bounded by the Lovázs numbers of these graphs. Moreover, these bounds are tight, i.e. they are precisely equal to the quantum bound. This fact manifests the deep connection of these graphs to classical and quantum theories. This is very important, as one can imagine theories offering stronger correlations than what quantum mechanics can provide. However, experiments until now only provide confirmation of quantum theory, which leads to classical mechanics when approximated in restricted sense (correspondence principle) i.e. in contrast to all possible theories, apparently only quantum mechanics gives the correct description of the physical world. Therefore, it is a quite interesting fact that the graphs constructed by pairwise exclusive outcomes of real experiments provide upper bound for quantum mechanics.

This feature of exclusivity graphs motivates the application of graph theory in the field of quantum information. Since the derivation of the new Bell inequalities– that we call pentagon Bell inequalities–is also based on the graphs, therefore, we will start the chapter with an introduction to the graph theory and some of its important terms that will be needed to understand the

[1] In this context, here and in the rest of the thesis by non-local correlation we mean correlations that cannot be explained by local realistic models.

Paper I. As an example we look at the graph of CHSH inequality. More details can be found in the attached published article.

4.1 An Introduction to Graph Theory

Graph theory is a wide and rapidly developing field of mathematics and computer science. Therefore here we will only describe concepts and terms which are required to understand later sections. In the following context, the word graph means a collection of points and lines which connect some of these points. The points are called *vertices* and the lines connecting some or all of these point are referred to as *edges*. The *degree of a vertex* is defined as the number of edges touching it. Moreover, all vertices of a graph can be collected in a set called *vertex set*, and the cardinality–number of members–of this set is called *vertex count* of the graph.

There are two main types of graphs called *directed* and *undirected* graphs. The type with which we are dealing here is undirected graphs. In this type of graphs, a vertex connected with other vertices has symmetric (or same) relation with them, meaning that the edges of the graph do not have any directional character.

In different fields vertices of a graph represent different parameters or quantities. Here, in this thesis we will consider graphs whose vertices represent events, and an edge will connect two vertices if and only if the two vertices represent mutually exclusive events. Such a graph will be called an *Exclusivity Graph*. In the following, we will introduce some important terms needed to understand later sections.

An independent vertex set is a subset of the vertex set containing only those vertices of the graph that are not connected to each other by edges. Note that one can form many different independent vertex sets for a given graph. The exact number will depend on the structure of the graph.

Independence number of a graph also known as vertex independent number, is defined as the cardinality of the largest independent vertex set. We will denote it by $\alpha(\mathbf{G})$, where $\mathbf{G}$ is a given graph. Note that for exclusivity graphs, independence number gives the upper bound for LHV theories. Computing independence number is not easy, since it requires finding the largest independent vertex set which is a NP-hard problem. This will mean that the effort needed to calculate this number grows very quickly with the size of the graph.

Lovász number was first introduced by László Lovász as an upper bound on the Shannon capacity of a graph [65]. However, in the context of this thesis it is the Lovász number itself which is the relevant quantity, as Lovász number of an exclusivity graph gives the upper bound for quantum mechanics in an experiment that can be faithfully represented by this graph. It is a real number and is denoted by $\vartheta(\mathbf{G})$. It can be calculated as follows.

Let B be a matrix with unit trace and range over all $n \times n$ symmetric positive semidefinite matrices such that $b_{ij} = 0$ when i and j form an edge in $\mathbf{G}$. Then

$$\vartheta(\mathbf{G}) = \max_{B} \mathrm{Tr}(BJ) \tag{4.1}$$

where J is a $n \times n$ matrix of ones. Therefore, $\mathrm{Tr}(BJ)$ is just the sum of all entries of B [65]. Another equivalent way of computing it is to assign a set of real normalized vectors v_i to each vertex of the graph such that two vectors are orthogonal if the corresponding vertices are adjacent. Then the Lovász number will be given by

$$\vartheta(\mathbf{G}) = \max_{|\varphi\rangle} \left(\sum_{i=1}^{n} |\langle \varphi | v_i \rangle|^2 \right) = \left\| \sum_{i=1}^{n} |v_i\rangle\langle v_i| \right\|_{\infty} \tag{4.2}$$

Here, $|\varphi\rangle$ and $|v_i\rangle$ are unit vectors in Euclidean space and the maximum is taken in any dimensions over all possible $|\varphi\rangle$ and $|v_i\rangle$, subject to orthogonality constraint. [17; 66]. Also, the interesting dimension turns out to be the lowest dimension in which the orthogonality constraint can be satisfy. Clearly, this definition has more quantum mechanical flavor and with this, one begins to see why the Lovász number is interesting in quantum mechanics.

It is an interesting fact that though Lovász number looks difficult to calculate, it can be efficiently computed using semi-definite programing. On the other hand, remember that for independence number no such effective algorithm exists. It is quite mysterious, when one considers the computational difficulty of these numbers together with their connections to classical and quantum upper bounds, as it could suggest that the basic principle behind quantum world may be simpler than the principle behind classical world.

Fig. 4.1 shows independence and Lovász number for some simple graphs, which are easy to calculate using the definitions above. Note that for a complete graph–in which all the vertices are connected together– independence and Lovász number are always 1. Also, the simplest graph for which $\alpha(\mathbf{G}) < \theta(\mathbf{G})$ is a pentagon as shown in Fig 4.3. Equipped with these definitions we will now discuss how to form a exclusivity graph for the CHSH inequality.

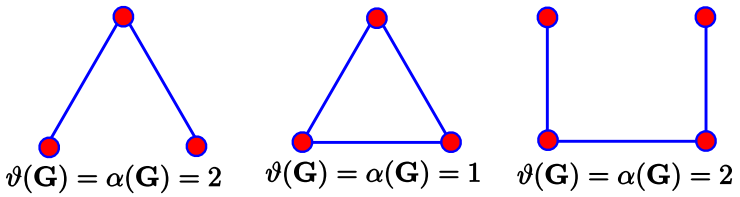

Figure 4.1: Independence and Lovász number for simple graphs.

4.2 Exclusivity Graph of CHSH inequality

Exclusivity graph represents the relation of the probabilities of different events, therefore, first we have to write CHSH inequality as a convex sum of probabilities, where by the term convex sum we mean weighted sum such that weights are not only non-negative but also add up to unity. From chapter 2, we know that, for positive correlations the CHSH inequality can be written as,

$$\begin{aligned} & E(A_0,B_0)+E(A_0,B_1)+E(A_1,B_0)-E(A_1,B_0) \leq 2 \\ \equiv \quad & \langle A_0B_0\rangle + \langle A_0B_1\rangle + \langle A_1B_0\rangle - \langle A_1B_1\rangle \overset{\text{LHV}}{\leq} 2 \end{aligned} \tag{4.3}$$

Where A_i and B_i represent operators measured using first or the second setting by Alice and Bob respectively. Note that here in the above equation the minus sign is with the different term compare to Eq. (2.25), this can be achieved by just renaming $A_0 \to A_1$ and $A_1 \to A_0$. The reason for doing this will be clear later. In our case these operators are σ_{A_i} and σ_{B_i} and $E(A_i,B_i)$ is the expectation value of the combined measurement and can be calculated as,

$$E(A_i,B_i) = \langle\psi|\sigma_{A_i}\otimes\sigma_{B_i}|\psi\rangle = \mathrm{Tr}\left(\rho \;.\; (\sigma_{A_i}\otimes\sigma_{B_i})\right). \tag{4.4}$$

Here, ρ is the density operator of the state in use. Further, in this thesis we will represent the probability of getting outcome a for Alice and b for Bob– while measuring with their first or the second setting that we represent by $x = \{0,1\}$ and $y = \{0,1\}$ for Alice and Bob respectively– as $P(a,b|x,y)$. Note that, since our operators are dichotomic, therefore, $a,b \in \{+1,-1\}$ and for simplicity we will just denote them by $+1 \to 0$ and $-1 \to 1$. Then, with these conventions, $P(0,1|1,0)$ will denote the probability of obtaining a result of $+1$ and -1 for Alice and Bob respectively, while Alice chooses her 2nd setting for measurement and Bob chooses his 1st setting. We will make clear in the context what we mean by 1st and 2nd settings.

Now, Suppose Alice and Bob together want to violate the CHSH inequality, then, as shown in the chapter 2, it can be achieved if Alice and Bob both chooses 2 different appropriate settings in which they measured the operators A_0, A_1, and B_0, B_1–as given in (4.3)–respectively. To do this they choose one

of the Bell states, say $|\Phi^+\rangle$, as defined in equation (2.28) which has positive correlations. Therefore, the expectation value $E(A_0,B_0)$, when Alice and Bob chooses 1st of their settings, can be written in terms of probabilities as

$$\begin{aligned} E(A_0,B_0) &= P(0,0|0,0)+P(1,1|0,0)-P(0,1|0,0)-P(1,0|0,0) \\ &= P(a\oplus b=0\ |x\to 0,y\to 0)-P(a\oplus b=1\ |x\to 0,y\to 0) \\ &= P(a\oplus b=0\ |0,0)-P(a\oplus b=1\ |0,0) \end{aligned}$$

where $x,y\in\{0,1\}$ and $a,b\in\{0,1\}$ and $\oplus$ denotes sum modulo 2. Note that the sum of all four probabilities in the above equation should be 1. Therefore,

$$E(A_0,B_0)=2\ P(a\oplus b=0\ |0,0)-1 \tag{4.5}$$

Similarly, other terms in equation (4.3) can also be represented in probabilities and the reader can check easily that the equation (4.3), in this case becomes,

$$\sum_{x,y=0}^{1} P(a\oplus b=x\wedge y\ |x,y)\leq 3 \tag{4.6}$$

Here, one can recognize the advantage of switching Alice settings. Note that probabilities represented by $P(a,b|x,y)$, can be inverted to give expectation value by using

$$P(a,b|x,y)=\frac{1}{4}\langle[\mathbb{1}+(-1)^a A_x][\mathbb{1}+(-1)^b B_y]\rangle \tag{4.7}$$

This is easy to derive if one notices that $\langle A_x^a\rangle=\mathrm{Tr}(\rho|\varphi_a\rangle\langle\varphi_a|)$, where ρ is any states and $|\varphi_a\rangle$ is an eigenvector of A_x with eigenvalue a and therefore it can be written as $\frac{1}{2}(\mathbb{1}+(-1)^a A_x)$. Now this sum of probabilities can be easily represented by an exclusivity graph. Note that this sum contains eight terms, so our graph will be an octagon. To form an exclusive relation between connected vertices note that two vertices, say $(a,b|x,y)$ and $(a',b'|x',y')$, of our octagon can be connected if one of the following conditions is fulfilled

1. $x=x'$ and $a\neq a'$, Meaning that Alice's outcomes are exclusive.
2. $y=y'$ and $b\neq b'$, Meaning that Bob's outcomes are exclusive.
3. (1) and (2) both are true, that is Alice and Bob both's outcomes are exclusive.

It can be checked easily that the resultant graph will be the one shown in figure 4.2. Note that in this case each vertex is connected to three other vertices; hence the degree of each vertex is 3.

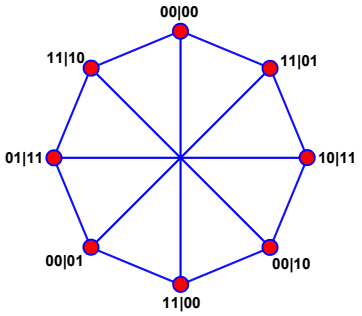

Figure 4.2: Exclusivity graph of CHSH inequality. Note that for this graph independence number $\alpha(\mathbf{G}) = 3$ and Lovász number $\vartheta(\mathbf{G}) = 2+\sqrt{2}$,

4.3 Simplest Exclusivity Graph With Quantum-Classical Gap

As mentioned earlier, the vertices in an exclusivity graph represent events or outcomes of some real experiments. all/some of these vertices are connected by edges using a simple rule that referred as exclusivity principle [66–68]. Note that the roots of this principle can be traced back to Ernst Specker [69; 70]. According to this principle, the sum of the probabilities of pairwise exclusive events–that we represent by two connected vertices on these graph–cannot exceed 1. Therefore, connected vertices in these graphs can be associated to the outcomes of a single experiment as they cannot both occur together i.e. if so connected they are exclusive. Thus, one can consider the vertices on these graphs as propositions whose truth and falsity can be checked in real experiments. In this sense, the independence number of such a graph must have the interpretation of being the largest number of these propositions that can be true at the same time according to classical physics. Whereas, the Lovász number as a tight bound for quantum mechanics, can be interpreted as the highest number of true statements in such experiments predicted by quantum mechanics. This fact reveals the deep connection of these graphs to physical theories.

Moreover, there are graphs for which Lovász number $\vartheta(\mathbf{G})$ is greater than independence number $\alpha(\mathbf{G})$. In the previous section we have seen an example of such a graph namely CHSH-graph. These graphs are important since they bring out the cases when quantum mechanics can outperform classical physics. We refer these graphs as exclusivity graphs with quantum-classical gap. It is known since 1979 [17; 65; 71] that the simplest graph for which $\alpha(\mathbf{G}) < \theta(\mathbf{G})$, is a pentagon as shown in Fig. 4.3, and it is associated to KCBS inequality that we described in Sec. 2.10. Due to the close relationship

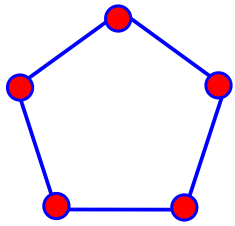

$$\alpha(\mathbf{G}) = 2, \quad \vartheta(\mathbf{G}) = \sqrt{5}$$

Figure 4.3: Exclusivity graph of a pentagon, which has a quantum-classical gap as $\alpha(\mathbf{G}) < \theta(\mathbf{G})$.

between contextuality and Bell inequality as described in Sec. 2.10, one can expect that there should be Bell inequalities connected to pentagons. In **Paper I** we investigated this point and found that there are actually three different Bell inequalities connected to a pentagon exclusivity structure. These are the simplest Bell inequalities in the sense of their logical structure and the cause of the violation of other Bell inequalities e.g. CHSH and I_{3322} can be traced back to the violation of these inequalities. Moreover, they also provide an argument for the impossibility of Popescu and Rohrlich (PR) non-signaling boxes [72]. In **Paper I**, we also present experimental violation of these inequalities. More details can be found in the attached published article.

5. Non-Local Games

Games involving two or more distant parties–that may or may not be space-like separated–are called non-local games. Furthermore, in these games, one can exploit intriguing aspect of quantum mechanics to achieve classically impossible tasks, in such scenarios; one regards these games as quantum non-local games. In the following context we are only concerned with a special type of quantum non-local games called CHSH-games and the aim of this chapter is to provide a brief introduction of the **Paper II**, where we present an experimental realization of CHSH-non-local game and also describe a real world application of such game based on a card game, Duplicate bridge. More details can be found in the attached published article.

We shall start the chapter by describing CHSH-games with biased and unbiased cases. This description will be based on the article [18].

5.1 CHSH Game

A non-local quantum game based of CHSH-inequality is called a CHSH-game. CHSH inequality can be expressed in different ways to describe a CHSH game, e.g. we can consider the form shown in expression (4.6), that can be rescaled and written as,

$$\sum_{x,y=0}^{1} \frac{1}{4} P(a \oplus b = x \wedge y \,|x,y) \overset{\text{LHV}}{\leq} \frac{3}{4} \tag{5.1}$$

In this form it is written as a sum of probabilities and therefore the CHSH-game corresponding to it can be formulated as follows. Alice and Bob measuring dichotomic observables with settings and outcomes denoted as $x, y \in \{0,1\}$ and $a, b \in \{0,1\}$ respectively. They can get positive score i.e. +1 if and only if $a \oplus b = x \wedge y$, and in all other cases they acquire -1. However, we want to generalize CHSH game to unbiased CHSH-games which is straightforward with the form given in expression (4.3). Therefore, we will consider this form to describe unbiased CHSH-game first.

5.1.1 Unbiased CHSH Game

The CHSH-game described above can be regarded as an unbiased CHSH-game if we impose the condition that the settings given by x and y are equally likely. This can be explicitly shown if one consider the CHSH inequality written in the form (4.3) and write the rescaled version of this expression as,

$$\frac{1}{4}\left[\langle A_0B_0\rangle + \langle A_0B_1\rangle + \langle A_1B_0\rangle - \langle A_1B_1\rangle\right] \overset{\text{LHV}}{\leq} \frac{1}{2} \tag{5.2}$$

In this form, one can formulates a quantum non-local CHSH game as follows. Suppose that two players Alice and Bob–which may be space-like separated–playing a game in which each of them got a particle emitted by a source. Then, according to the procedure of the game, they have to perform a dichotomic measurement, giving possible outcomes as +1 and -1, which will correspond to their scores and the goal of the game is to achieve as high score as possible. Now, the inequality above, in this case can be regarded as their average score in this game over many rounds and the factor $\frac{1}{4}$ can be recognized as the averaging factor for four different types of measurement's combinations. Note that this factor is same for all terms meaning that each measurement combination is equally likely. Now, to get positive score, expectation values can be written as,

$$\langle A_iB_j\rangle = \frac{N(A_iB_j=1) - N(A_iB_j=-1)}{N(A_iB_j=1) + N(A_iB_j=-1)} \tag{5.3}$$

where $i,j \in \{0,1\}$ and, $N(A_iB_j=1)$ and $N(A_iB_j=-1)$ represent the total number of rounds giving score $+1$ and -1 respectively for corresponding measurements. We will now consider a more general situation of this game.

5.1.2 Biased CHSH Game

Since the factor $\frac{1}{4}$ in the expression is recognized as averaging factor, therefore, when the probabilities of choosing different measurement's settings are unequal then we can write CHSH inequality as,

$$\begin{aligned} CHSH(p,q) = {} & pq\langle A_0B_0\rangle + p(1-q)\langle A_0B_1\rangle + (1-p)q\langle A_1B_0\rangle \\ & - (1-p)(1-q)\langle A_1B_1\rangle \overset{\text{LHV}}{\leq} \frac{1}{2} \end{aligned} \tag{5.4}$$

Here, p and q denote probabilities with which Alice and Bob choose their first measurement settings. If we assume that $p,q \geq \frac{1}{2}$, then, it is easy to see that the maximum classical value is achieved by a simple strategy, e.g. when all

the expectation values are $+1$, we will get the classical maximum as,

$$\begin{aligned} CHSH_{Cl}(p,q) &= p+q-pq-(1-p)(1-q) \\ &= 1-1+p+q-pq-(1-p)(1-q) \\ &= 1-2\,(1-p)(1-q) \end{aligned} \tag{5.5}$$

and the quantum bound can be calculated as describe in the article [18]. I will just quote the result here which is

$$\begin{aligned} CHSH_Q(p,q) \leq \quad & p\sqrt{q^2+(1-q)^2+q(1-q)\alpha} \\ + \quad & (1-p)\sqrt{q^2+(1-q)^2-q(1-q)\alpha} \end{aligned} \tag{5.6}$$

where $\alpha = \langle\psi|\mathbb{1}\otimes(B_0B_1+B_1B_0)|\psi\rangle$ in which B_i are Hermitian operators on Bob's Hilbert space such that $B_i^2 = \mathbb{1}$ and $|\psi\rangle$ is an arbitrary pure state. The maximum of (5.6) occurs when

$$\alpha = \min\left\{2, \frac{(q^2+(1-q)^2)(p^2-(1-p)^2)}{q(1-q)(p^2+(1-p)^2)}\right\}. \tag{5.7}$$

which implies that we have two regions in (p,q) space.

Region 1: When $1 \geq p \geq (2q)^{-1} \geq 1/2$, the maximum value occurs for $\alpha = 2$ and the optimal is

$$CHSH_{Cl}(p,q) = CHSH_Q(p,q) = 1-2\,(1-p)(1-q) \tag{5.8}$$

Region 2 : When $1 \geq (2q)^{-1} > p \geq 1/2$, in this case quantum protocols or strategies can outperform their classical counterparts and quantum bound will be given by,

$$CHSH_Q(p,q) \leq \sqrt{2}\sqrt{q^2+(1-q)^2}\sqrt{p^2+(1-p)^2} \tag{5.9}$$

Now, the experimental settings with which maximum quantum bound can be achieved are as follow,

$$\begin{aligned} A_0 \quad &= \frac{\sigma_x\,(q+(1-q)\;cos\;\beta)+\sigma_z(1-q)\;sin\;\beta}{\sqrt{(q+(1-q)\;cos\;\beta)^2+(1-q)^2\;sin^2\;\beta}} \\ A_1 \quad &= \frac{\sigma_x\,(q+(1-q)\;cos\;\beta)+\sigma_z(1-q)\;sin\;\beta}{\sqrt{(q+(1-q)\;cos\;\beta)^2+(1-q)^2\;sin^2\;\beta}} \\ B_0 \quad &= \sigma_x\;cos\;\beta+\sigma_z\;sin\;\beta \\ B_1 \quad &= \sigma_x \\ |\psi\rangle \quad &= \frac{1}{2}(\;|0\rangle|0\rangle+|1\rangle|1\rangle\;) \end{aligned} \tag{5.10}$$

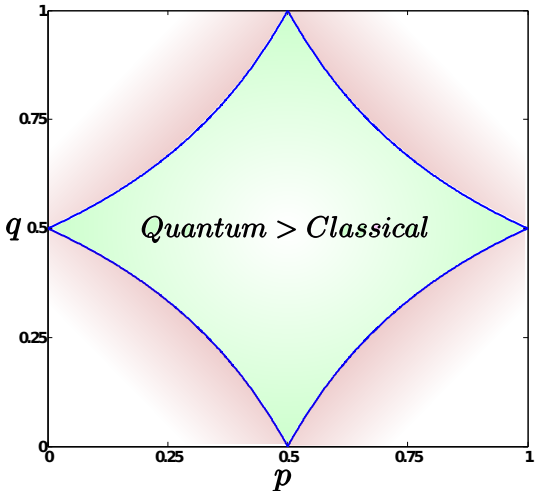

Figure 5.1: (p,q) space containing region I–where quantum mechanics does not provide any advantage–and region II–where quantum mechanics does provide some advantage.

where σ_i denote Pauli matrices and

$$cos\ \beta = \frac{1}{2}\frac{\left(q^2+(1-q)^2\right)\left(p^2-(1-p)^2\right)}{q(1-q)\left(p^2+(1-p)^2\right)} \tag{5.11}$$

During all this description, we assumed that $p,q \geq \frac{1}{2}$. For all other cases the situation is quite symmetric and depicted in figure 5.1. Also, if instead of (5.4) one considers (5.1) for biased case as,

$$\begin{aligned} I = \quad & pq\ P(A\oplus B = x\wedge y\ |x=0,y=0) \\ + \quad & p(1-q)\ P(A\oplus B = x\wedge y\ |x=0,y=1) \\ + \quad & (1-q)p\ P(A\oplus B = x\wedge y\ |x=1,y=0) \\ + \quad & (1-p)(1-q)\ P(A\oplus B = x\wedge y\ |x=1,y=1) \overset{\text{LHV}}{\leq} \frac{3}{4}, \end{aligned} \tag{5.12}$$

then it is easy to see that the two forms are connected as,

$$I = \frac{1+CHSH(p,q)}{2} \tag{5.13}$$

In this work we have successfully achieved experimental realization of this CHSH-game by choosing different values of p and q and the results are presented in **Paper II**.

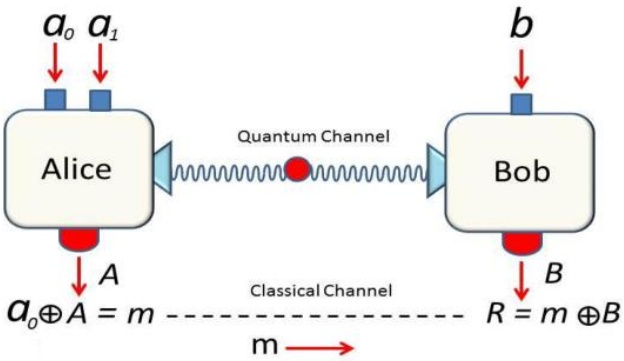

Figure 5.2: Quantum Bridge Scheme. Alice and Bob (West and East partners in Bridge game) are given two bits a_0 and a_1 and one bit $y = b$ respectively. Alice receives two bits a_0 and a_1 with the respective probabilities $p_0(0)$ and $p_1(0)$ of them being 0. She chooses her measurement setting to be $x = a = a_0 \oplus a_1$. After reading out her outcome A, Alice prepares the message $m = A \oplus a_0$ which she transmits to Bob. He then computes R by adding the message to his outcome: $R = B \oplus m$.

5.2 Quantum Duplicate Bridge: An Application of CHSH Game

Under this heading we are not inventing any new game, rather, by the word *"Quantum duplicate bridge"*, we are emphasizing the application of quantum mechanics on the famous card game of *duplicate bridge*.

Contract bridge is a partnership game and the essence of a successful play is efficient communication between the partners. Due to the rules of the game, the form and the amount of the information exchanged between the partners is severely restricted. Nevertheless, using our technique that we have presented in **Paper II** attached with this thesis, the players can increase their winning probability without violating any rule of the game [73]. In our scheme, the players need to share an entangled state, which they can do before the beginning of the game. During the game they just need to do local measurements on their subsystems which is not in any sense against the rules of the World Bridge Federation [73].

The protocol used here to increase the wining probability is based on $2 \rightarrow 1$

entanglement assisted random access code [74]. This can be applied to duplicate bridge as there are situations in the game when one partner–that we can assume as Alice–has two bits of information and the other partner, say Bob, could be interested in any one of them. However, the communication between them is restricted due to the rules of the game, therefore Bob cannot freely ask the information he is interested in. Thus, Alice has to guess which bit he might be interested in and then she sends this bit. However, the situation can be considered as it consists of many such rounds and therefore we are interested in a optimized protocol that Alice could use. In this situation she could use $2 \rightarrow 1$ entanglement assisted random access code which is more advantageous than any other classical protocol [74]. Fig. 5.2 explains quantum protocol briefly. More details can be found in the attached paper.

6. Measurement-Device-Independent Entanglement Detection

In the last chapters, we have seen how the correlation in entangled states leads to the violation of Bell inequalities and how these correlations can be used to perform task more efficiently than can be done using classical resources. Except these, entanglement has been used in numerous other protocols and recognized as a fundamental resource in quantum information science. Consequently, detection and quantification of entanglement is of the utmost importance and thus has been a subject of intensive research in recent years.

In **Paper III**, we have implemented a measurement-device-independent way to detect entanglement in a bipartite system. Such an implementation is quite useful in certifying entanglement in the case when one cannot access the resource or cannot trust the measurement devices. The aim of this chapter is to briefly describe the background of **Paper III** and present its short introduction. Further details can be found in the attached published article.

6.1 Quantum State Verification and Entanglement Detection

In almost all experimental situations when one tries to produce a quantum state, he ends up in preparing a state close to the desired one and often has to find out how close the state is to the target state. Fortunately there are some measures available to define a distance between the two states e.g. trace distance, fidelity, relative entropy etc. Unfortunately, to calculate these measures we need to know the density operator of the state prepared, which is not always possible either due to the complexity of the preparation procedure or due to the miserable generation rates.

Whereas, sometimes one only desires to prepare a state with certain properties e.g. entanglement or bound entanglement–which is the topic of the next chapter–etc. In such cases it suffices to just measure or infer the properties one desires. In this chapter our desired characteristic is entanglement so we will

briefly mention some methods to detect it, more details can be found in [75]. However, we start by defining fidelity of a quantum state.

6.1.1 Fidelity of a Quantum State

Fidelity of a quantum state with respect to a given state is a measure which quantitatively describes how close the two states are [64; 76]. Suppose the two states under consideration are represented as ρ_1 and ρ_2 then fidelity is defined as[1]

$$F(\rho_1,\rho_2) = \mathrm{Tr}\left(\sqrt{\sqrt{\rho_1}\rho_2\sqrt{\rho_1}}\right) \tag{6.1}$$

Note that $F(\rho_1,\rho_2) = 1$ when $\rho_1 = \rho_2$, and is zero when the two states are orthogonal. In general, $0 \leq F(\rho_1,\rho_2) \leq 1$. Also, it is invariant under unitary transformations i.e.

$$F(\hat{U}\rho_1\hat{U}^\dagger, \hat{U}\rho_2\hat{U}^\dagger) = F(\rho_1,\rho_2) \tag{6.2}$$

Moreover, fidelity is symmetric in its arguments. In case when the two states are commuting or can be diagonalized with the same representations or basis we will have $F(\rho_1,\rho_2) = \sum_{i=0}^{n}\sqrt{\lambda_i^{(1)}\lambda_i^{(2)}}$. Here $\lambda_i^{(1)}$ and $\lambda_i^{(2)}$ are the eigenvalues of the two states ρ_1 and ρ_2 respectively and n represents their dimensionality.

In most of the experiments one of the states–usually the one an experimentalist aims to produce–is pure, in such cases one can check easily that Eq. (6.1) becomes

$$F(\rho_1,\rho_2) = \sqrt{\langle\psi|\rho_2|\psi\rangle} = \sqrt{\mathrm{Tr}\,(\rho_2|\psi\rangle\langle\psi|)}, \tag{6.3}$$

where, we assumed $\rho_1 = |\psi\rangle\langle\psi|$. This is a quite useful expression as for instance, it provides a connection between entanglement visibility and fidelity for the Bell states (2.28) as given in [78], where we define visibility as

$$V_i = \langle(\hat{\sigma}_i \otimes \hat{\sigma}_i)\rangle = \frac{N(\hat{\sigma}_i \otimes \hat{\sigma}_i = 1) - N(\hat{\sigma}_i \otimes \hat{\sigma}_i = -1)}{N(\hat{\sigma}_i \otimes \hat{\sigma}_i = 1) + N(\hat{\sigma}_i \otimes \hat{\sigma}_i = -1)}, \tag{6.4}$$

Here $\hat{\sigma}_i = \vec{r}_i.\vec{\sigma}$ and the term $N(\hat{\sigma}_i \otimes \hat{\sigma}_i = 1)$ indicates total number of coincidences obtained when the two photons measured under the setting $\hat{\sigma}_i \otimes \hat{\sigma}_i$ and

[1] Some articles e.g. [75; 77; 78] and many others especially experimentalist define fidelity as

$$F(\rho_1,\rho_2) = \left(\mathrm{Tr}\left[\sqrt{\sqrt{\rho_1}\rho_2\sqrt{\rho_1}}\right]\right)^2$$

In order to be consistent with others we have also used this formula for the calculation of fidelity in our experiments.

result in eigenvalues whose product is $+1$. Similarly the second term in the numerator represents coincidences obtained when the product of the resulted eigenvalues is -1. With this definition, for any Bell state we will have

$$F = \sqrt{\frac{1}{4}(1+V_x+V_y+V_z)}. \tag{6.5}$$

6.1.2 Violation of Bell Inequality

We have seen in chapter 2 that the violation of a Bell inequality is an evidence of non-classical behavior and imply that the system possesses quantum correlations manifesting the entanglement among its constituents. Thus, violating a Bell inequality can certify presence of entanglement. However, it has been shown that one can violate Bell inequality and even quantum mechanics (only apparently) by either exploiting some loopholes or by adopting some hacking strategies [79; 80]. Hence, for such a certification one has to reply on loophole free violation of a Bell inequality. Moreover, once achieved such a violation will guarantee the presence of entanglement, independently of the measurement settings used,[1] the precision accomplished in implementing them, or the dimensionality of the system under consideration. Moreover, the fact that, for a bipartite system all pure entangled states violates a Bell inequality [81; 82], further increases the usefulness of such certification.

However, there are bipartite mixed entangled states which do not violate any Bell inequality [24; 83] as their correlation can be explained by a local model. Werner states [24] provides such examples, and are defined as those bipartite states which do not change when the two parties transform their subsystems using the same unitary operators i.e.

$$\rho_W = (U \otimes U)\rho_W(U^\dagger \otimes U^\dagger) \tag{6.6}$$

where with ρ_W we represent a Werner state. When the sub-systems are 2-dimensional, a Werner state can be formed by a mixture of the singlet and the completely mixed state as

$$\rho_W = p|\Psi^-\rangle\langle\Psi^-| + (1-p)\frac{\mathbb{1}}{4} \tag{6.7}$$

It is straight forward to check that CHSH violation for this state is $CHSH = 2\sqrt{2}p$ and as depicted in Fig 6.1, CHSH inequality cannot certify entanglement when $p \leq \frac{1}{\sqrt{2}}$, though it can be evident with positive partial transposition (PPT) method as we will see in the next section.

[1] As far as, one fulfills the requirement of the Bell inequality under consideration that is, for instance CHSH inequality is a two-two settings Bell inequality and therefore will not work for any other number of measurement settings.

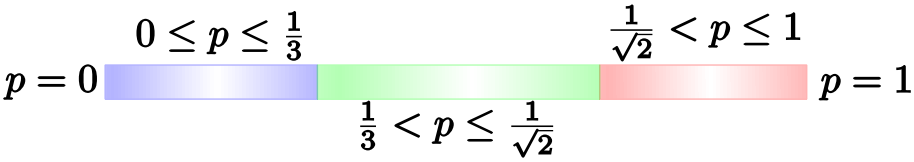

Figure 6.1: Varying p in Eq. (6.7) leads to (a) $0 \leq p \leq \frac{1}{3}$ state is separable. (b) $\frac{1}{3} < p \leq \frac{1}{\sqrt{2}}$, state is entangled and entanglement is detectable by PPT criterion. (c) $\frac{1}{\sqrt{2}} < p \leq 1$ state is entangled and entanglement is detectable even with CHSH violation.

6.1.3 Positive Partial Transpose (PPT) Criterion

Positive partial transpose (PPT), is actually a necessary condition for separability discovered by Asher Peres [84]. According to this a density matrix representing a state ρ_{AB} can be separable only if $\rho_{AB}^{T_B}$ is also a legitimate density operator and therefore have non-negative eigenvalues. The partial transpose operation on a bipartite state ρ_{AB} can be elaborated as

$$\rho_{AB}^{T_B} = \left(\sum_{ijkl} c_{ijkl} |i\rangle\langle j| \otimes |k\rangle\langle l| \right)^{T_B} = \sum_{ijkl} c_{ijkl} |i\rangle\langle j| \otimes |l\rangle\langle k| \tag{6.8}$$

Similarly one can also define partial transpose with respect to sub-system A. Also note that in case of the systems consisting of qubit-qubit or qubit-qutrit i.e. when the dimension of the composite system is six or less, this condition is not only necessary for separability but sufficient also. Hence, PPT criterion completely characterize separability in such systems [25; 85].

Now if one applies this criterion to calculate the necessary condition for a Werner state given in Eq. (6.7) to be separable, then it is easy to see that the eigenvalues of the partially transpose density matrix are $\frac{1}{4}(1-3p), \frac{p+1}{4}, \frac{p+1}{4}$, and $\frac{p+1}{4}$. Demanding that the least eigenvalue is non-negative will give $0 \leq p \leq \frac{1}{3}$, and hence the Werner state for such values of p will be separable. This is depicted in Fig. 6.1.

PPT is a powerful criterion for testing when a state is separable i.e. not entangled. However it requires the knowledge of the density operator of the state under consideration and as pointed out earlier this is not always possible in experimental situations. Another way to detect entanglement, which is comparably more practical, is witness method.

6.1.4 Witness Method

An observable $\mathcal{W}$ is referred to as an entanglement witness (EW) for an entangled state ρ if $\mathrm{Tr}(\mathcal{W}\rho) \geq 0$ for all separable states, whereas $\mathrm{Tr}(\mathcal{W}\rho) < 0$

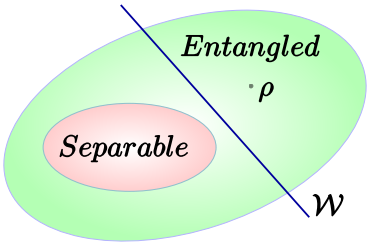

Figure 6.2: An Entanglement Witness, separating an entangled state ρ from the set of separable states.

at least for the state ρ [25; 75]. Thus, a negative expectation value of the observable $\mathcal{W}$ will be considered as evidence of entanglement in ρ. Note that an entanglement witness is a directly measurable quantity and therefore detection of entanglement through measuring the witness is a very feasible experimental method.

EWs are actually hyperplanes in the space of all states which contains separable states as a convex set. Moreover, planes defined by EWs can be drawn from any direction and hence are able to discriminate any entangled states from the set of separable states, as can be inferred from Fig. 6.1.

For an entangled pure state $|\psi\rangle$, an EW can be constructed by using the fact that states in the close vicinity of an entangled state should also be entangled. Therefore

$$\mathcal{W} = \alpha \mathbb{1} - |\psi\rangle\langle\psi|. \tag{6.9}$$

In this case the expectation value of the witness $\mathcal{W}$ clearly depends on the $\mathrm{Tr}(\rho'|\psi\rangle\langle\psi|)$, which can be understood as the fidelity (or square of fidelity, according to the other definition) of ρ' with respect to $|\psi\rangle\langle\psi|$. Here ρ' can be any state around $|\psi\rangle\langle\psi|$. When this fidelity is higher than some critical value $\alpha = \max_{\phi \in S} |\langle\psi|\phi\rangle|^2$ the state is entangled, where S represents the set of separable states. For the Werner states given in (6.7), $\alpha = \frac{1}{2}$ and hence EW for this state is

$$\mathcal{W} = \frac{1}{2}\mathbb{1} - |\psi\rangle\langle\psi|. \tag{6.10}$$

EW has been used in various experiments, for instance, implementation of this method for 2,3 and 4-photons can be found in [86; 87]. To experimentally implement this method one first optimally decompose a witness into a minimal number of local projective measurements [88; 89], as otherwise it could involve more than one qubit operations. Thus, the validity of this technique depends on the precision involved in implementing these measurements, i.e. it demands perfect implementation. Therefore, in case of imperfect measurement

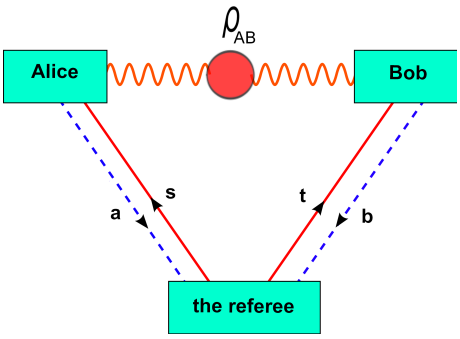

Figure 6.3: Scheme for a semi-quantum nonlocal game.

devices it can lead to false entanglement detection [90; 91]. In comparison, violation of Bell inequality is more robust, though this technique has its own disadvantages. In **Paper III** we experimentally implement a method which can overcome these drawbacks.

6.2 Measurement-Device-Independent Entanglement Witness

As mentioned before, loophole free violation of a Bell inequality can be used as a device-independent entanglement detection method. However with this, one cannot detect all entangled states. An example is, Werner states, as these states for certain values of p admit a local realistic model. There are some other methods to overcome these problems, for instance, measuring more than one copy of the same state simultaneously [92], however it is unclear if such methods can be used to detect all entangled state.

In [19], Francesco Buscemi has generalized the concept of so-called nonlocal games [93] to include quantum inputs from a referee for specifying in which basis the participating parties should measure their shared entangled state. He showed that in such games all entangled states can give an advantage over separable states. The scheme of such a game is presented in Fig. 6.3. Here, s and t are quantum inputs, whereas a and b are outcomes (eigenvalues) of the measurements performed by Alice and Bob respectively. In reference [20], this point is further clarified and used to devise a method to obtain a measurement-device-independent EW for all entangled states. In **Paper III** we experimentally implement such an approach, more details can be found in the article attached to this thesis.

7. Bound Entanglement: Generation and Activation

In previous chapters we have seen the importance and applications of entanglement in quantum information science. The fact that one cannot produce entanglement using classical techniques makes it a resource for accomplishing classically unachievable task. Therefore it plays a key role in the field of quantum cryptography, communication and computation. However, in real experiments entanglement can be easily destroyed due to decoherence induced by the environment. Such uncontrollable interactions introduce noise and transform, for instance, maximally entangled states into mixed states. Fortunately, some distillation protocols and techniques have been discovered. Therefore, these mixed states can be distilled via local operations and classical communication (LOCC) to get maximally entangled states, and can be useful again for further information processing. However, this distillation is not always possible leading to a kind of trapped entanglement that we called bound entanglement.

In **paper IV, V** and **VI**, we are dealing with this kind of entanglement. In these papers we prepared and investigated three and four-partite bound entangled states. In **paper VI** we also experimentally realized activation scheme for a bound entangled state and show that these states are indeed useful resources. This chapter gives the necessary background for these papers, results and details of the experiments can be found in the attached papers.

7.1 LOCC Operations

In the field of quantum information and communication sometimes we impose restrictions due to some natural or artificial origin to investigate how fruitful quantum resources can be. For instance, in chapter 5, we saw that the communication between two partners could be more effective by sharing an entangled pair beforehand, when during one way communication a partner is restricted to send only a single classical bit. Here, only one-way communication was allowed with severe limitations. Similarly, other form of restriction classes have been considered and investigated.

One such restriction class is called local operations (LO), in which two

parties–that we named as Alice and Bob–who shared some state ρ_{AB} are only allowed to perform local operations i.e. no communication (classical or quantum) between them is allowed [25; 94]. Mathematically such an operation can be represented as

$$\Lambda_{LO}(\rho_{AB}) = \sum_{i,j}(A_i \otimes B_j)\rho_{AB}(A_i^\dagger \otimes B_j^\dagger) \tag{7.1}$$

Here, $\sum_i A_i^\dagger A_i = \mathbb{1}_N$ and also $\sum_i B_i^\dagger B_i = \mathbb{1}_N$. Naturally, one could extend this to include classical communication; such restriction class is known as local operations and classical communication (LOCC). Note that here by local operation we mean any kind of quantum operations including measurements, with the only restriction that they be performed locally on each subsystem. Moreover, the results of these measurements and other information can be shared, however no quantum information transfer is allowed. Note that, via classical communication one cannot share entanglement, therefore with LOCC entanglement remains a resource.

One can distinguish LOCC from the separable operation class (SO) [95] defined as

$$\Lambda_{sep}(\rho_{AB}) = \sum_{i}(A_i \otimes B_i)\rho_{AB}(A_i^\dagger \otimes B_i^\dagger) \tag{7.2}$$

Although it is hard to see, (SO) class is more general than (LO) or (LOCC) class as LO $\subset$ LOCC $\subset$ SO. It can be a bit clear if one notices that special choice of indexing in the above equation implies correlation between Alice and Bob's measurements which comes from classical communication. However, Eq. (7.2) includes operations that are not present in LOCC, details for this can be found in [96; 97].

7.2 Distillation and Bound Entanglement

In many quantum information applications including teleportation, superdense coding, entanglement swapping etc. one needs pure maximally entangled Bell states. However, real experiments in most of the cases lead to mixed entangled states due to the noise induced by the environment or imperfections of the experiment itself. Thus, at the output we have to deal with mixed entangled states rather than pure maximally entangled states. Therefore, it is important to know, how to get pure or more concentrated entangled states from some mixed states, as the former are clearly more advantageous. Solely achieving this goal is called distillation of entanglement [25; 75].

In this context, one considers that there are arbitrary but finite number of copies available of the state that needs to be distilled. Moreover, these copies

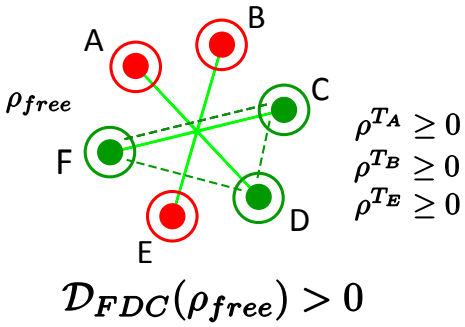

Figure 7.1: The red (green) circles symbolize that PPT with respect to the subsystems they mark is satisfied (violated). Only between the pairs with two green circles (marked by green dashed lines) pure entanglement can be distilled.

are distributed between two parties that we call Alice and Bob, as usual, and they are allowed to perform any LOCC operations on these copies such that in the end they share a maximally entangled state or a state close to it. This problem for pure and mixed entangled states was first considered by Bennett et al. in [98; 99]. In [99], it was shown that the two distant parties, Alice and Bob, sharing n copies of a noisy mixed bipartite entangled state ρ, can perform LOCC operations to acquire in turn some number k of copies (where $k < n$) of a state close to a maximally entangled state, containing more concentrated entanglement. The procedure with which this task is achieved, using LOCC, is referred to as entanglement purification or entanglement distillation protocol.

Observe that it is proved in [100] that all two-qubit entangled states are distillable. However, for higher dimensional systems this is not always true i.e. there are entangled states which are not distillable by LOCC. These states are known as bound entangled (BE) states. This is because to prepare these states one needs entanglement, however, once driven into bound entanglement regime it is not possible to distill maximally entangled states from them anymore. Therefore, one can discriminate between two forms of entanglement here, free and bound, which are defined according to their distillability.

The positive partial transpose (PPT) criterion of separability, discussed in section 6.1.3, is closely connected to distillation. One cannot distill entanglement from separable states by LOCC, as the set of separable states is closed under these operations. Therefore separable states are PPT and non-distillable. It is also shown in [101; 102] that violation of PPT criterion is a necessary condition for distillation. Fig. 7.1, provides an example, where the PPT criterion is used to show that there exists free entanglement in the state. Moreover, creation of BE states are examples of irreversible processes in quantum sys-

tems, as these states can be created from pure free entangled states via LOCC operations. Nevertheless, once this free entanglement is brought into a bound entangled regime then it cannot be reversed. Interestingly, sometimes bound entanglement can be activated via some activation protocol, in the sense that at the end we left with some free entanglement. We present such an experiment in **Paper VI**.

7.3 Smolin States

In the experiment, which demonstrates the first experimental realization of bound entangled states, Smolin states were produced [103; 104], where they also presented its unlocking, a process which leads to distillable free entanglement. Smolin states are mixed Bell states given as

$$\rho_s^{ABCD} = \frac{1}{4}\sum_{i=1}^{4} |\Psi_i^{AB}\rangle\langle\Psi_i^{AB}| \otimes |\Psi_i^{CD}\rangle\langle\Psi_i^{CD}| \tag{7.3}$$

where $|\Psi\rangle_{i=1}^{4} = \{|\Psi^-\rangle, |\Psi^+\rangle, |\Phi^+\rangle, |\Phi^-\rangle\}$. It is easy to check that this state can also be written as

$$\rho_{s_1}^{ABCD} = \frac{1}{16}\left(\hat{\sigma}_{\mathbb{1}}^{\otimes 4} + \hat{\sigma}_x^{\otimes 4} + \hat{\sigma}_y^{\otimes 4} + \hat{\sigma}_z^{\otimes 4}\right) \tag{7.4}$$

When one of the qubits in this state is rotated locally with $\hat{\sigma}_y$, $\hat{\sigma}_z$ and $\hat{\sigma}_x$ we get

$$\begin{aligned}
\rho_{s_2}^{ABCD} &= \frac{1}{16}\left(\hat{\sigma}_{\mathbb{1}}^{\otimes 4} - \hat{\sigma}_x^{\otimes 4} + \hat{\sigma}_y^{\otimes 4} - \hat{\sigma}_z^{\otimes 4}\right) \\
\rho_{s_3}^{ABCD} &= \frac{1}{16}\left(\hat{\sigma}_{\mathbb{1}}^{\otimes 4} - \hat{\sigma}_x^{\otimes 4} - \hat{\sigma}_y^{\otimes 4} + \hat{\sigma}_z^{\otimes 4}\right) \\
\rho_{s_4}^{ABCD} &= \frac{1}{16}\left(\hat{\sigma}_{\mathbb{1}}^{\otimes 4} + \hat{\sigma}_x^{\otimes 4} - \hat{\sigma}_y^{\otimes 4} - \hat{\sigma}_z^{\otimes 4}\right)
\end{aligned} \tag{7.5}$$

Note that these are obtained by just local rotations of a BE state and therefore are all bound entangled also. Moreover, these four states are also mutually orthogonal, since $\mathrm{Tr}\left(\rho_{s_i}\rho_{s_j}\right) = \frac{\delta_{ij}}{4}$ i.e. one can imagine these four states as orthogonal vectors in a 4-dimensional space. In this case the tetrahedron depicted in Fig. (1) of the paper VI attached, can be visualized as a 3-dimensional plane containing all these four states. Moreover, the center of this tetrahedron will be a completely mixed state.

To see how these states are bound entangled, note that the mixture of maximally entangled Bell states given in Eq. (7.6) is by construction bi-separable, however if the two parties, say A and B meet and perform a Bell measurement with their qubits then they can determine the maximally entangled Bell state

shared by the other two parties, C and D. i.e. this process will leave the other two qubits entangled. Conversely, the parties C and D could meet to perform Bell measurement; this will leave the states shared between A and B entangled. Therefore, clearly Smolin states contain entanglement. Moreover, these states are completely symmetric in terms of the labeling of the parties, this is easy to see from the equivalent form given in Eq. (7.5). Therefore, the above argument can be applied to any of the two parties. However, as mentioned earlier, these states are bi-separable also across every possible cut e.g. AB|CD, AC|BD and AD|BC. This implies that these states are separable between every pair of the pairs, therefore no entanglement can be distilled across these cuts and hence as long as the parties are distant, and only LOCC operations are allowed, these states are BE [105]. Note however that when any two of the four parties meet they can unlock entanglement hidden in these states.

7.4 Experimental bound entanglement through a Pauli channel

In **Paper VI**, we experimentally investigated the case when a product of Bell states transmits through a lossless quantum channel, which induces bit-flips and/or phase-flips errors. For this we first generated a product of singlet state given as

$$\rho^{ABCD} = |\Psi^{-}_{AB}\rangle\langle\Psi^{-}_{AB}| \otimes |\Psi^{-}_{CD}\rangle\langle\Psi^{-}_{CD}| \tag{7.6}$$

Then, via the action of a lossless quantum channel (correlated LO operations i.e. LOCC operations) we were able to transform this state to a mixture of all maximally entangled Bell states. Also, by adding noise in a controllable fashion we drove this mixture to BE regime and were able to produced states shown in Eq. (7.4) and (7.5). We experimentally investigated the set of states span by these four orthogonal states. Also, by controlling the amount of noise we were able to produce BE states that violates a Bell inequality. Moreover, we experimentally investigated the boundary regime between free entanglement, bound entanglement and separable states. More details can be found in the attached published article.

7.5 Three-Qubit Bound Entanglement Generation

In **Paper V**, we experimentally generated a high fidelity mixed three qubit polarization bound entangled state. This is also the first experimental realization of a three-qubit BE state. The state that we generated was

$$\rho^{ABC}_{bound} = \frac{1}{3}|\Psi_{GHZ}\rangle\langle\Psi_{GHZ}| + \frac{2}{3}\frac{P}{4} \tag{7.7}$$

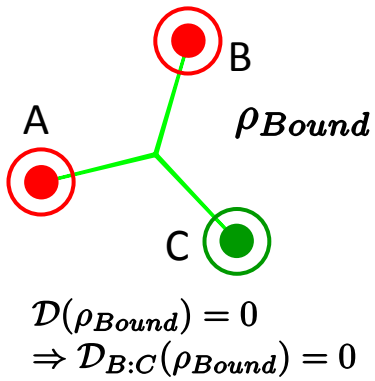

Figure 7.2: Three-qubit bound entangled state ρ^{ABC}_{bound}. The red (green) circles symbolize that PPT with respect to the subsystems they mark is satisfied (violated).

where $|\Psi_{GHZ}\rangle$ is a GHZ state given as

$$|\Psi_{GHZ}\rangle = \frac{1}{\sqrt{2}}(|000\rangle + |111\rangle) \tag{7.8}$$

and the projection P projects onto $\{|010\rangle, |011\rangle, |100\rangle, |101\rangle\}$ i.e.

$$P = |010\rangle\langle 010| + |100\rangle\langle 100| + \frac{1}{\sqrt{2}}(|011\rangle\langle 011| + |101\rangle\langle 101|). \tag{7.9}$$

Characteristics of this state are illustrated in Fig. 7.2. Using quantum state tomography [106], we have fully reconstructed its density matrix and demonstrated all its entanglement properties. The experimental details can be found in the attached manuscript. Note that this is the first experimental realization of a bound entangled state that can be used for generation of multipartite bound information [107]. Most importantly bound entanglement in this state can be activated as we have shown in **Paper VI**.

7.6 Three-Qubit Bound Entanglement Activation

In **Paper VI**, we present activation scheme for the state in Eq. (7.7), using a free entangled pair, that we can represent as

$$\rho^{A'B'C'}_{free} = [|\Psi^+\rangle\langle\Psi^+|]_{A'B'} \otimes [|\Omega\rangle\langle\Omega|]_{C'} \tag{7.10}$$

Both of the resources i.e. ρ^{ABC}_{bound} and $\rho^{A'B'C'}_{free}$ are depicted in Fig. 7.3 together. The special bound entangled 3-qubit state ρ^{ABC}_{bound} is depicted symbolically on

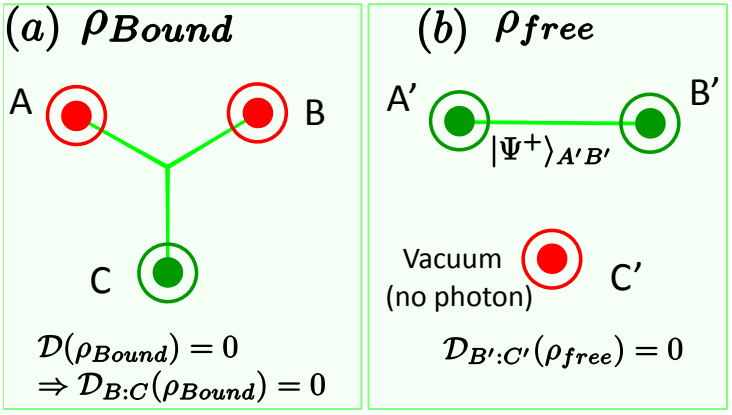

Figure 7.3: The two resources (states) that are used in the activation protocol.

the left hand side. Since in each pair of qubits there is always at least one of them guaranteeing PPT property, therefore with the original 3-qubit state there is no chance to distill any pure entanglement out of the state. Thus distillable entanglement vanishes, $\mathcal{D}(\rho_{bound}) = 0$. In particular no singlet can be distilled between B and C which we write as $\mathcal{D}_{B:C}(\rho_{bound}) = 0$. However there is still some entanglement in the state since the PPT test is violated with respect to the subsystem C. Thus the state is entangled and, since it is non-distillable, therefore it is bound entangled. The second, free entangled state ρ_{free} corresponds to two-qubit singlet and the virtual (vacuum) part. Clearly there is no chance to distill entanglement between B' and C' from ρ_{free}. Thus there is no possibility of distillation of free entanglement between B and C from an arbitrary number of copies of any of the state ρ_{bound} or ρ_{free}. In that sense any of the two states alone is weak since some important quantum entanglement ingredient is completely absent in any of them.

In **Paper VI** we present activation of ρ^{ABC}_{bound} [108]. Importantly, the very unique feature of quantum mechanics revealed by our experiment is its "something-out-of-nothing" character; an ingredient completely absent in any of the two resources suddenly emerges after putting the two resources together. This phenomenon lies at the very heart of the quantum information. More details can be found in the attached manuscript of **paper VI**.

8. Conclusion

This thesis consists of six papers. In the following we will present the conclusion of each part separately.

In **paper I** we identified three bipartite inequalities based on the pentagon exclusivity graph, which is the simplest exclusivity graph for which there exist a quantum-classical gap. We also experimentally violated all three inequalities and obtained results in good agreement with quantum mechanics. We also show that one of our inequalities is algebraically equivalent to CHSH inequality, whereas other inequalities can be identified as building blocks of CHSH and I_{3322} inequalities. Therefore the quantum violation of CHSH and I_{3322} inequalities can be traced back to the violation of pentagon inequalities. Furthermore, by linking CHSH inequality to a pentagon inequality, we are able to provide a simple argument for the impossibility of Popescu and Rohrlich (PR) nonlocal boxes.

In **paper II** we present experimental realization of biased and unbiased CHSH games. We also found a remarkable application of these games, in a famous card game of duplicate bridge. In the paper we described this application along with its successful experimental realization. Note that this is the first demonstration of a quantum communication complexity protocol usable in a real-life scenario. We also show in the paper that our quantum bridge game corresponds to a biased non-local CHSH game, and it is equivalent to a $2 \to 1$ entanglement assisted quantum random access code. Therefore, our experiment is also a realization of a $2 \to 1$ entanglement assisted random access code. Interestingly our application of quantum communication complexity protocol on duplicate bridge game will have influence on its future and/or on the rules of this game. As it is up to the World Bridge Federation to decide whether to allow quantum resources and encoding strategies in Bridge championships, making this technique the first commonplace application of quantum communication complexity, or to forbid quantum strategies and thus, constituting the very first everyday regulation of quantum resources.

In **paper III**, we have presented an implementation of a recently discovered method with which one can certify entanglement in a measurement-device-independent way [19; 20]. This certification is based on the witness method and therefore could be easily applied for many entangled states. Using this method we detect entanglement in a set of two-photon Werner states.

Our results are in good agreement with the theory. Our experiment can be viewed as a demonstration of Buscemi game with quantum input which leads to a trust-free entanglement detection. Methods and techniques used here can open the door for other applications i.e. the measurement-device-independent determination of properties of quantum systems, realization of quantum communication and cryptographic protocols etc.

In **paper IV** we experimentally investigated a lossless quantum channel, inducing phase-flip and bit-flip errors. We analyze, what happens when a product of Bell's state passes through this noisy channel. This way we were able to produce four-partite bound entangled states, known as Smolin states. We also show that such a channel can generate a set of bond entangled states that can violate CHSH-inequality. Moreover, we experimentally investigated the boundary regime between free entanglement, bound entanglement and separable states.

In **paper V**, for the first time we prepared a high fidelity mixed three qubit polarization bound entangled state. Using quantum state tomography we have fully reconstructed its density matrix and demonstrated all its entanglement properties. In **Paper VI**, we present activation scheme for this state using a free entangled pair. Importantly, the very unique feature of quantum mechanics revealed by our experiment is its "something-out-of-nothing" character; an ingredient completely absent in any of the two resources suddenly emerges after putting the two resources together. This phenomenon lies at the very heart of the quantum information. We strongly believe that the results reported here will help in the development of novel quantum information and communication protocols and in deeper understanding of foundations of quantum mechanics.

A. Correlation function for GHZ state

We define measurement settings for each qubit on the corresponding Bloch spheres with $\sigma_{n_i} = \hat{n}_i.\vec{\sigma}$, where $i = 1,2,3,4$ and

$$\hat{n}_i = \begin{pmatrix} \sin\theta_i \ \cos\phi_i \\ sin\theta_i \ \sin\phi_i \\ cos\theta_i \end{pmatrix}, \tag{A.1}$$

therefore

$$\sigma_{n_i} = \hat{n}_i.\vec{\sigma} = \begin{pmatrix} \cos\theta_i & e^{-i\phi_i}\sin\theta_i \\ e^{i\phi_i}\sin\theta_i & -\cos\theta_i \end{pmatrix}. \tag{A.2}$$

As, $|GHZ\rangle$ is given as,

$$|GHZ\rangle = \frac{1}{\sqrt{2}} \ (\ |0011\rangle + |1100\rangle \ ). \tag{A.3}$$

Then correlation function will becomes

$$\begin{aligned} E^{GHZ}(\hat{n}_1,\hat{n}_2,\hat{n}_3,\hat{n}_4) =& \langle GHZ|(\sigma_{n_1}\otimes\sigma_{n_2}\otimes\sigma_{n_3}\otimes\sigma_{n_4})|GHZ\rangle \\ =& \frac{1}{2}\langle 0011|(\sigma_{n_1}\otimes\sigma_{n_2}\otimes\sigma_{n_3}\otimes\sigma_{n_4})|0011\rangle \\ &+ \langle 0011|(\sigma_{n_1}\otimes\sigma_{n_2}\otimes\sigma_{n_3}\otimes\sigma_{n_4})|1100\rangle \\ &+ \langle 1100|(\sigma_{n_1}\otimes\sigma_{n_2}\otimes\sigma_{n_3}\otimes\sigma_{n_4})|0011\rangle \\ &+ \langle 1100|(\sigma_{n_1}\otimes\sigma_{n_2}\otimes\sigma_{n_3}\otimes\sigma_{n_4})|1100\rangle. \end{aligned} \tag{A.4}$$

Note that

$$\begin{aligned} \langle 0|\sigma_{n_i}|0\rangle &= \begin{pmatrix} 1 & 0 \end{pmatrix} \begin{pmatrix} \cos\theta_i & e^{-i\phi_i}\sin\theta_i \\ e^{i\phi_i}\sin\theta_i & -\cos\theta_i \end{pmatrix} \begin{pmatrix} 1 \\ 0 \end{pmatrix} \\ &= \cos\theta_i \end{aligned} \tag{A.5}$$

$$\begin{aligned} \langle 0|\sigma_{n_i}|1\rangle &= \begin{pmatrix} 1 & 0 \end{pmatrix} \begin{pmatrix} \cos\theta_i & e^{-i\phi_i}\sin\theta_i \\ e^{i\phi_i}\sin\theta_i & -\cos\theta_i \end{pmatrix} \begin{pmatrix} 0 \\ 1 \end{pmatrix} \\ &= e^{-i\phi_i}\sin\theta_i \end{aligned} \tag{A.6}$$

$$\begin{aligned}\langle 1|\sigma_{n_i}|0\rangle &= \begin{pmatrix} 0 & 1 \end{pmatrix} \begin{pmatrix} \cos\theta_i & e^{-i\phi_i}\sin\theta_i \\ e^{i\phi_i}\sin\theta_i & -\cos\theta_i \end{pmatrix} \begin{pmatrix} 1 \\ 0 \end{pmatrix} \\ &= e^{i\phi_i}\sin\theta_i \end{aligned} \tag{A.7}$$

$$\begin{aligned}\langle 1|\sigma_{n_i}|1\rangle &= \begin{pmatrix} 0 & 1 \end{pmatrix} \begin{pmatrix} \cos\theta_i & e^{-i\phi_i}\sin\theta_i \\ e^{i\phi_i}\sin\theta_i & -\cos\theta_i \end{pmatrix} \begin{pmatrix} 0 \\ 1 \end{pmatrix} \\ &= -\cos\theta_i \end{aligned} \tag{A.8}$$

Using these relations and the fact that $\cos x = \frac{e^{ix}+e^{-ix}}{2}$, we get

$$\begin{aligned}E^{GHZ}(\hat{n}_1,\hat{n}_2,\hat{n}_3,\hat{n}_4) =& cos\ \theta_1\ cos\ \theta_2\ cos\ \theta_3\ cos\ \theta_4 \\ & -sin\ \theta_1\ sin\ \theta_2\ sin\ \theta_3\ sin\ \theta_4\ cos\ (\phi_1+\phi_2-\phi_3-\phi_4)\end{aligned}$$

This is the desired relation [33].

References

[1] DAVID BOHM. *Quantum theory*. Courier Dover Publications, 1951. 1, 13

[2] A. EINSTEIN, B. PODOLSKY, AND N. ROSEN. **Can quantum-mechanical description of physical reality be considered complete?** *Physical review*, **47**(10):777, 1935. 1, 12

[3] NIELS BOHR. **Can quantum-mechanical description of physical reality be considered complete?** *Physical review*, **48**(8):696–702, 1935. 1, 14

[4] ERWIN SCHRÖDINGER. **Die gegenwärtige Situation in der Quantenmechanik**. *Naturwissenschaften*, **23**(49):823–828, 1935. 1, 20

[5] ERWIN SCHRÖDINGER. **Discussion of probability relations between separated systems**. In *Mathematical Proceedings of the Cambridge Philosophical Society*, **31**, pages 555–563. Cambridge Univ Press, 1935. 1

[6] J. F. CLAUSER, M. A. HORNE, A. SHIMONY, AND R. A. HOLT. **Proposed experiment to test local hidden-variable theories.** *Phys. Rev. Lett.*, **23**(21):880–884, 1969. 1, 17

[7] JOHN S. BELL. **On the problem of hidden variables in quantum mechanics.** *Reviews of Modern Physics*, **38.3**(447-452), 1966.

[8] JOHN S. BELL. *Speakable and Unspeakable in Quantum Mechanics: Collected papers on quantum philosophy.* Cambridge University Press, 2004. 1

[9] STUART J FREEDMAN AND JOHN F CLAUSER. **Experimental test of local hidden-variable theories**. *Physical Review Letters*, **28**(14):938, 1972. 2, 17

[10] ALAIN ASPECT, PHILIPPE GRANGIER, AND GÉRARD ROGER. **Experimental tests of realistic local theories via Bell's theorem.** *Physical Review Letters*, **47.7**(460-463), 1981.

[11] ALAIN ASPECT, JEAN DALIBARD, AND GÉRARD ROGER. **Experimental test of Bell's inequalities using time-varying analyzers**. *Physical review letters*, **49**(25):1804, 1982. 17

[12] MARY A ROWE, DAVID KIELPINSKI, VOLKER MEYER, CHARLES A SACKETT, WAYNE M ITANO, CHRISTOPHER MONROE, AND DAVID J WINELAND. **Experimental violation of a Bell's inequality with efficient detection**. *Nature*, **409**(6822):791–794, 2001.

[13] MARISSA GIUSTINA, ALEXANDRA MECH, SVEN RAMELOW, BERNHARD WITTMANN, JOHANNES KOFLER, JÖRN BEYER, ADRIANA LITA, BRICE CALKINS, THOMAS GERRITS, SAE WOO NAM, ET AL. **Bell violation using entangled photons without the fair-sampling assumption**. *Nature*, **497**(7448):227–230, 2013. 17

[14] BG CHRISTENSEN, KT MCCUSKER, JB ALTEPETER, B CALKINS, T GERRITS, AE LITA, A MILLER, LK SHALM, Y ZHANG, SW NAM, ET AL. **Detection-loophole-free test of quantum nonlocality, and applications**. *Physical review letters*, **111**(13):130406, 2013.

[15] BAS HENSEN, H BERNIEN, AE DRÉAU, A REISERER, N KALB, MS BLOK, J RUITENBERG, RFL VERMEULEN, RN SCHOUTEN, C ABELLÁN, ET AL. **Loophole-free Bell inequality violation using electron spins separated by 1.3 kilometres**. *Nature*, **526**(7575):682–686, 2015. 17

[16] MARISSA GIUSTINA, MARIJN AM VERSTEEGH, SÖREN WENGEROWSKY, JOHANNES HANDSTEINER, ARMIN HOCHRAINER, KEVIN PHELAN, FABIAN STEINLECHNER, JOHANNES KOFLER, JAN-ÅKE LARSSON, CARLOS ABELLÁN, ET AL. **Significant-loophole-free test of Bell's theorem with entangled photons**. *Physical review letters*, **115**(25):250401, 2015. 2

[17] ADAN CABELLO, SIMONE SEVERINI, AND ANDREAS WINTER. **(Non-) Contextuality of Physical Theories as an Axiom.** *arXiv preprint arXiv:1010.2163*, 2010. 2, 51, 53, 56

[18] LAWSON THOMAS, NOAH LINDEN, AND SANDU POPESCU. **Biased nonlocal quantum games.** *arXiv:1011.6245*, 2010. 2, 59, 61

[19] FRANCESCO BUSCEMI. **All entangled quantum states are nonlocal**. *Physical review letters*, **108**(20):200401, 2012. 3, 70, 79

[20] CYRIL BRANCIARD, DENIS ROSSET, YEONG-CHERNG LIANG, AND NICOLAS GISIN. **Measurement-device-independent entanglement witnesses for all entangled quantum states**. *Physical review letters*, **110**(6):060405, 2013. 3, 70, 79

[21] MICHAEL REED AND BARRY SIMON. *Methods of modern mathematical physics: Functional analysis*, **1**. Gulf Professional Publishing, 1980. 6

[22] J. J. SAKURAI. *Modern Quantum Mechanics.* Addison-Wesley Publishing Company, 1994. 7

[23] LLUÍS MASANES, YEONG-CHERNG LIANG, AND ANDREW C DOHERTY. **All bipartite entangled states display some hidden nonlocality**. *Physical review letters*, **100**(9):090403, 2008. 11

[24] REINHARD F WERNER. **Quantum states with Einstein-Podolsky-Rosen correlations admitting a hidden-variable model**. *Physical Review A*, **40**(8):4277, 1989. 11, 67

[25] RYSZARD HORODECKI, PAWEŁ HORODECKI, MICHAŁ HORODECKI, AND KAROL HORODECKI. **Quantum entanglement**. *Reviews of modern physics*, **81**(2):865, 2009. 11, 68, 69, 72

[26] JOHN S BELL. **Introduction to the hidden-variable question**. *Foundations of quantum mechanics*, pages 171–181, 1971. 14

[27] LESLIE E. BALLENTINE. *Quantum Mechanics: a modern development.* World Scientific Publishing Company, 1998. 14

[28] BORIS S CIREL'SON. **Quantum generalizations of Bell's inequality**. *Letters in Mathematical Physics*, **4**(2):93–100, 1980. 17

[29] LUCIEN HARDY. **Nonlocality for two particles without inequalities for almost all entangled states**. *Physical Review Letters*, **71**(11):1665, 1993. 18

[30] ADÁN CABELLO, PIOTR BADZIĄG, MARCELO TERRA CUNHA, AND MOHAMED BOURENNANE. **Simple Hardy-like proof of quantum contextuality**. *Physical review letters*, **111**(18):180404, 2013. 18, 22

[31] N DAVID MERMIN. **What's Wrong with this Temptation?** *Physics Today*, **47**(6):9–11, 1994.

[32] ERNESTO F GALVÃO. **Foundations of quantum theory and quantum information applications**. *arXiv preprint quant-ph/0212124*, 2002. 18

[33] DANIEL M GREENBERGER, MICHAEL A HORNE, ABNER SHIMONY, AND ANTON ZEILINGER. **Bell's theorem without inequalities**. *Am. J. Phys*, **58**(12):1131–1143, 1990. 19, 20, 21, 82

[34] DANIEL GREENBERGER, MICHAEL HORNE, ANTON ZEILINGER, AND MAREK ŻUKOWSKI. **A Bell theorem without inequalities for two particles, using inefficient detectors**. *arXiv preprint quant-ph/0510207*, 2005. 21

[35] N DAVID MERMIN. **Is the moon there when nobody looks? Reality and the quantum theory**. *Physics today*, **38**(4):38–47, 1985. 22

[36] N DAVID MERMIN. **Quantum mysteries revisited**. *Am. J. Phys*, **58**(8):731–734, 1990. 22

[37] BRENO MARQUES, JOHAN AHRENS, MOHAMED NAWAREG, ADÁN CABELLO, AND MOHAMED BOURENNANE. **Experimental observation of Hardy-like quantum contextuality**. *Physical review letters*, **113**(25):250403, 2014. 22

[38] BERTHOLD-GEORG ENGLERT, CHRISTIAN KURTSIEFER, AND HARALD WEINFURTE. **Universal unitary gate for single-photon two-qubit states.** *Physics Letters A*, **63.3**(032303), 2001. 27, 34

[39] RICHARD A CAMPOS, BAHAA EA SALEH, AND MALVIN C TEICH. **Quantum-mechanical lossless beam splitter: SU (2) symmetry and photon statistics**. *Physical Review A*, **40**(3):1371, 1989. 30

[40] MARK BECK. *Quantum Mechanics: Theory and Experiment*. Oxford University Press, 2012. 30

[41] PAUL G KWIAT, KLAUS MATTLE, HARALD WEINFURTER, ANTON ZEILINGER, ALEXANDER V SERGIENKO, AND YANHUA SHIH. **New high-intensity source of polarization-entangled photon pairs**. *Physical Review Letters*, **75**(24):4337, 1995. 38

[42] ANTIA LAMAS-LINARES, JOHN C HOWELL, AND DIK BOUWMEESTER. **Stimulated emission of polarization-entangled photons**. *Nature*, **412**(6850):887–890, 2001. 38

[43] PIETER KOK AND BRENDON W LOVETT. *Introduction to optical quantum information processing*. Cambridge University Press, 2010. 38

[44] CHARLES H BENNETT, GILLES BRASSARD, CLAUDE CRÉPEAU, RICHARD JOZSA, ASHER PERES, AND WILLIAM K WOOTTERS. **Teleporting an unknown quantum state via dual classical and Einstein-Podolsky-Rosen channels**. *Physical review letters*, **70**(13):1895, 1993. 41, 45, 48

[45] DIK BOUWMEESTER, JIAN-WEI PAN, KLAUS MATTLE, MANFRED EIBL, HARALD WEINFURTER, AND ANTON ZEILINGER. **Experimental quantum teleportation**. *Nature*, **390**(6660):575–579, 1997. 41, 45, 48

[46] M ŻUKOWSKI, A ZEILINGER, MA HORNE, AND AK EKERT. **" Event-ready-detectors" Bell experiment via entanglement swapping**. *Physical Review Letters*, **71**(26):4287–4290, 1993. 41, 45

[47] JIAN-WEI PAN, DIK BOUWMEESTER, HARALD WEINFURTER, AND ANTON ZEILINGER. **Experimental entanglement swapping: Entangling photons that never interacted**. *Physical Review Letters*, **80**(18):3891, 1998. 41, 45

[48] CK HONG, ZY OU, AND LEONARD MANDEL. **Measurement of subpicosecond time intervals between two photons by interference**. *Physical Review Letters*, **59**(18):2044, 1987. 41

[49] L MANDEL. **Quantum effects in one-photon and two-photon interference**. *Reviews of Modern Physics Supplement*, **71**:S274–S282, 1999. 41

[50] ZHE-YU JEFF OU. *Multi-photon quantum interference*. Springer, 2007. 43

[51] FW SUN, ZY OU, AND GC GUO. **Projection measurement of the maximally entangled N-photon state for a demonstration of the N-photon de Broglie wavelength**. *Physical Review A*, **73**(2):023808, 2006.

[52] NIKOLAI KIESEL, CHRISTIAN SCHMID, ULRICH WEBER, RUPERT URSIN, AND HARALD WEINFURTER. **Linear optics controlled-phase gate made simple**. *Physical review letters*, **95**(21):210505, 2005. 43

[53] JIAN-WEI PAN, ZENG-BING CHEN, CHAO-YANG LU, HARALD WEINFURTER, ANTON ZEILINGER, AND MAREK ŻUKOWSKI. **Multiphoton entanglement and interferometry**. *Reviews of Modern Physics*, **84**(2):777, 2012. 44, 47

[54] CHARLES H BENNETT AND STEPHEN J WIESNER. **Communication via one-and two-particle operators on Einstein-Podolsky-Rosen states**. *Physical review letters*, **69**(20):2881, 1992. 45

[55] N LÜTKENHAUS, J CALSAMIGLIA, AND K-A SUOMINEN. **Bell measurements for teleportation**. *Physical Review A*, **59**(5):3295, 1999. 45

[56] PHILIP WALTHER AND ANTON ZEILINGER. **Experimental realization of a photonic Bell-state analyzer**. *Physical Review A*, **72**(1):010302, 2005. 45

[57] LING-JUN KONG, YONGNAN LI, YU SI, RUI LIU, CHENGHOU TU, AND HUI-TIAN WANG. **Near-complete polarization Bell-state analysis based on symmetry-broken scheme with linear optics**. *arXiv preprint arXiv:1512.01131*, 2015. 45

[58] SAMUEL L BRAUNSTEIN AND A MANN. **Measurement of the Bell operator and quantum teleportation**. *Physical Review A*, **51**(3):R1727, 1995. 45

[59] HARALD WEINFURTER. **Experimental Bell-state analysis**. *EPL (Europhysics Letters)*, **25**(8):559, 1994. 45

[60] JIAN-WEI PAN AND ANTON ZEILINGER. **Greenberger-Horne-Zeilinger-state analyzer**. *Physical Review A*, **57**(3):2208, 1998. 46

[61] ANTON ZEILINGER, MICHAEL A HORNE, HARALD WEINFURTER, AND MAREK ŻUKOWSKI. **Three-particle entanglements from two entangled pairs**. *Physical review letters*, **78**(16):3031, 1997. 46

[62] RUPERT URSIN, F TIEFENBACHER, T SCHMITT-MANDERBACH, H WEIER, THOMAS SCHEIDL, M LINDENTHAL, B BLAUENSTEINER, T JENNEWEIN, J PERDIGUES, P TROJEK, ET AL. **Entanglement-based quantum communication over 144 km**. *Nature physics*, **3**(7):481–486, 2007. 48

[63] WILLIAM K WOOTTERS AND WOJCIECH H ZUREK. **A single quantum cannot be cloned**. *Nature*, **299**(5886):802–803, 1982. 48

[64] MICHAEL A NIELSEN AND ISAAC L CHUANG. *Quantum computation and quantum information*. Cambridge university press, 2010. 48, 66

[65] L. LOVÁSZ. **On the Shannon capacity of a graph**. *Trans. Inf. Theory*, **25**(1), 1979. 53, 56

[66] BIN YAN. **Quantum correlations are tightly bound by the exclusivity principle**. *Physical review letters*, **110**(26):260406, 2013. 53, 56

[67] ADÁN CABELLO. **Simple explanation of the quantum violation of a fundamental inequality**. *Physical review letters*, **110**(6):060402, 2013.

[68] MOHAMED NAWAREG, FABRIZIO BISESTO, VINCENZO D'AMBROSIO, ELIAS AMSELEM, FABIO SCIARRINO, MOHAMED BOURENNANE, AND ADAN CABELLO. **Bounding quantum theory with the exclusivity principle in a two-city experiment**. *arXiv preprint arXiv:1311.3495*, 2013. 56

[69] YEONG-CHERNG LIANG, ROBERT W SPEKKENS, AND HOWARD M WISEMAN. **Specker's parable of the overprotective seer: A road to contextuality, nonlocality and complementarity**. *Physics Reports*, **506**(1):1–39, 2011. 56

[70] ADAN CABELLO. **Specker's fundamental principle of quantum mechanics**. *arXiv preprint arXiv:1212.1756*, 2012. 56

[71] R. DIESTEL. Graph Theory*, Graduate Texts in Mathematics*. Springer, Heidelberg, 2010. 56

[72] S. POPESCU AND D. ROHRLICH. **Quantum nonlocality as an axiom.** *Found. Phys.*, **24**(379), 1994. 57

[73] **General conditions of contest: www.worldbridge.org/Data/Sites/1/media/documents/regulations/generalconditionsofcontest.pdf**. 63

[74] M. PAWŁOWSKI AND M. ŻUKOWSKI. **Entanglement assisted random access codes.** *Phys. Rev. A*, **81**(042326), 2010. 64

[75] OTFRIED GÜHNE AND GÉZA TÓTH. **Entanglement detection**. *Physics Reports*, **474**(1):1–75, 2009. 66, 69, 72

[76] STIG STENHOLM AND KALLE-ANTTI SUOMINEN. *Quantum approach to informatics.* Wiley-Interscience, 2005. 66

[77] RICHARD JOZSA. **Fidelity for mixed quantum states**. *Journal of modern optics*, **41**(12):2315–2323, 1994. 66

[78] CLAUDIA WAGENKNECHT, CHE-MING LI, ANDREAS REINGRUBER, XIAO-HUI BAO, ALEXANDER GOEBEL, YU-AO CHEN, QIANG ZHANG, KAI CHEN, AND JIAN-WEI PAN. **Experimental demonstration of a heralded entanglement source**. *Nature Photonics*, **4**(8):549–552, 2010. 66

[79] JAN-ÅKE LARSSON. **Loopholes in Bell inequality tests of local realism**. *Journal of Physics A: Mathematical and Theoretical*, **47**(42):424003, 2014. 67

[80] JONATHAN JOGENFORS, ASHRAF MOHAMED ELHASSAN, JOHAN AHRENS, MOHAMED BOURENNANE, AND JAN-ÅKE LARSSON. **Hacking the Bell test using classical light in energy-time entanglement–based quantum key distribution**. *Science Advances*, **1**(11), 2015. 67

[81] NICOLAS GISIN. **Bell's inequality holds for all non-product states**. *Physics Letters A*, **154**(5):201–202, 1991. 67

[82] NICOLAS GISIN AND ASHER PERES. **Maximal violation of Bell's inequality for arbitrarily large spin**. *Physics Letters A*, **162**(1):15–17, 1992. 67

[83] ANTONIO ACÍN. **Werner States**. In *Compendium of Quantum Physics*, pages 843–845. Springer, 2009. 67

[84] ASHER PERES. **Separability criterion for density matrices**. *Physical Review Letters*, **77**(8):1413, 1996. 68

[85] MICHAŁ HORODECKI, PAWEŁ HORODECKI, AND RYSZARD HORODECKI. **Separability of mixed states: necessary and sufficient conditions**. *Physics Letters A*, **223**(1):1–8, 1996. 68

[86] M BARBIERI, F DE MARTINI, G DI NEPI, P MATALONI, GM D'ARIANO, AND C MACCHIAVELLO. **Detection of entanglement with polarized photons: experimental realization of an entanglement witness**. *Physical review letters*, **91**(22):227901, 2003. 69

[87] MOHAMED BOURENNANE, MANFRED EIBL, CHRISTIAN KURTSIEFER, SASCHA GAERTNER, HARALD WEINFURTER, OTFRIED GÜHNE, PHILIPP HYLLUS, DAGMAR BRUSS, MACIEJ LEWENSTEIN, AND ANNA SANPERA. **Experimental detection of multipartite entanglement using witness operators**. *Physical review letters*, **92**(8):087902, 2004. 69

[88] MACIEJ LEWENSTEIN, B KRAUS, JI CIRAC, AND P HORODECKI. **Optimization of entanglement witnesses**. *Physical Review A*, **62**(5):052310, 2000. 69

[89] O GÜHNE, P HYLLUS, D BRUSS, A EKERT, M LEWENSTEIN, C MACCHIAVELLO, AND A SANPERA. **Detection of entanglement with few local measurements**. *Physical Review A*, **66**(6):062305, 2002. 69

[90] PATRICK SKWARA, HERMANN KAMPERMANN, MATTHIAS KLEINMANN, AND DAGMAR BRUSS. **Entanglement witnesses and a loophole problem**. *Physical Review A*, **76**(1):012312, 2007. 70

[91] TOBIAS MORODER, OTFRIED GÜHNE, NORMAND BEAUDRY, MARCO PIANI, AND NORBERT LÜTKENHAUS. **Entanglement verification with realistic measurement devices via squashing operations**. *Physical Review A*, **81**(5):052342, 2010. 70

[92] ASHER PERES. **Collective tests for quantum nonlocality**. *Physical Review A*, **54**(4):2685, 1996. 70

[93] RICHARD CLEVE, PETER HØYER, BENJAMIN TONER, AND JOHN WATROUS. **Consequences and limits of nonlocal strategies**. In *Computational Complexity, 2004. Proceedings. 19th IEEE Annual Conference on*, pages 236–249. IEEE, 2004. 70

[94] INGEMAR BENGTSSON AND KAROL ZYCZKOWSKI. *Geometry of quantum states: an introduction to quantum entanglement*. Cambridge University Press, 2007. 72

[95] VLATKO VEDRAL, MARTIN B PLENIO, MICHAEL A RIPPIN, AND PETER L KNIGHT. **Quantifying entanglement**. *Physical Review Letters*, **78**(12):2275, 1997. 72

[96] CHARLES H BENNETT, DAVID P DIVINCENZO, CHRISTOPHER A FUCHS, TAL MOR, ERIC RAINS, PETER W SHOR, JOHN A SMOLIN, AND WILLIAM K WOOTTERS. **Quantum nonlocality without entanglement**. *Physical Review A*, **59**(2):1070, 1999. 72

[97] ERIC CHITAMBAR, DEBBIE LEUNG, LAURA MANČINSKA, MARIS OZOLS, AND ANDREAS WINTER. **Everything you always wanted to know about LOCC (but were afraid to ask)**. *Communications in Mathematical Physics*, **328**(1):303–326, 2014. 72

[98] CHARLES H BENNETT, HERBERT J BERNSTEIN, SANDU POPESCU, AND BENJAMIN SCHUMACHER. **Concentrating partial entanglement by local operations**. *Physical Review A*, **53**(4):2046, 1996. 73

[99] CHARLES H BENNETT, DAVID P DIVINCENZO, JOHN A SMOLIN, AND WILLIAM K WOOTTERS. **Mixed-state entanglement and quantum error correction**. *Physical Review A*, **54**(5):3824, 1996. 73

[100] MICHAŁ HORODECKI, PAWEŁ HORODECKI, AND RYSZARD HORODECKI. **Inseparable two spin-1 2 density matrices can be distilled to a singlet form**. *Physical Review Letters*, **78**(4):574, 1997. 73

[101] PAWEL HORODECKI. **Separability criterion and inseparable mixed states with positive partial transposition**. *arXiv preprint quant-ph/9703004*, 1997. 73

[102] MICHAŁ HORODECKI, PAWEŁ HORODECKI, AND RYSZARD HORODECKI. **Mixed-state entanglement and distillation: is there a "bound" entanglement in nature?** *Physical Review Letters*, **80**(24):5239, 1998. 73

[103] ELIAS AMSELEM AND MOHAMED BOURENNANE. **Experimental four-qubit bound entanglement**. *Nature Physics*, **5**(10):748–752, 2009. 74

[104] JOHN A SMOLIN. **Four-party unlockable bound entangled state**. *Physical Review A*, **63**(3):032306, 2001. 74

[105] ELIAS AMSELEM. **Dynamics of Quantum Correlations with Photons: Experiments on bound entanglement and contextuality for application in quantum information**. 2012. 75

[106] JOSEPH B ALTEPETER, EVAN R JEFFREY, AND PAUL G KWIAT. **Photonic state tomography**. *Advances in Atomic, Molecular, and Optical Physics*, **52**:105–159, 2005. 76

[107] ANTONIO ACIN, J IGNACIO CIRAC, AND LL MASANES. **Multipartite bound information exists and can be activated**. *Physical review letters*, **92**(10):107903, 2004. 76

[108] PAWEŁ HORODECKI, MICHAŁ HORODECKI, AND RYSZARD HORODECKI. **Bound entanglement can be activated**. *Physical review letters*, **82**(5):1056, 1999. 77